NTNU – Trondheim
Norwegian University of
Science and Technology

Hydrodynamic Analysis for a Logistical HUB

Erik Løken

Marine Technology
Submission date: June 2012
Supervisor: Jan Vidar Aarsnes, IMT

Norwegian University of Science and Technology
Department of Marine Technology

PREFACE

This thesis is submitted to the Norwegian University of Science and Technology (NTNU) for fulfillment of the requirements for the degree of Master of Science.

The work with this master thesis has been performed at the Department of Marine Technology, NTNU, Trondheim, with Jan Aarsnes as supervisor. The work is a continuation of the summer project done at Sevan Marine during the summer 2011 and the project thesis performed during the autumn of 2011 as the course TMR 4520.

First, I would like to thank my supervisor, Prof. Jan Aarsnes, for his guidance and encouragement throughout the work of this thesis. His knowledge and insight into the research topic gave my thesis a solid foundation.

I would also like to thank Adjunct Associate Professor Zhen Gao for his assistance in Wadam.

I would like to thank the professors and the staffs at Department of Marine Technology for their help and availability during my master study.

Trondheim 08.06.2012

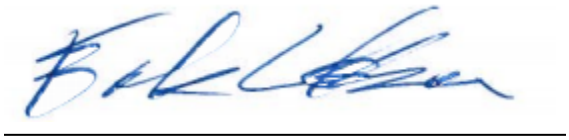

Erik Løken

ABSTRACT

The conventional way of transporting personnel from shore to offshore platforms is done by helicopter. For large distances of transportation this results in high costs due to the limitations in the maximum number of persons each helicopter can transport per trip and due to the high prices on helicopter fuel. In this thesis is an alternative solution to this conventional transportation proposed by the utilization of a logistical HUB. The concept is based ferries doing the transportation of personnel from shore to the HUB and helicopters doing the remaining, relatively short, transfer from the HUB to the respective platforms. The HUB evaluated is based on the characteristic Sevan 650 design, having a cylindrical shape with diameter $D = 78m$ in the waterline.

The models that have been analyzed in this thesis were modeled in GeniE, the hydrodynamic analyses were done in Wadam and the post processing was performed using Postresp.

Models of a platform with a single tunnel cut out with varying tunnel length L have been evaluated, and the motions of these models as well as the surface elevation inside the tunnel were studied in detail. It was recorded a two peaked response in heave for the models with tunnel lengths ranging from $30m < L < 40m$. This unexpected behavior was found to be due to diverging values for the added mass in heave for increasing tunnel lengths for models with intact tunnel bottoms. This was adjusted for by removing the bottom of the tunnel to add damping to the system, resulting in the usual one peaked response in heave being retrieved. The reason the two peaked response in heave occurred was concluded to be due to Wadam neglecting viscous effects including the viscous damping. This leads to the system having little or no damping and the added mass to diverge towards negative infinity giving unphysical motion representations.

Since critical situations for the platform-ferry interaction will occur during loading and unloading of personnel from the ferry to the platform and during entry of a ferry into a tunnel, the wave pattern inside and on the immediate outside of this tunnel have been studied and evaluated. A total of 4 different designs for the layout of the tunnels have been proposed and evaluated to find the design that results in the least surface elevation inside the tunnel and at the tunnel entrance. A window of acceptance for the incoming wave headings were established with the intention of minimizing the surface elevation. The designs were also evaluated regarding their ability to resist large motion for a variety of incoming wave periods. It was concluded that a three tunnel solution with the tunnels being shifted 120 degrees relative each other would result in the smallest platform motions for wave periods smaller than $18s$. A design consisting of 4 tunnels, where three of the tunnels are shifted 30 degrees relative each other and the last tunnel being located opposite of these three would result in the smallest surface elevations. An operability study was done for all 4 designs proposed based on the elevations inside and at the tunnel entrance. It was found that the 4 tunnel design described above would result in the largest operability for the platform. It was also found that this 4 tunnel solution would be unstable in roll due to an unsatisfactory low transverse metacentric height. This low metacentric height could be adjusted for by installing a vertical wall in the waterline in the transverse direction of the tunnels orientation.

SAMMENDRAG

Den konvensjonelle måten å transportere personell fra land til offshore plattformer gjøres i dag med helikopter. For transport over store avstander resulterer dette i høye kostnader på grunn av ett lavt antall personer som fraktes per helikoptertur og høye priser på drivstoff. I denne avhandlingen er en alternativ løsning på denne konvensjonelle måten for transport foreslått, ved bruk av en logistikk HUB. Konseptet er basert på er at ferger gjør den lange transporten av personell fra land til HUB, mens helikoptre blir satt til å gjøre den gjenværende, forholdsvis korte transporten fra HUBen til de ulike plattformene. HUBen som her er evaluert er basert på ett karakteristisk Sevan 650 design, og har en sylindrisk form med diameteri vannlinjen $D = 78m$.

Modellene som er analysert i denne avhandlingen er blitt modellert i GeniE, de hydrodynamiske analysene er gjort i Wadam og etterbehandlingen av resultatene er blitt utført ved bruk av Postresp.

Modeller av en plattform med ett tunnel utkutt i skroget for varierende tunnel lengde L har blitt evaluert, og bevegelsene til disse modellene samt overflate hevingen inne i tunnelen ble studert i detalj. En to- toppet response i hiv ble observert for modeller med tunnel lengder fra $30m < L < 40m$. Denne uventede oppførselen av modellene ble funnet til å være grunnet divergerende added mass A_{33} for økende tunnellengder for modeller med intakt tunnel bunn. Dette ble korrigert for ved å fjerne bunnen for å tilføre demping til systemet, hvilket resulterte i at den vanlige, ene toppede hiv responsen ble observert. Grunnen til at den to- toppede responsen i hiv oppstod, ble funnet til å være fordi Wadam neglisjerer viskøse effekter og da også inkludert viskøs demping. Dette fører til at systemet har liten eller ingen demping og added mass til å divergere mot negativ uendelig , resulterende i ufysiske bevegelses representasjoner.

Ettersom kritiske situasjoner for interaksjon mellom plattform og ferge vil være under av- og på-stigning av personell fra fergen til plattform, samt under innkjøring av en ferge i tunnel, har bølgemønsteret i disse situasjonene blitt studert. Totalt har 4 forskjellige layouter for plasseringen av tunneler blitt foreslått og vurdert for å finne det designet som resulterer i minst overflateheving ved kritiske situasjoner. Et vindu for aksept for den innkommende bølgeretningen har blitt etablert med hensikt å minimere bølgebevegelsen inne i tunnelen. Designene ble også evaluert med hensyn til designets evne til å motstå bevegelser for forskjellige bølgeperioder. Det ble konkludert med at en designløsning med tre tunnel, hvor tunnelene er plassert 120 grader i forhold til hverandre vil resultere i minst plattform bevegelser for alle bølgeperioder mindre enn 18 sekunder. Ett design bestående av 4 tunneler, hvor tre av disse er forskjøvet 30 grader relativ hverandre og den siste tunnelen er plassert motsatt av disse tre, vil resultere i minst bølgebevelgse ved de kritiske situasjoner. En studie for oppetid har blitt gjort for alle 4 foreslåtte design, basert på bevegelse inne i tunnel og ved inngangen til denne. Det ble funnet at utformingen med 4 tunneler som beskrevet ovenfor ville resultere i den største operabiliteten av de evaluerte designene. Det ble også funnet at denne løsningen ville være ustabil i tverrretning på grunn av utilfredsstillende lav metasenterhøyde i denne retningen. Denne usabiliteten kan kompanseres for ved å installere en vertikal vegg i vannlinjen i midten av HUBen.

TABLE OF CONTENTS

PREFACE I

ABSTRACT II

SAMMENDRAG III

TABLE OF CONTENTS IV

TABLE OF FIGURES VI

TABLE OF TABLES VIII

1 INTRODUCTION AND MOTIVATION 1

1.1 PROJECT CONCEPT 1
1.2 DESIGN CONCEPT AS OF TODAY 1
1.3 SCOPE OF WORK 5

2 WAVE CONDITIONS IN THE SANTOS BASIN 6

3 DISCUSSION OF TUNNEL EFFECT ON HYDRODYNAMIC RESPONSE 8

3.1 WADAM 8
3.1.1 First computations done for a model with a single tunnel cut out in Wadam *9*
3.1.2 Computation for a concept model *13*
3.2 GENERAL DISCUSSION OF DESIGN SOLUTIONS WITH INTACT TUNNEL BOTTOM 16
3.2.1 Occurrence of a standing wave *16*
3.2.2 Sloshing *17*
3.2.3 Computational results for a single, closed tunnel *19*
3.2.4 Basic evaluation of structure motion for varying tunnel lengths *20*
3.2.5 Short Term Response for tunnels with intact bottom *23*
3.2.6 Detailed evaluation of tunnel impact on structure motion *28*
3.2.7 Viscous effects *35*

4 COMPUTATIONAL EVALUATION OF DIFFERENT DESIGN SOLUTIONS 37

4.1 OUTLINE OF PROPOSED DESIGNS 38
4.2 WAVE CONDITION IN THE SANTOS BASIN 39
4.3 PROPOSED DESIGN SOLUTION #1 40
4.4 PROPOSED DESIGN SOLUTION #2 48
4.5 PROPOSED DESIGN SOLUTION #3 53
4.6 PROPOSED DESIGN SOLUTION #4 60
4.7 COMPARISON OF COMPUTATIONAL RESULTS FOR THE DIFFERENT DESIGN SOLUTIONS 67

5 TUNNEL MODIFICATIONS 74

5.1 CENTRAL WHARF SEPARATING THE TUNNELS 74
5.2 PERFORATED BOTTOM 74

6 CONCLUSION 75

7 LIST OF REFERENCES 76

APPENDIX A **78**

Response Amplitude Operators in heave for models with a single tunnel with intact bottom of varying length L 78

APPENDIX B **80**

Surface elevations for a model with a single tunnel of length L=35m, without bottom, for varying y- coordinates and incoming wave heading = 270 degrees 80

APPENDIX C **82**

Surface elevation for a model with a single tunnel of length L=35m, without bottom, at y=-10m and for varying incoming wave headings 82

APPENDIX D **84**

Motions for the 4 evaluated designs with central wharf separating the tunnels 84

APPENDIX E **87**

Surface elevation at y=-10m for design #1-4 with central wharf separating the tunnels 87

APPENDIX F **88**

Surface elevation at y=-10m for design #1-4 as Short Term Responses. The limiting factor for the regularity study is SAT to be 5m. 88

Surface elevation at tunnel entrance y=-39m for design #1-4 as Short Term Responses. The limiting factor for the regularity study is SAT to be 5m. 90

APPENDIX G **92**

Surface elevation at y=-10m for design #1-4 as Short Term Responses. The limiting factor for the regularity study is SAT to be 2.5m 92

Surface elevation at tunnel entrance y=-39m for design #1-4 as Short Term Responses. The limiting factor for the regularity study is SAT to be; 2.5m 94

TABLE OF FIGURES

Figure 1 - Characteristic Sevan design 5
Figure 2 - Wave statistics in the Santos basin 7
Figure 3 - GeniE model of single tunnel, tunnel length L=35m 9
Figure 4 - Heave RAO for tunnel lenght L=35 11
Figure 5 - Pitch RAO for tunnel length L=35m 11
Figure 6 - Roll RAO for tunnel length L=35m 12
Figure 7 - Surge RAO for tunnel length L=35m 12
Figure 8 - Wave heading definition 13
Figure 9 - Heave RAO concept model 14
Figure 10 - Pitch RAO concept model 15
Figure 11 - Roll RAO concept model 15
Figure 12 - Standing wave inside a closed tunnel 17
Figure 13 - Elevations inside a closed tunnel of length L=35m for incoming wave direction 0 degrees 19
Figure 14 - Elevations inside a closed tunnel of length L=35m for incoming wave direction 270 degrees 20
Figure 15 - Heave RAO for tunnel length L=15m 21
Figure 16 - Heave RAO for tunnel length L=30m 21
Figure 17 - Heave RAO for tunnel length L=35m 22
Figure 18 - Heave RAO for tunnel length L=37.5m 22
Figure 19 - Heave RAO for tunnel length L=55m 23
Figure 20 - Short Term Response in heave for varying tunnel length L 24
Figure 21 - Short Term Response in pitch for varying tunnel length L 24
Figure 22 - Short Term Response in surge for varying tunnel length L 25
Figure 23 - Short Term Response in sway for varying tunnel length L 25
Figure 24 - Short Term Response in roll for varying tunnel length L 27
Figure 25 - Short Term Response in sway for 45m<L<55m 28
Figure 26 - Excitation force in heave F_3 for models with varying tunnel lengths 29
Figure 27 - Excitation force in heave F_3 for the concept model 30
Figure 28 - Added mass A_{33} for models with varying tunnel lengths 31
Figure 29 - Added mass A_{33} for tunnel length L=35m, without bottom. 33
Figure 30 - Excitation force F_3 for tunnel length L=35m, without bottom. 34
Figure 31 – Heave RAO for tunnel length L=35m, without tunnel bottom. 35
Figure 32 – Proposed design #1 38
Figure 33 - Proposed design #2 38
Figure 34 - Proposed design #3 38
Figure 35 - Proposed design #4 38
Figure 36 - Percentage average distribution of where the incoming waves are coming from in the Santos basin 39
Figure 37 - Proposed design solution #1 41
Figure 38 - Relation between incoming wave direction and desired tunnel for ferry entry for design solution #1 41

Figure 39 - Heave RAO for design #1 42
Figure 40 - Pitch RAO for design #1 43
Figure 41 - Roll RAO for design #1 43
Figure 42 - Pitch RAO for design #1, 7s<T<10s 44
Figure 43 – A_{33} for design #1, 7s<T<10s 45
Figure 44 - A_{53} for design #1, 7s<T<10s 45
Figure 45 – A_{55} for design #1, 7s<T<10s 46
Figure 46 - Surface elevation at y=-10m for design #1. 47
Figure 47 - Surface elevation at tunnel entrance for design #1 47
Figure 48 - Proposed design solution #2 49
Figure 49 - Relation between incoming wave direction and desired tunnel for ferry entry for design solution #2 49
Figure 50 - Heave RAO for design #2 50
Figure 51 - Pitch RAO for design #2 51
Figure 52 - Roll RAO for design #2 51
Figure 53 - Surface elevation at y=-10m for design #2 52
Figure 54 - Surface elevation at tunnel entrance for design #2 53
Figure 55 - Proposed design solution #3 54
Figure 56 - Relation between incoming wave direction and desired tunnel for ferry entry for design solution #3 55
Figure 57 - Heave RAO for design #3 57
Figure 58 - Pitch RAO for design #3 57
Figure 59 - Roll RAO for design #3 58
Figure 60 - Surface elevation at y=-10m for design #3 59
Figure 61 - Surface elevation at the tunnel entrance for design #3 59
Figure 62 - Proposed design solution #4 61
Figure 63 - Relation between incoming wave direction an tunnel of entry for design solution #4 62
Figure 64 - Heave RAO for design #4 63
Figure 65 - Pitch RAO for design #4 64
Figure 66 - Roll RAO for design #4 64
Figure 67 - Surface elevations at y=-10m for design #4 65
Figure 68 - Surface elevation at the tunnel entrance for design #4 66
Figure 69 - STR in heave for design #1-4 67
Figure 70 - STR in pitch for design #1-4 68
Figure 71 - STR in surge for design #1-4 68
Figure 72 - STR in sway for design #1-4 69
Figure 73 - STR in roll for design #1-4 69
Figure 74 - Short term response for surface elevation at y=-10m for design #1-4 71
Figure 75 - Short term response for surface elevation at y=-39m for design #1-4 71

TABLE OF TABLES

Table 1 - Sevan 650 main dimensions 3
Table 2 - Main parameters of proposed design 39
Table 3 - Regularity for design #1-4 with limiting factor =5m 72
Table 4 - Regularity for design #1-4 with limiting factor =2.5m 72

1 INTRODUCTION AND MOTIVATION

1.1 Project concept

The transportation of people over large distances at sea is conventionally done by helicopters. When the distance of transportation is long, transportation by helicopter leads to large expenditures due to limitations in the number of passengers available per trip and due to high prices on helicopter fuel. It has been proposed a solution to this problem by utilizing a logistical HUB offshore, where ferries transport people back and forth from shore to the HUB. In addition to reducing the costs of transportation, this solution makes the personnel transfer less dependent on air fluctuations, which are considered to be more unpredictable than ocean fluctuations. Helicopters are proposed to do the remaining, short transfer from the HUB to the different platforms. Since a ferry will have significantly smaller fuel costs and can transport a larger amount of passengers than a helicopter, this will reduce the total transportation costs and thus be preferable.

The proposed design for this logistical HUB is based on the Sevan 650 hull, where ferries can load and unload personnel safely before chartering back to shore. To make sure that the loading and unloading of personnel is done safely, it is proposed that the hull has cut outs acting as entrances to tunnels inside the hull. The concept is that when a ferry enters a tunnel, the gate closes behind it and the loading/unloading of personnel inside the hull is performed with very little surface motion. The tunnels are planned to be spread around the hull in a fashion so that the ferries always can enter the hull on the leeward side of the incoming waves.

Initial computer simulations have indicated that problems might appear considering wave motions in a tunnel when the gate is open and a vessel is entering/ exiting. Some of these problems are for high wave periods, when the wave length is approximately twice the length of the tunnel, which would lead to large pressure differences between the inside and outside of the tunnel. Other problems occur for smaller wave periods, which are believed to be due to diffraction effects.

1.2 Design concept as of today

Reduced movements are of great importance both for units used for drilling and for units used for oil production. During drilling operations the tolerance for heave motion is the limiting factor, but the tolerance of rolling and pitching angles are also of importance. For production units, the process equipment is often sensitive to extensively large movements and these have to be reduced as much as possible to achieve a high uptime. It is therefore critical to achieve a reduction in heave motion and of rolling and pitching movements to get an efficient unit for drilling after or production of oil and gas (Syvertsen and Smedal, 2005).

Conventional FPSOs as of today are recognized by their large storage capacity and high deck load. The downside is that these FPSOs are sensitive to incoming wave direction even in moderate seas. The sensitivity to wave direction is where the Sevan Stabilized Platform concept differs from the conventional FPSOs. The main objective with the Sevan design is to provide an offshore platform which is constructed with a focus on achieving reduced rolling and pitching movement in addition to reduced heave motions. Other objectives of the design are (Syvertsen and Lopes);

- To provide a platform which will combine the positive characteristics from units based on vessels and units based on semi-submersible platforms.
- Provide a platform which has a simple construction and low building costs.

The Sevan Stabilized Platform concept is basically a mono hull with circular shape, depending on the same stability principles as the conventional FPSOs. The circular shape dispenses the unit of any heading changes, because the sea faces the same vessel hydrodynamic resistance indifferent of the direction of the waves. The consequence of this is that the Sevan platform does not need any expensive turrets or swivels, which reduce the cost of production and maintenance substantially. The design is developed for offshore installations and meets the challenges for versatility, flexibility and fast deployment that is sat by the oil and gas industry. The design has proven to be able to perform operations in water depths ranging from $30m$ to more than $3000m$ and Sevan units may operate in both benign and harsh environments (Syvertsen and Lopes).

The characteristic dimension for the Sevan platform is the diameter. This makes it a highly modular design, with the diameter determining the size of the platform. The stability principles for the Sevan platform are the same as for a ship shaped vessel, and the large water plane area provides high stability and a large deck load capacity. If needed, the available deck area can be further increased with a cantilevered deck (Syvertsen and Lopes).

The main particulars of the Sevan 650 FPSO are summarized in table 1;

Parameter	*Unit*	*Dimensions*
Diameter Main Hull Cylinder	m	**78.0**
Diameter Main Deck	m	**86.0**
Diameter Process Deck	m	**92.0**
Area Process Deck	m^2	**6 650**
Diameter Pontoon	m	**95.0**
Height Pontoon	m	**/**
Elevation Main Deck	m	**36.0**
Elevation Process Deck	m	**42.0**
Elevation start flare	m	**28.0**
Radius of gyration in roll	m	**25**
Radius of gyration in pitch	m	**25**
Radius of gyration in yaw	m	**36**
Ballast Draft		
Draft	m	**16.5**
Displacement	Ton	**88 100**
Freeboard to MD	m	**19.5**
Freeboard to PD	m	**25.5**
VCG	m	**22.0**
GM (inclusive correction for free surface)	m	**6.5**
Loaded Draft		
Draft	m	**23.0**
Displacement	Ton	**119 900**
Freeboard to MD	m	**13.0**
Freeboard to PD	m	**19.0**
VCG	m	**20.3**
GM (inclusive correction for free surface)	**m**	**5.5**

Table 1 - Sevan 650 main dimensions

One of the big advantages of the Sevan design is the large storage room found inside the hull. The FPSOs utilize the hull for cargo storage and segregated ballast tanks as well as for marine and utility systems. Mobile Offshore Drilling Units (MODU) use the built in storage capacity to store mud and drill water as well as cargo and ballast tanks. Pumps and other utility systems related both to the drilling equipment and to the marine systems are also located inside the hull.

Due to the symmetrical shape, access to all tanks, ballast and cargo can be made through a central compartment. No piping is needed inside any of the tanks, which greatly simplifies the engineering design, construction and operation. It is estimated that the Sevan design will reduce the required piping to 30% of the piping needed in conventional FPSOs. The amount of cabling will also be reduced due to

the beneficial compact design. The internal tank layouts place the ballast tanks at the platform periphery, giving it a double hull configuration. The double hull on the Sevan platform is designed to maximize operational and environmental safety. The ballast tanks are protecting the cargo tanks to prevent direct leaks to the sea in the event of an accident. The double hull also adds stiffness to the structure in combination with the upper deck and central shaft. In total, this results in a lighter steel weight and thus reduced construction costs. The cylindrical shape gives lower flexing moments on the structure and low fatigue stress levels. The Sevan designed platform also has a bilge box at the base that provides damping to the vertical and angular motions of the vessel (Syvertsen and Lopes).

The hydrodynamic functions of the Sevan platform have been extensively tested in the ocean basin at Marintek in Trondheim, where it was verified that the platform has excellent angular and vertical motions. The low motion behavior of the Sevan design leads to the following positive effects (Syvertsen and Lopes);

- The plant`s efficiency increases due to reduced downtime.
- The riser life is elongated due to small riser motion.
- Increased overall operational safety level.
- The interactional motions between a tanker and the platform are much lower than that between a tanker and a conventional FPSO due to the much smaller surge and sway motions resulting from the Sevan design.

The Sevan concept has a wide range of applications, from large units operating in deep water, to production in small fields in shallow areas. The concept offers a flexible solution where adjustments can easily be done to tailor the platform to a number of applications. The Sevan designed platform may be used as a full-fledged ultra-deep water FPSO, or, with a large number of risers it may be used as a shallow water storage unit in combination with a fixed production platform or as a DP unit, designed for early production (Syvertsen and Lopes).

Figure 1 - Characteristic Sevan design

1.3 Scope of Work

In this master thesis have the occurring wave pattern at the entrance and inside the tunnels located on the HUB been evaluated. Different design solutions for the layout of the tunnels have been proposed and evaluated for minimization of the surface elevations at these critical conditions. Results from this in addition to relevant weather statistics have then been utilized to establish the regularity of the concept.

In chapter 2 is the essential wave statistics in the Santos basin presented, which will be critical for the computations done in this thesis.

In chapter 3 is the computer programs that have been utilized in this master thesis presented. The impact from the installation of a tunnel on the hydrodynamic response to a Sevan platform is discussed here.

In chapter 4 is different design solutions proposed with varying layouts for the locations of the tunnels presented. The layouts have as been constructed with the purpose of minimizing the surface elevation inside the tunnel. The motions of the different design solutions are discussed, and the results of the wave pattern and motions are compared. The motions and surface elevations are presented as response amplitude operators and as short term responses. The designs have been studied for separated as well as for interconnected tunnel solutions and the changes this modification results in. A study of the regularity based on the surface elevations for the proposed designs is also included in chapter 4.

In chapter 5 is practical modifications that can be done to the tunnels briefly discussed.

2 WAVE CONDITIONS IN THE SANTOS BASIN

To find an optimal design solution for the problem discussed in this report, it is of interest to map the weather conditions in the area where the HUB is intended to be located, which is in the Santos basin off the coast of Brazil. This is important because it will provide insight to what kind of waves one can expect regarding period, height and direction, as these factors will have a big influence on the design and layout of the hull.

With the development of accurate ocean- atmosphere interaction models such as the NOAA WaveWatch 3 (NWW3) it has become possible to obtain long term time series data from model hindcast (Pianca et al., 2010). Comparison of wave height and direction acquired from the model and observations done over a year along the Brazilian coast, show that the overall wave climate is well represented by the model. Thus, it seems reasonable to assume that the modeled wave data are representative for the wave climate in the studied area.

The wave data acquired for this study is based on an eleven year time series from January 1997 to December 2007. The data are provided at 3-hour intervals, every day over the period in question. Previous information about the wave climate in Brazilian waters has been based on occasional short term observations.

In the report considered (Pianca et al., 2010), the wave climate along the entire coast of Brazil is analyzed. Here will the part of the report that concerns the wave climate in the area of the Santos basin be concerned, as this is the area where the HUB is intended to be located.

The wave regime in the Southeast area (Santos basin) is mostly determined by the South Atlantic High and the passage of synoptic cold fronts (Pianca et al., 2010). The wave data acquired shows that the most energetic waves are from the south and are generated by strong winds associated with the passage of cold fronts. It has also been measured that the waves have the highest energy during the winter months. Wave power has been calculated as: $P = \frac{\rho g^2 H^2 T}{32\pi}$, where ρ is water density, g is the gravitational acceleration, H is the wave height and T is the wave period.

In the Santos basin, the measured data shows that the majority of the incoming waves are coming from the south and east. This is logical due to the fact that the area subject for discussion is shielded by the Brazilian coast to the north and west. Wave size, period and direction are illustrated in figure 2. By consideration of these data, it can be concluded that the main incoming waves are coming from south, southeast, east and northeast. The largest waves have north/north-east directional heading, with a wave height of approximately $6.5m$ and wave period of approximately $14s$.

The maximum design criteria in the Santos basin are for the 100-year return period is: $H_{max} = 20.58m$ and corresponding period $T = 17.90s$. While for the 10- year return period, the design criteria is: $H_{max} = 17m$, and corresponding period $T = 16.18s$ (Petrobras, 2008).

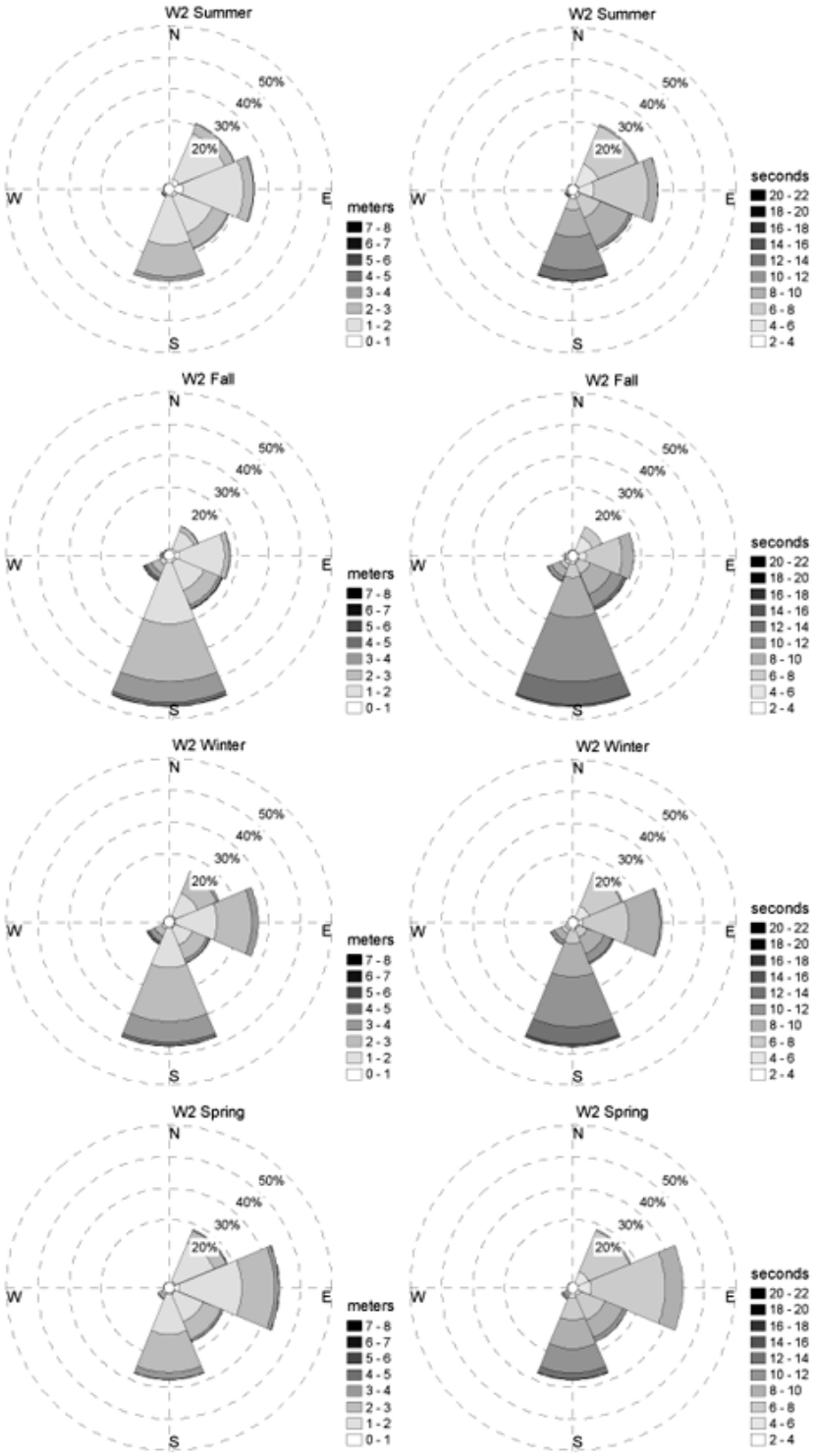

Figure 2 - Wave statistics in the Santos basin

3 DISCUSSION OF TUNNEL EFFECT ON HYDRODYNAMIC RESPONSE

Conventional computer programs used to simulate hydrodynamic effects are relying on mathematical expressions to represent the reality in a simplified way. These mathematical expressions representing the reality are in a varying degree accurate to the real world behavior. Some of the computer programs are based on very complex mathematical expressions that represent the reality in a very exact manner, but these programs usually require large computational time. Other programs are based on more simplified mathematical expressions and thus require shorter computational time. These programs are very applicable for doing computations in several cases, as long as the user is aware of the limitations in the program and the implications these limitations can lead to in the final results.

In this master thesis have HydroD been utilized. HydroD is an interactive application for computation of hydrostatics and stability, wave loads and motion response for ships and offshore structures (DNV). The wave motions are computed by Wadam. Wadam is a general hydrodynamic analysis program for calculating wave-structure interactions for fixed and floating structures of arbitrary shape (DNV). Wadam is based on linear methods for marine hydrodynamics, and neglects the impact from viscous effects. This might be a source of error and it is important to be aware of this when reviewing the results as they might give an unphysical representation of the reality. The results from the Wadam analyze was acquired by Postresp. Postresp is a graphical postprocessor for statistical processing and presentation of response in frequency and time domain (DNV). Postresp does statistical postprocessing of general responses given as transfer functions in the frequency domain or as time series in the time domain.

Before being able to perform hydrodynamic computations for a structure, it was necessary to create a model representing the structure which was done in GeniE. GeniE is a tool for designing and analyzing offshore and maritime structures made up of beams and plates. It is based upon the use of concepts to represent the physical structure and the equipment it supports (DNV).

3.1 Wadam

Wadam stands for Wave Analysis by Diffraction and Morison theory, and some of the analysis capabilities in Wadam that will be used in this master thesis are:

- Calculations of hydrostatic data and inertia properties
- Calculations of global responses including:
    - First and second order wave exciting forces and moments
    - Hydrodynamic added mass
    - First and second order rigid body motion

3.1.1 First computations done for a model with a single tunnel cut out in Wadam

The first model evaluated was a cylinder shaped platform with diameter $\mathrm{D} = 78\mathrm{m}$ in the waterline, a draft equal to $12m$ and with a single entrance solution. This model was constructed first because the geometry was fairly simple which made it easy to model. In addition it was reasonable to expect that this design would give a good indication of what wave pattern one could expect on the inside and in the vicinity of the tunnel.

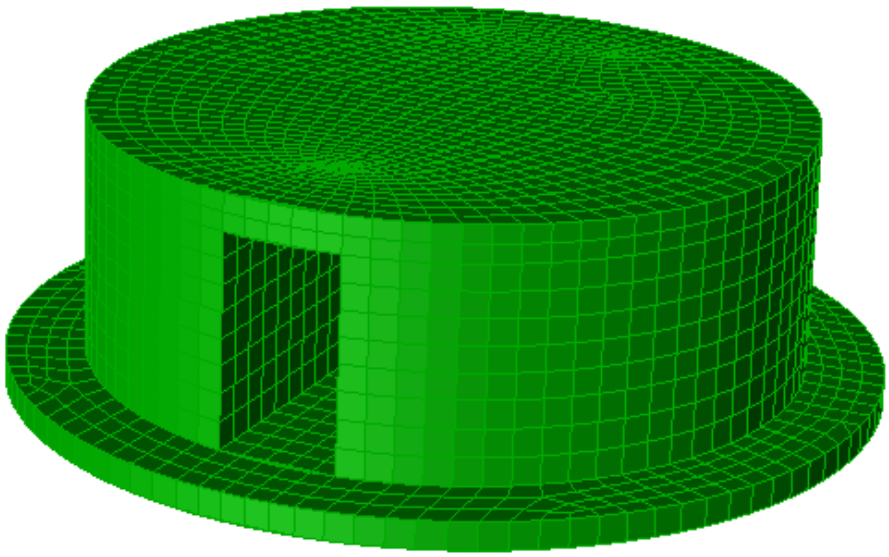

Figure 3 - GeniE model of single tunnel, tunnel length L=35m

For the first model, a platform with a single tunnel cut out with dimensions length $\mathrm{L} = 35\mathrm{m}$, breadth $\mathrm{B} = 13\mathrm{m}$ and height $H = 23m$ was modeled. These dimensions were chosen preliminary because they were concluded to be the required dimensions for entry of a ferry in the summer project prior to this master thesis (Syvertsen et al., 2011). The model was created in GeniE with a mesh-density of $3m$ before it was imported into HydroD as a .FEM file. The mesh density was chosen after experimenting with different values of density, and as it turned out, a mesh size of $3m$ resulted in sufficiently accurately results for the analyses in this thesis without requiring unpractical large computational time. With this mesh density the model consisted of approximately 1500 panels, and the computations took on average approximately 200 seconds.

After performing a computation, the result file created in Wadam was evaluated to ensure that:

- The mass of the displaced volume was equal to the mass of the structure.

- The center of gravity was located in the same x- and y- coordinates as the center of buoyancy so that the model was in balance.
- The three volumes displaced of the panel model $Vol1$, $Vol2$ and $Vol3$ were equal. The three volumes represent the volume calculated by evaluating the elements along the x- y- and z-axis.
- $GM_4 = GM_5 \approx 10m$. This would mainly concern symmetric design, as it is natural that asymmetric designs would result in $GM_4 \neq GM_5$. Desirable metacentric height was achieved by setting the vertical distance between the center of gravity (COG) and the center of buoyancy (COB) to be $20m$. This lead to an unphysical location of the gravity center, but it results in satisfactory GM- values, which was the main aspect of interest in this thesis. The unphysical location of gravity in the model will not be discussed any further in this master thesis.

When these points were checked and satisfied for a model, the motions could be evaluated to check if they behaved as expected by comparison with provided comparison data (Sevan, 2010). To evaluate the motions, the Response Amplitude Operators (RAO) for the model in heave, pitch and roll were considered. The $RAOs$ are used to determine the effect that the incoming wave period would have on the motion of a floating structure. To retrieve the $RAOs$ of a structure, it was assumed that the structure motions are linearly connected to the incoming waves, so that the equation of motion is applicable:

Eq. of motion: $$[M + A(\omega)]\ddot{\eta} + B(\omega)\dot{\eta} + C\eta = F(\omega) \quad \textbf{(3.1)}$$

ω is the oscillatory frequency

M is the structural mass

$A(\omega)$ is the added mass

$B(\omega)$ is the linear damping

C is the restoring force

$F(\omega)$ is the harmonic excitation force proportional to the motion η and the wave height ζ_a.

When this is solved for η, the RAO can be expressed as (Faltinsen, 1998);

$$RAO(\omega) = \frac{\eta}{\zeta_a} = \frac{F_0}{C - \big(M + A(\omega)\big)\omega^2 - iB(\omega)\omega} \quad \textbf{(3.2)}$$

F_0 is the linear excitation force amplitude (on complex form) per wave height.

The plot of the motions for the model in heave, pitch, roll and surge are here presented as response amplitude operators as functions of incoming wave direction and wave period. These can be seen in figure 4, 5, 6 and 7 in the following. In the figures representing the $RAOs$ are the unit on the vertical axis given as m/m for heave and surge and as rad/m for pitch and roll motion;

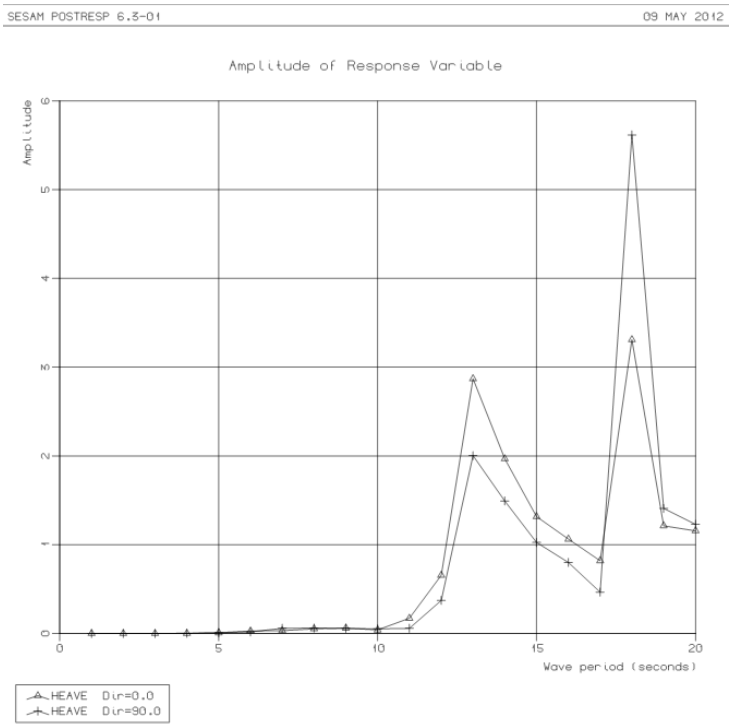

Figure 4 - Heave RAO for tunnel lenght L=35

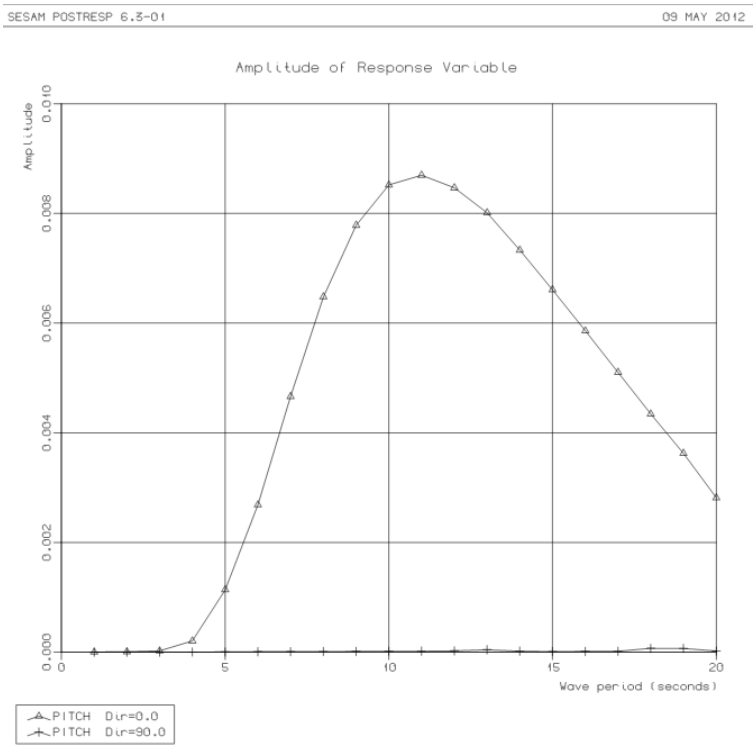

Figure 5 - Pitch RAO for tunnel length L=35m

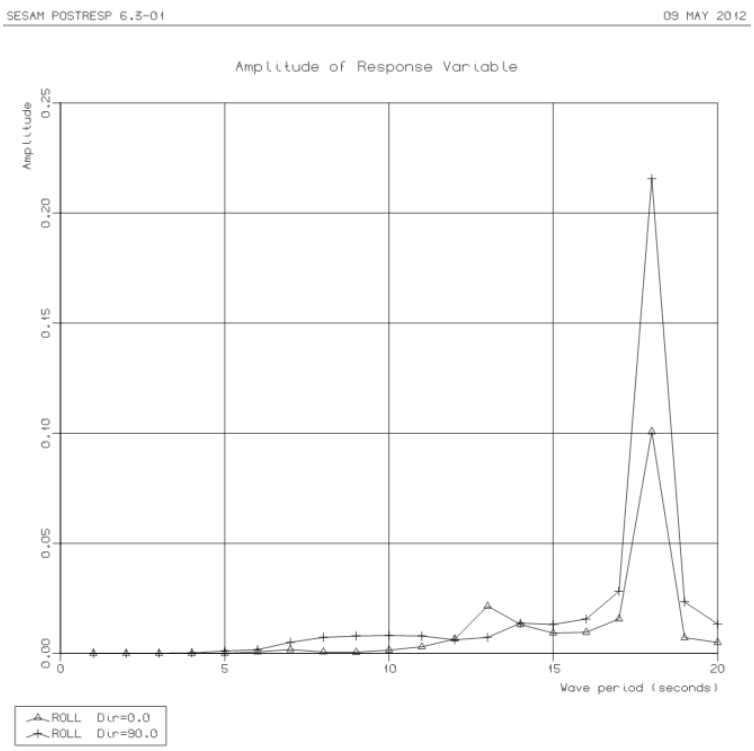

Figure 6 - Roll RAO for tunnel length L=35m

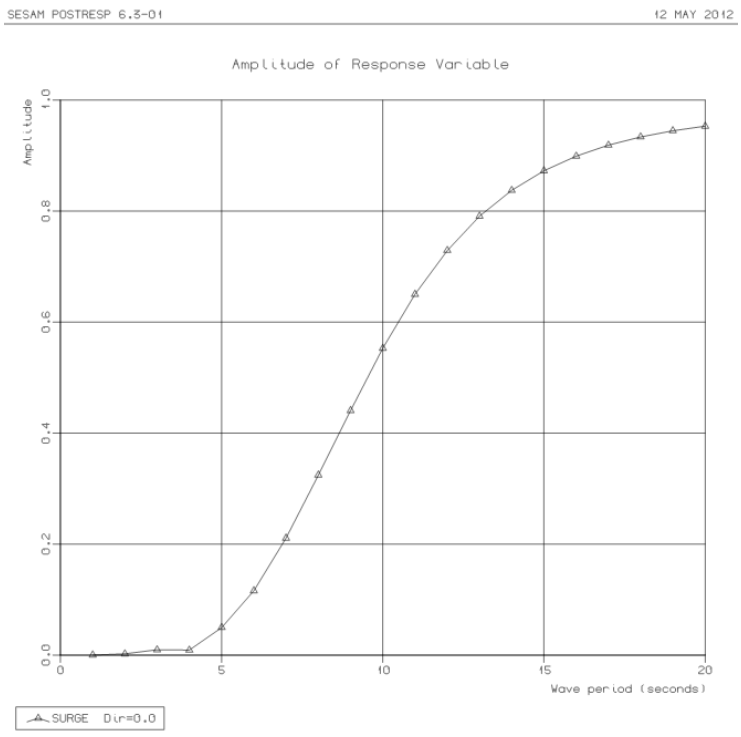

Figure 7 - Surge RAO for tunnel length L=35m

The computation of the heave, pitch and roll $RAOs$ were done for two incoming wave-headings; 0 and 90 degrees, while the surge motion was calculated for incoming wave direction 0 degrees. The incoming wave headings and single tunnel location is defined and illustrated in figure 8 below;

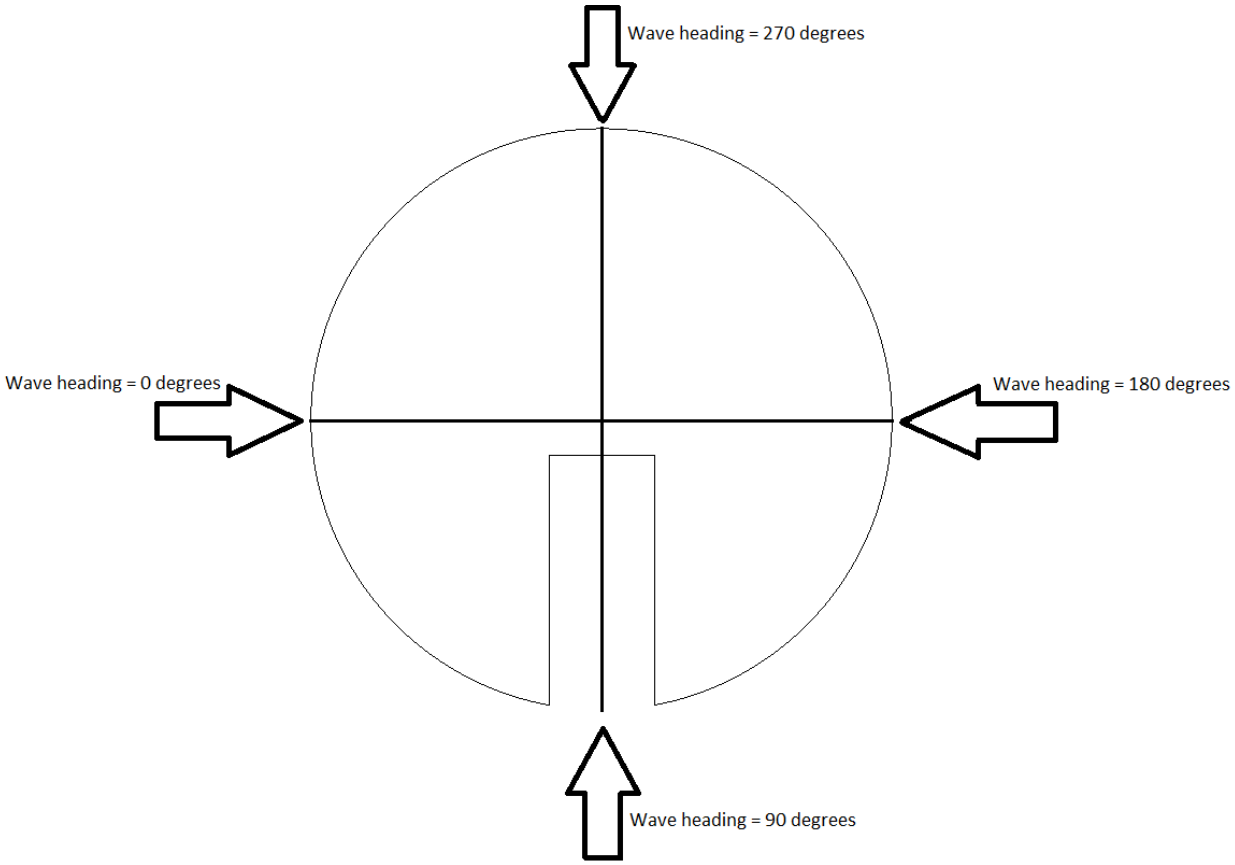

Figure 8 - Wave heading definition

In the plot for the pitch RAO, it was observed that the RAO was equal to zero for wave heading 90 degrees. This was a consequence of the wave direction resulting in pure heave-, sway- and roll- motion. The roll-RAO was somewhat surprising, as it was expected that wave heading 0 degrees would result in zero roll for the model as this heading would lead to pure heave-, surge- and pitch- motion. The plot showed that wave heading 0 degrees gave a roll RAO greater than zero for wave periods greater than 10 seconds. In addition the roll motion took unexpectedly large values for $T > 15s$, which was expected to have similar magnitude and shape as the pitch RAO. These effects were suspected to be a result of the impact the tunnel had on the motion of the platform. It was suspected that the reason the tunnel did not impact the pitch motion to the same degree as it impacted the roll motion was that the tunnel was cut in the transverse direction of the platform. Thus will waves with 0 degrees heading, cause the tunnel to have water flowing in and out of it, causing the platform to have motion in roll. Water flowing in and out of a transversely oriented tunnel will not have any significant impact on the pitch motion.

3.1.2 COMPUTATION FOR A CONCEPT MODEL

When the figure for the heave RAO for the model with tunnel cut out as shown in figure 4 was evaluated, it showed an unexpected two peaked formation where it was expected to have only one. This effect needed to be studied more in detail, and in order to see the impact of the tunnel cut out on the motions more explicitly, a model of a standard Sevan platform with diameter $D = 78m$ was made for comparison. The RAO plots for this concept model can be seen in the following;

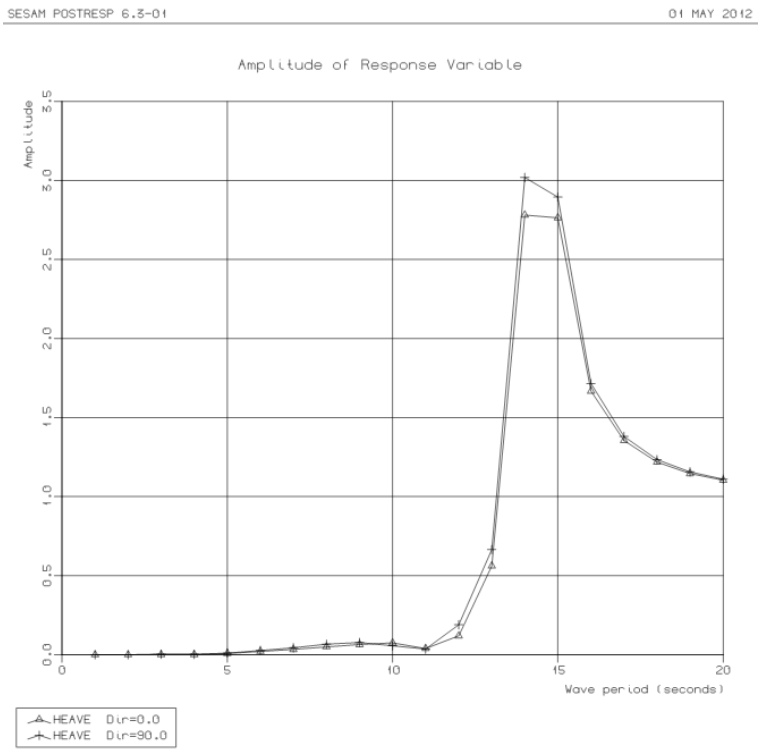

Figure 9 - Heave RAO concept model

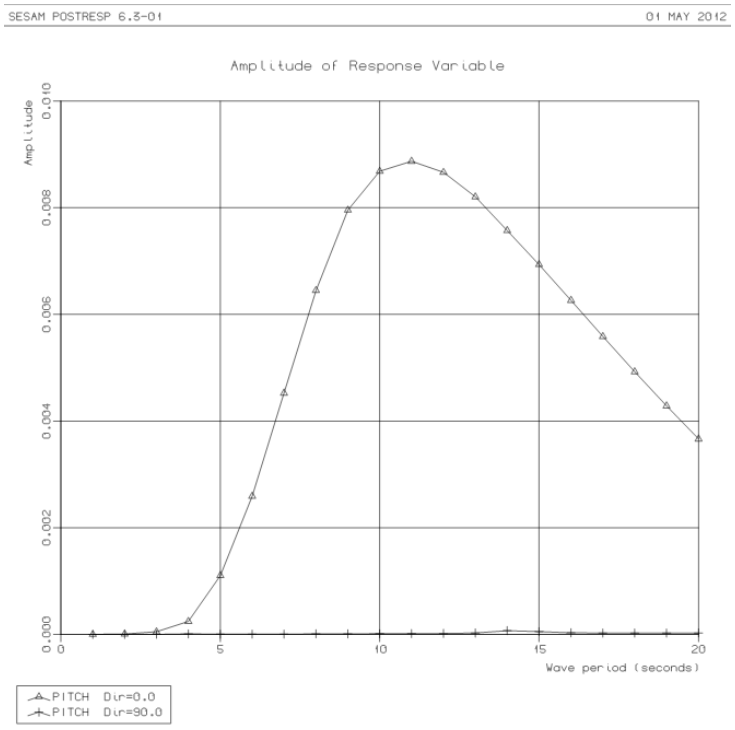

Figure 10 - Pitch RAO concept model

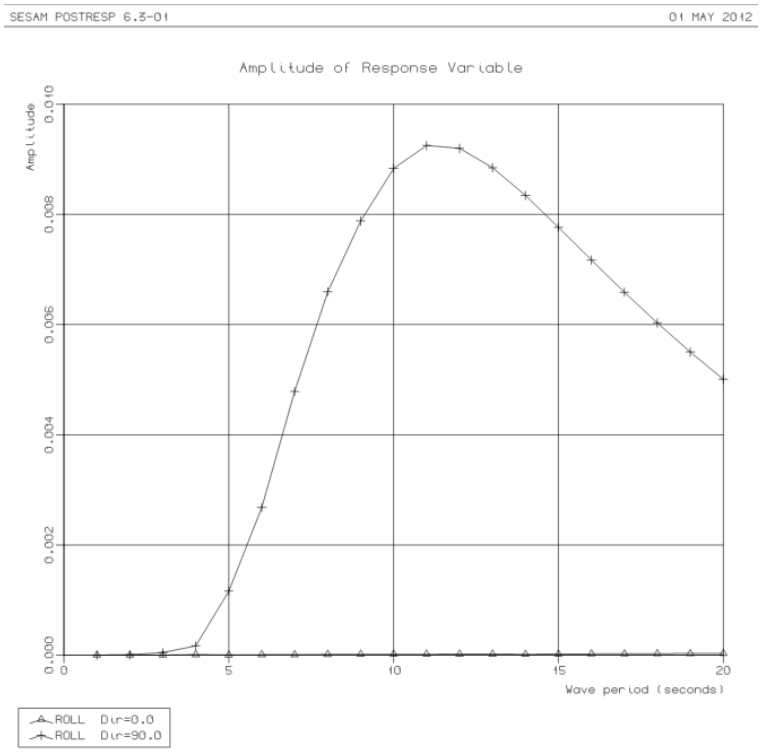

Figure 11 - Roll RAO concept model

As seen in the plots presented for the concept model, the heave-, pitch- and roll- $RAOs$ all behaved as expected when compared to data provided from Sevan Marine for models of similar dimensions (Sevan, 2010). Thus was it reasonable to assume that the somewhat unexpected heave- and roll- $RAOs$ shown in figure 4 and 6 was due to tunnel effects. A further discussion of what can be expected for a tunnel with intact tunnel bottom is presented in the following.

3.2 General discussion of design solutions with intact tunnel bottom

If a design solution for tunnels with intact bottom is evaluated, some distinct effects might occur as each tunnel represents a closed system when the tunnel port is closed. Each tunnel will represent a pool with the port being closed, and platform motion can then result in violent fluid motion. This may result in critical situations during loading or unloading of personnel and is thus important to study further in detail to achieve a brief overview of the situation. This inner fluid motion in the pool will also influence the total motion response of the floater.

3.2.1 Occurrence of a standing wave

A critical situation may occur when a standing wave is created inside the tunnel. This will most likely occur when the wave length inside the tunnel is $\lambda = \frac{L}{2}$, where L is the length of the tunnel. By simplifying and assuming that a wave inside a tunnel can be represented by a regular sinusoidal wave, one can use the dispersion relation for finite water depth according to linear theory to find the critical periods where the occurrence of a standing wave may be critical. For finite water depth;

Dipersion relation:
$$\frac{\omega^2}{g} = k\tanh(kh) \tag{3.3}$$

Where the different variables are defined as:

$$\omega = \frac{2\pi}{T},$$

$$k = \frac{2\pi}{\lambda},$$

h is the depth at mean water level

T is the wave period

λ is the wave length.

Inserting $\lambda = \frac{L}{2}, L = 35m, h = 9m$ and solving for the period T gives:

$$T = \sqrt{\frac{4\pi L}{g \tanh(\frac{\pi h}{L})}} = 8{,}2s \qquad (3.4)$$

Based on this calculation one can expect a violent fluid motion and thus large wave elevations inside the closed tunnel for wave periods in the vicinity of $8{,}2s$. An illustration of the situation calculated here is shown in figure 12;

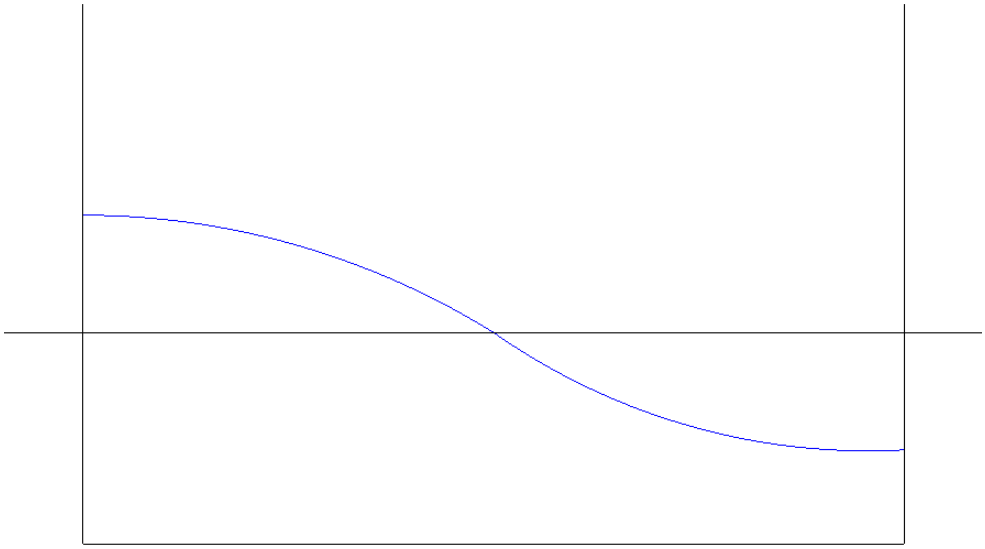

Figure 12 - Standing wave inside a closed tunnel

3.2.2 SLOSHING

Sloshing refers to the surface motion of a liquid inside another object which is typically undergoing motion. When interacting with its container, the free liquid surface can exhibit motion in the form of energy exchange between interacting modes. Modulated free surface occurs when the free liquid surface motion interacts with the container dynamics in the neighborhood of internal resonance conditions. The basic problem of liquid sloshing involves the estimation of hydrodynamic pressure distribution, forces, moments and natural frequencies of the free liquid surface. These parameters have a direct effect on the dynamic stability of moving containers. In general it can be said that the hydrodynamic pressure of liquids in moving, rigid containers has two distinct components; One proportional to the acceleration of the tank and is caused by the fluid moving with the same velocity as the tank. The other component is known as convective pressure and represents the free surface liquid motion according to R. Ibrahim (Ibrahim, 2005).

The motion of a liquid inside a container has an infinite number of natural frequencies, but it is the lowest few modes that are most likely to be excited by the motion of a vehicle/ship. Due to this, most studies done this far have focused on investigating forced harmonic oscillations near the lowest natural frequencies, predicted by the linear equations of the fluid field. However, nonlinear effects result in the frequency of maximum response being slightly different from the linear natural frequency. Nonlinear

effects include amplitude jump, parametric resonance, chaotic liquid surface motion and nonlinear sloshing mode interaction due to the occurrence of internal resonance among the liquid sloshing modes. It is worth noting that nonlinearities associated with free surface motion inside a moving container are different from those nonlinear effects described for water waves in ocean.

Considering linear sloshing dynamics, sloshing phenomena in moving rectangular tanks can usually be described by considering two-dimensional fluid flow if the tank width is much smaller than its length. For this case, the potential function ϕ must satisfy the Laplace equation;

Laplace equation: $$\frac{\partial^2 \phi}{\partial x^2} + \frac{\partial^2 \phi}{\partial z^2} = 0 \qquad \textbf{(3.5)}$$

Solving this for the period T and ignoring the surface tension will result in equation (3.4**)**.

Tanks with two-dimensional flow are divided into tanks for low and high liquid fill depths. The low fill depth case is characterized by the formation of hydraulic jumps and traveling waves for excitation periods around resonance. For higher fill depths, large standing waves are usually formed in the resonance frequency range. When hydraulic jumps or traveling waves are present, extremely high impact pressures can occur on the container walls.

When considering nonlinear theories of forced sloshing in a rectangular tank, these have been developed by Bauer (Bauer, 1965), Verhagen and WijmGaarden (Verhagen and WijnGaarden, 1965), Faltinsen (Faltinsen, 1974), Khosropour (R.Khosropour et al., 1995), Young-Sun and Chung-Bang (Young-Sun and Chung-Bang, 1996), Lukovskii and Timokha (Lukovskii and Timokha, 1999) and Faltinsen and Timokha (Faltinsen and Timokha, 2001). These studies pertain to lateral excitation of the whole tank and the nonlinear effects were manifested as a soft spring characteristic. Linear theory fails to correctly describe the wave response in the vicinity of the cutoff frequencies (the boundary in a system`s frequency response at which energy flowing through the system begins to be reduced rather than passing through). In order to account for the finite wave amplitude that can be observed experimentally at the cutoff frequency, nonlinear effects have to be considered although dissipation can be crucial under certain, specific circumstances.

Three domains of fluid depth-to-length ratio for the two-dimensional, irrotational flow in rectangular containers have been classified according to Dean and Darymple (Dean, 1992) as; finite domain $\frac{h}{L} \geq 0.24$, intermediate $0.1 \leq \frac{h}{L} \leq 0.24$ and shallow $\frac{h}{L} \leq 0.1$. Each domain is characterized by its own resonant behavior. The modifications of the sloshing behavior associated with decreasing depth ratio $\frac{h}{L}$, and increasing excitation amplitude were examined by Faltinsen and Timokha (Faltinsen and Timokha, 2002b), (Faltinsen and Timokha, 2002a). These methods involve Fourier representation of the free-surface wave height and the velocity potential with time-dependent coefficients.

These effects and their implications will have to be evaluated more in detail if a more thorough analyze is going to be done for a tunnel for intact tunnel bottom. In the following the results are presented from computations done for a closed tunnel in HydroD using Wadam.

3.2.3 COMPUTATIONAL RESULTS FOR A SINGLE, CLOSED TUNNEL

Computations have been done in HydroD for a model with a single, closed tunnel with tunnel length $L = 35m$. The elevations inside the tunnel were calculated in point $x = 0$ (representing the center of the tunnel), and $y = -10m$. This was done for incoming wave directions 0 and 270 degrees. The computations can be seen in figure 13 and 14;

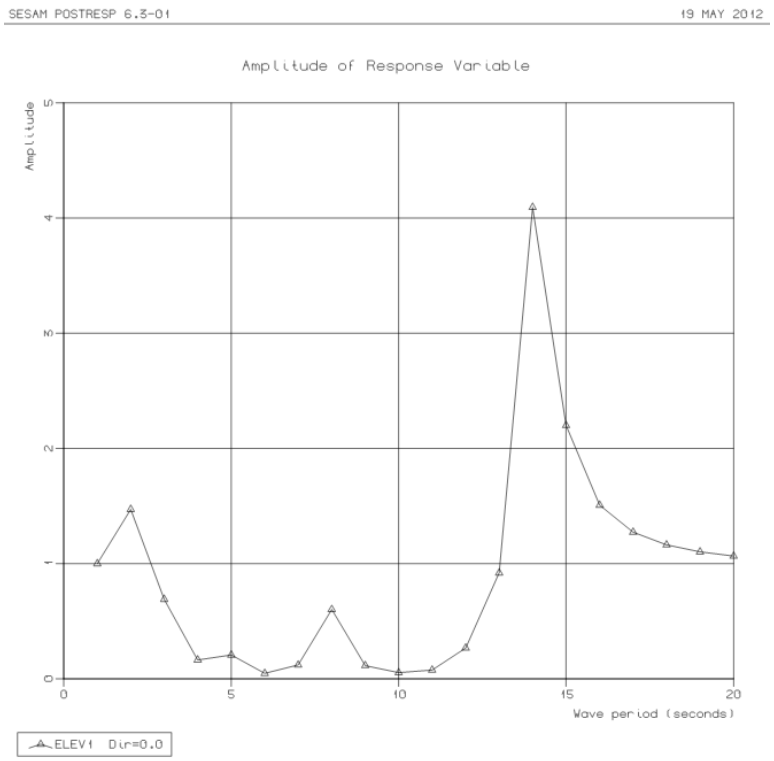

Figure 13 - Elevations inside a closed tunnel of length L=35m for incoming wave direction 0 degrees

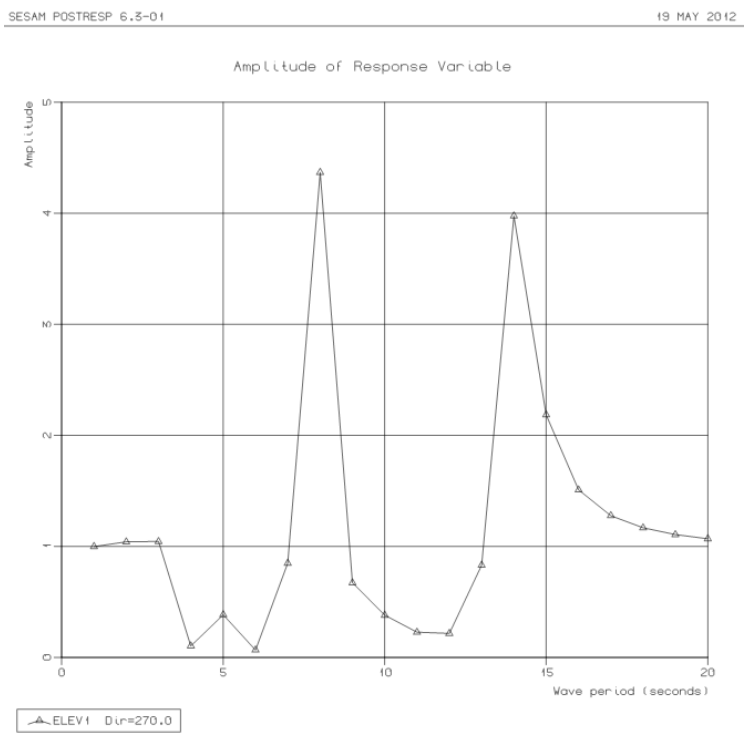

Figure 14 - Elevations inside a closed tunnel of length L=35m for incoming wave direction 270 degrees

As seen in the plot for wave direction equal to 0 degrees in figure 13, the surface elevation inside the tunnel follows the heave motion of the platform as shown in figure 9 fairly close. For incoming wave direction 270 degrees, the surface elevation has two distinct peaks, one peak occurring around wave period $T = 14s$ which is the resonance frequency of the platform in heave. The other resonance period is in the proximity of the period calculated by hand previously $T = 8s$. It is thus reasonable to conclude that this peak in the surface elevation is due to violent wave motions as a result of the occurrence of a standing wave inside the tunnel. The standing wave is a result of the platform`s sway motion of a sufficiently large magnitude to create inner waves of periods approximately equal to 8 seconds.

3.2.4 BASIC EVALUATION OF STRUCTURE MOTION FOR VARYING TUNNEL LENGTHS

To further study the strange heave RAO found in figure 4, several platforms were modeled with tunnel lengths varying from $0 - 78m$ and the $RAOs$ for these geometries were evaluated more closely. It was found that the two-peaked RAO in heave occurred more distinct for tunnels of length ranging for $30m < L < 40m$. For the model with a tunnel cutting through the entire model ($L = 78m$), the heave RAO was of similar shape as for the concept model shown in figure 9. In the following is the heave RAO presented for tunnel length $= 15m,\ L = 30m, L = 35m, L = 37.5m$ and $L = 70m$. $RAOs$ for the heave motion for the rest of the tunnel lengths evaluated can be found in appendix A.

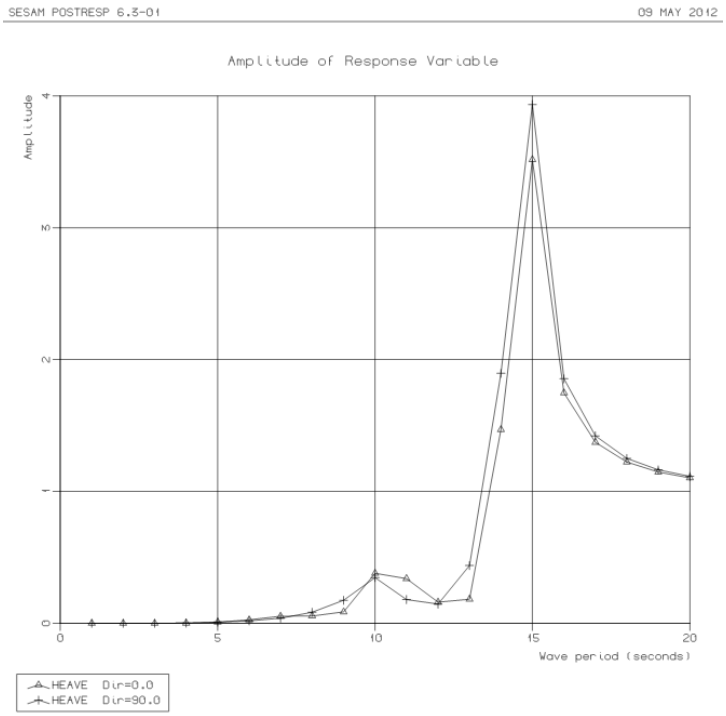

Figure 15 - Heave RAO for tunnel length L=15m

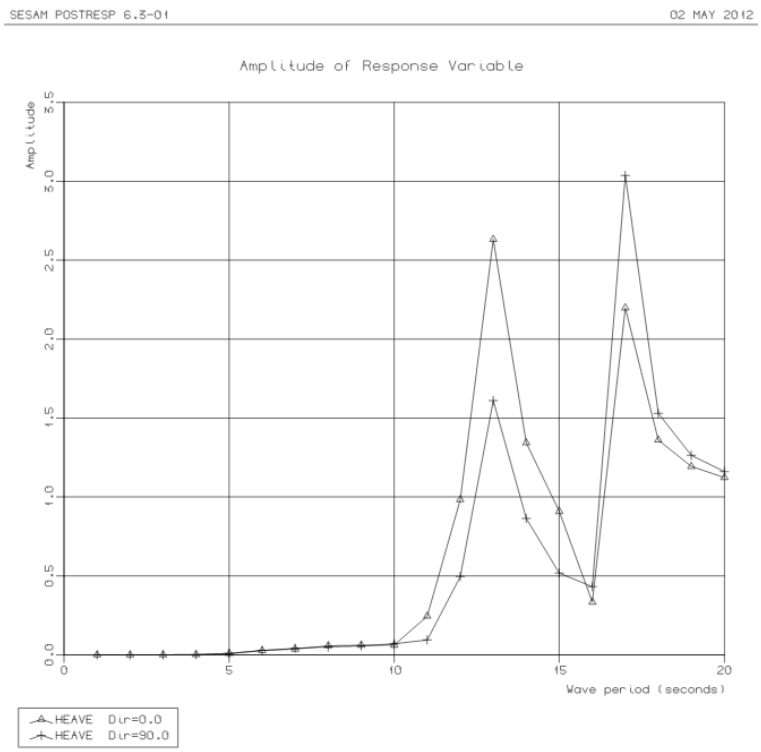

Figure 16 - Heave RAO for tunnel length L=30m

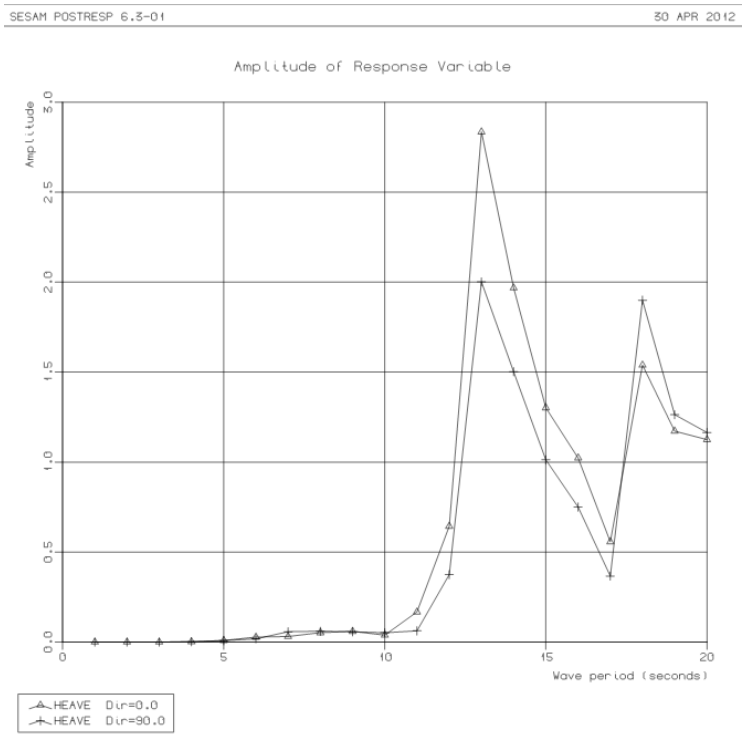

Figure 17 - Heave RAO for tunnel length L=35m

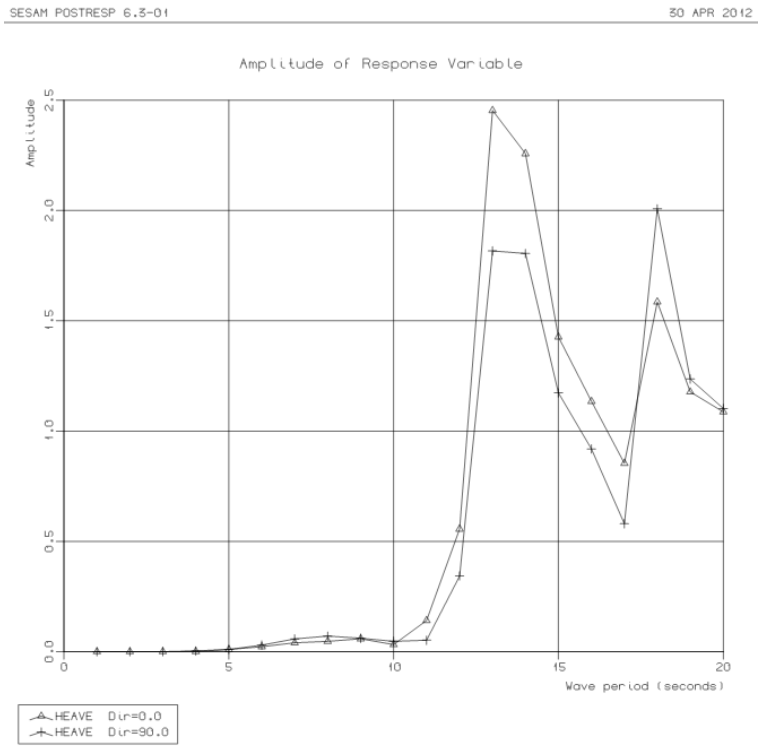

Figure 18 - Heave RAO for tunnel length L=37.5m

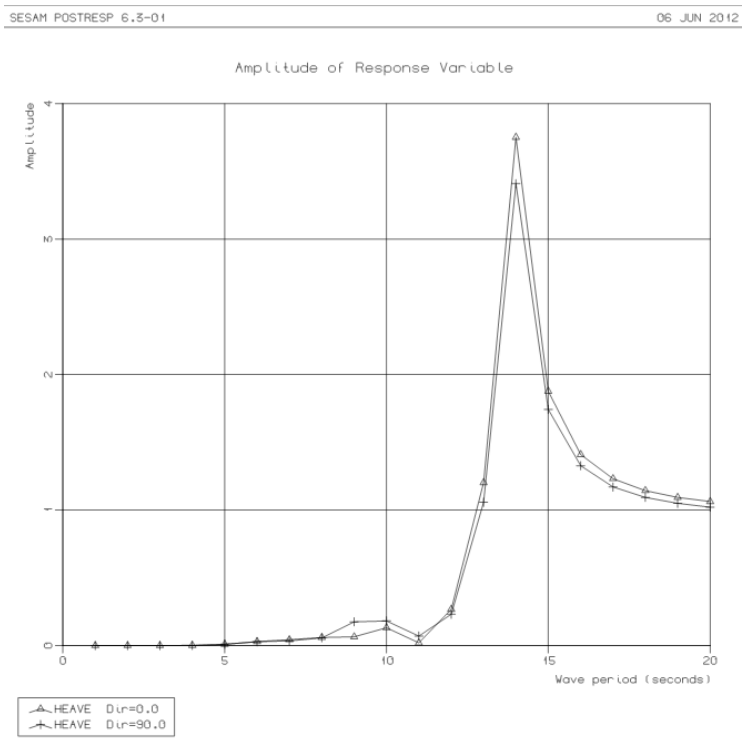

Figure 19 - Heave RAO for tunnel length L=55m

The effect from the tunnel on the heave RAO is seen distinctly as a two-peaked formation in figure 16-18. The reason for the unexpected motion was not clear after evaluating the heave motion for the varying tunnel lengths. To further study the impact the tunnels had on the model`s motion, it had to be done a more closely evaluation of the motion as a function of tunnel lengths.

3.2.5 SHORT TERM RESPONSE FOR TUNNELS WITH INTACT BOTTOM

The short term response is way a presenting the motions of a model based on the response amplitude operators. A very compact way of presentation of the short term response (STR) in irregular waves is to give the significant response amplitude calculated for $H_S = 1m$ as a function of spectral peak period T_P. Due to linearity, the significant response amplitude can then be directly obtained simply by multiplying with the actual H_S value, if a 2 parameter PM spectrum is assumed.

In the following is the short term response for varying tunnel lengths L presented. By default, Postresp presents the significant double amplitude as a function of the zero cross period T_Z. Here is the STR presented as a function of spectral peak period $T_P = 1{,}41 * T_Z$ and the significant amplitude = $\frac{1}{2} *$ significant double amplitude, where the significant double amplitude = 2* the standard deviation of the response, as this is the conventional way to present the results. The short term response in heave, pitch and surge is calculated for wave heading 0 degrees, while the short term response for the sway is calculated for wave heading 270 degrees;

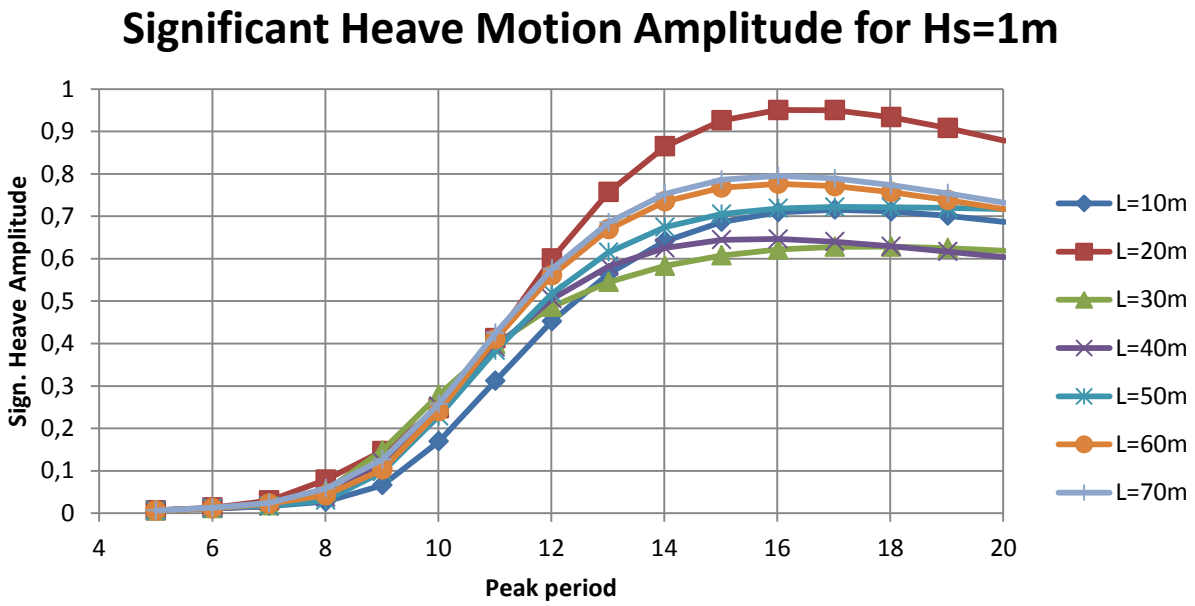

Figure 20 - Short Term Response in heave for varying tunnel length L

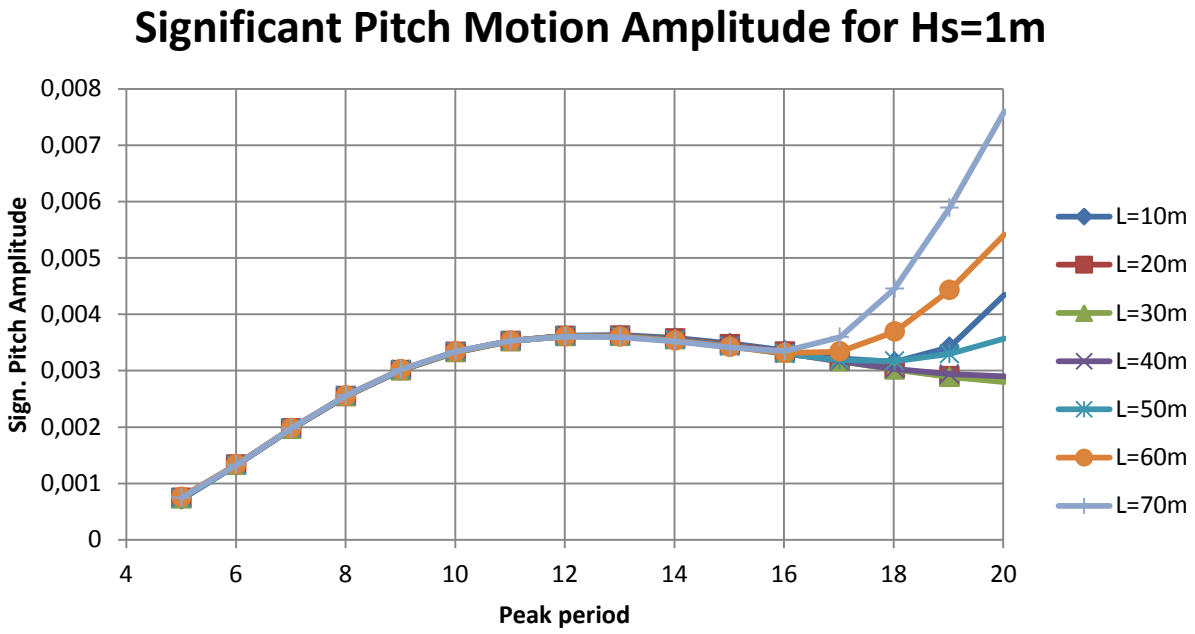

Figure 21 - Short Term Response in pitch for varying tunnel length L

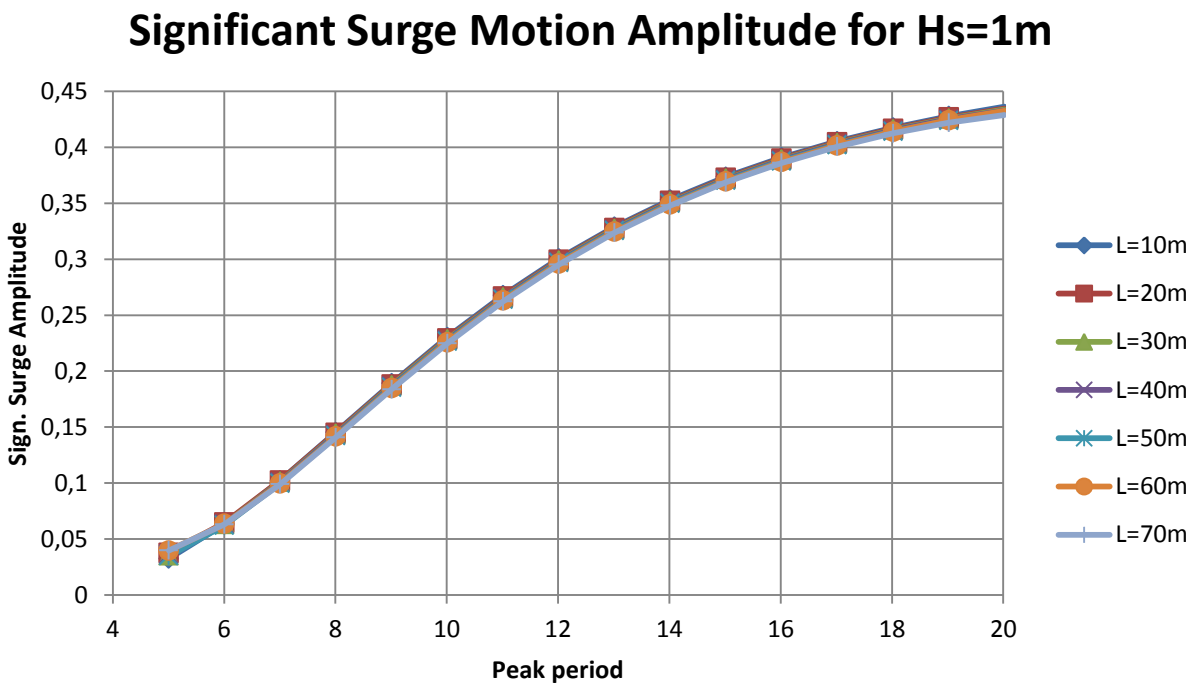

Figure 22 - Short Term Response in surge for varying tunnel length L

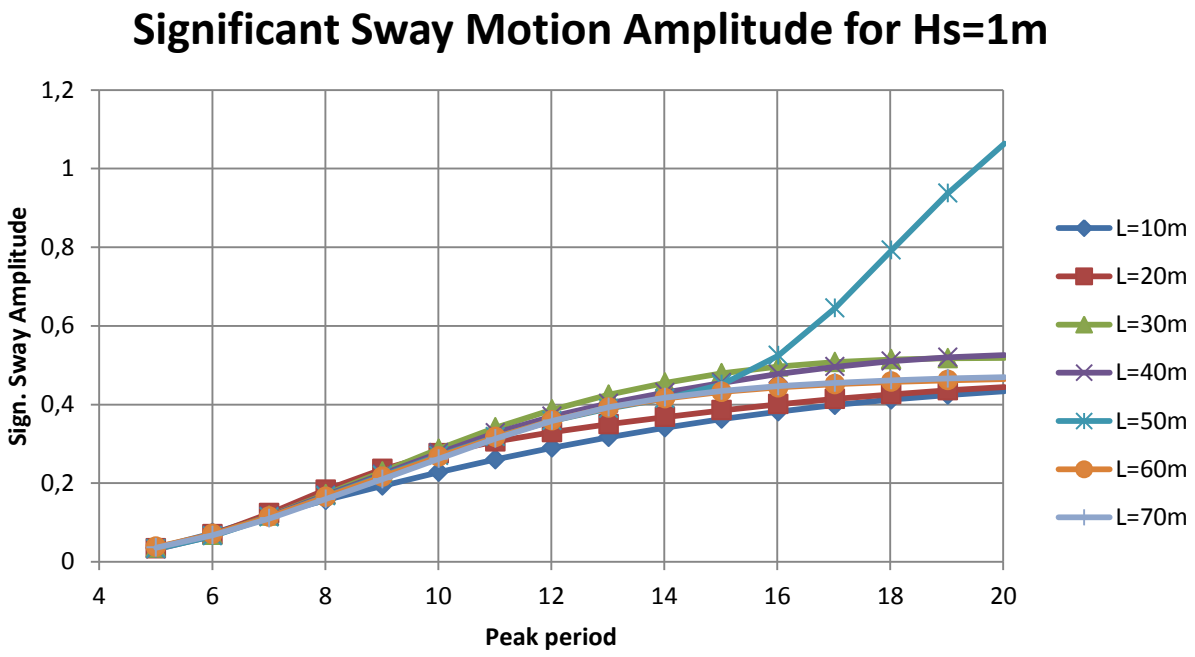

Figure 23 - Short Term Response in sway for varying tunnel length L

As it can be seen from the plots of STR in surge, increasing tunnel length does not have any significant impact on this motion which is logical as the cut is done in the structure`s transverse direction.

For the short term response in pitch, as shown in figure 21, it can be observed that the pitch motion for high periods tend to increase with increasing tunnel length. It is here worth noting that it was observed in the result file computed in Wadam, that as the tunnel length increased, the GM_4 decreased while the GM_5 increased. GM_4 decreased from $6.43m$ for tunnel length $L = 10m$ to $5.55m$ for $L = 70m$, while GM_5 increased from $8.73m$ for $L = 10m$ to $12.13m$ for $L = 70m$. For the computations done for the models with different tunnel lengths the distance from the center of buoyancy to the center of gravity was kept constant equal to $20m$. This was a surprising result, and will be looked further into in the following. The metacentric height for small angles of heel is calculated by;

$$GM = KB + \frac{I}{\nabla} - KG$$

Where KB and KG are held constant. As the tunnel cut out is done, both I and ∇ will change. Considering one fixed tunnel length, the change in volume ∇ will be the same for GM_4 as for GM_5. However, the second moment of area I will change more significantly for GM_4 than it will for GM_5. As ∇ is the same for the two, but I will be smaller oriented about the x-axis (GM_4) than about the y-axis (GM_5), this results in an decreasing GM_4, and increasing GM_5 with increasing tunnel length. The increasing metacentric height in pitch will only be correct as long as the change in the second moment of area is smaller than the change in volume displacement for longer tunnels.

As shown in the plot of STR in sway in figure 23, the model with tunnel length $L = 50m$ is deviating significantly from the other models. It was made several models with this geometry to conclude if it was a modeling error that lead to this deviation. Three models were made with the same geometry and tunnel length $L = 50m$ and all gave the same deviating results for the STR in sway. The contributions from the roll motion should be investigated more in detail to see if the reason for the deviating short term response in sway for $L = 50m$ can be found. The STR in roll is calculated using wave heading equal 270 degrees;

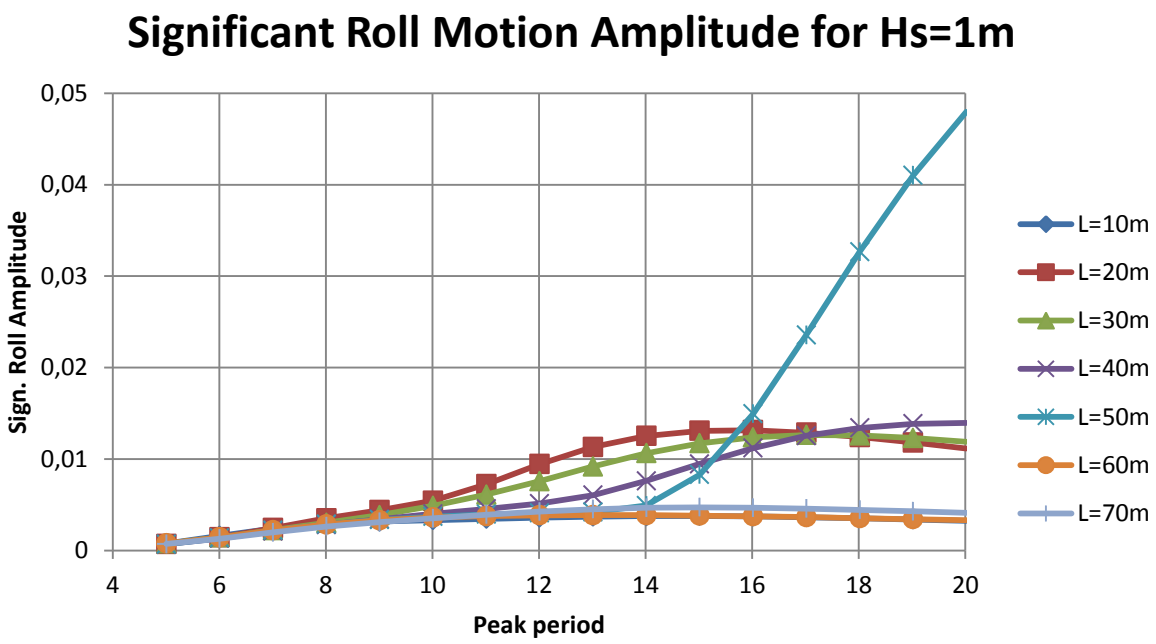

Figure 24 - Short Term Response in roll for varying tunnel length L

As shown in figure 24 above, the short term response in roll for the model with tunnel length $L = 50m$ is deviating significantly from the norm. It is still not clear what causes the large sway STR for models with tunnel length $L = 50m$. But it seems from figure 24 reasonable to conclude that large roll motions contributes to the unphysical behavior in sway, as seen in figure 23.

The most noteworthy about the behavior of the sway STR in figure 23, is that for $L = 50m$ it is increasing for all $T \geq 16s$, but for models with $L \geq 60m$ it follows the normal trend for large wave periods. To look further in detail into this deviation from the norm, 5 models were made with tunnel length L varying between $45m$ and $55m$ with $\Delta L = 2.5m$. The short term response in sway for these models was evaluated, and can be seen in figure 25;

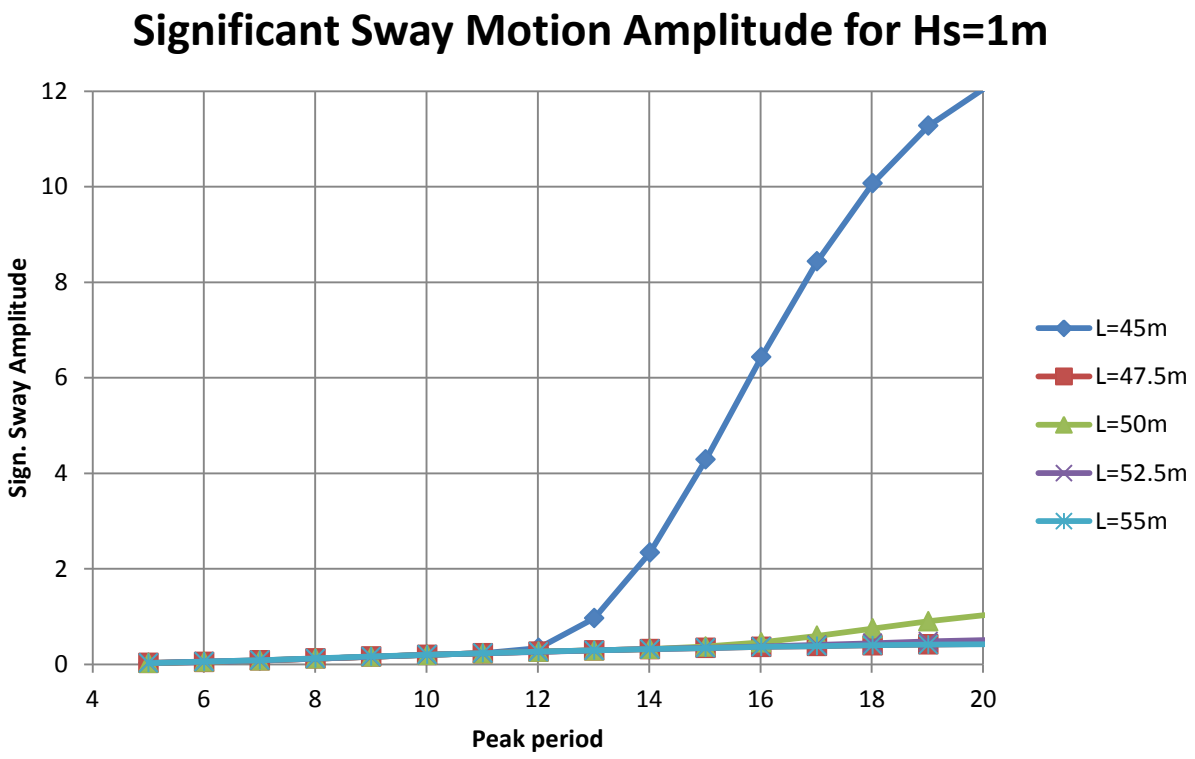

Figure 25 - Short Term Response in sway for 45m<L<55m

As seen in figure 25, the model with tunnel length $L = 50m$ is somewhat deviating compared to $L = 47.5m, L = 52.5m, L = 55m$. However, the STR for the model with tunnel length $L = 45m$ is the biggest deviation from the norm. Figure 25 shows that the short term response for this tunnel length is more than 10 times as large as the STR for the other models. Also here was it made several models with the same geometry and $L = 45m$ to confirm that the deviating result not was a consequence of modeling errors. It is not any clear pattern in the behavior of the STR in sway for the different tunnel lengths and thus it is difficult to conclude with a logical explanation for why the models behave differently.

3.2.6 Detailed evaluation of tunnel impact on structure motion

The next step in investigating the unexpected motions in heave for the models, observed in figure 16-18, was to look further in detail into the different factors influencing the motion of the models. Factors that are known to influence the heave motion is the excitation force F_3 and the added mass A_{33}. The excitation force F_3 was first evaluated to see whether there were any irregularities in these values that could lead to the unexpected heave motion found in figure 16-18. Figure 26 shows the accumulation of the excitation force in heave F_3 for varying tunnel lengths L as a function of incoming wave period $0s < T < 20s$.

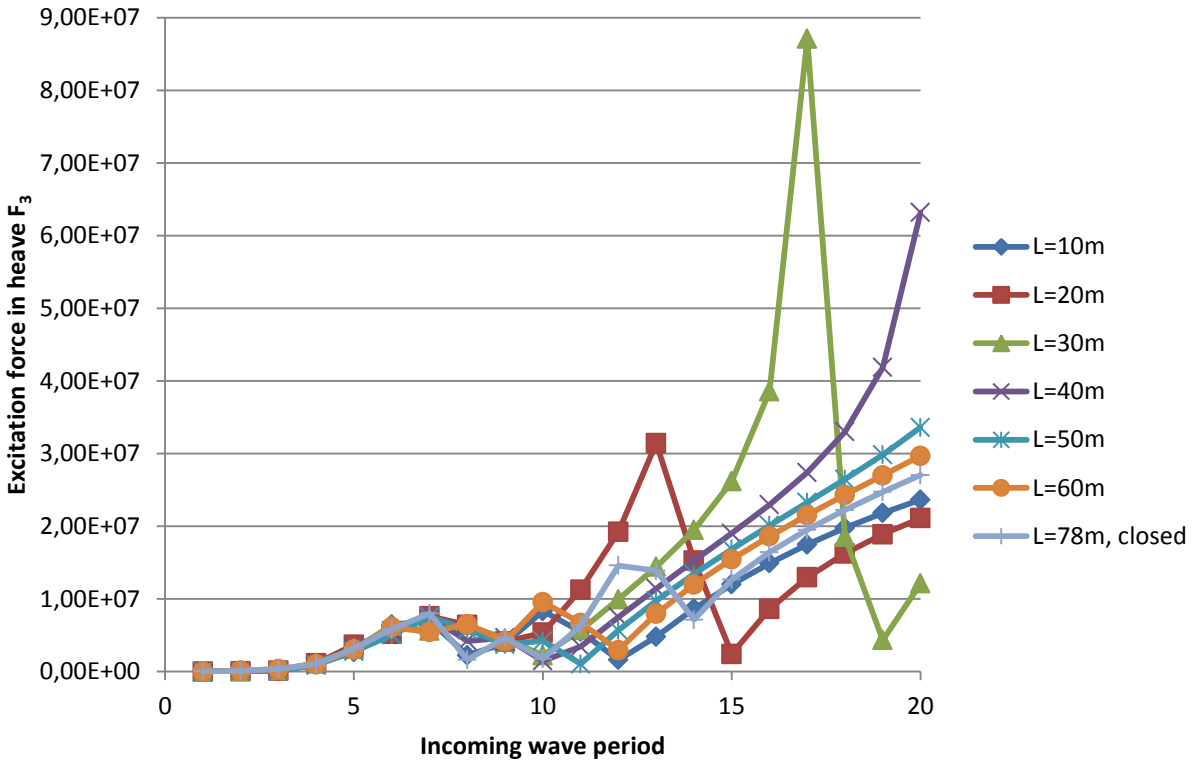

Figure 26 - Excitation force in heave F_3 for models with varying tunnel lengths

When the development of the excitation force in relation to the tunnel length as shown in figure 26 was considered, it was observed that the excitation force achieved very large values for tunnel lengths $20m < L \leq 40m$. To find the reason for this behavior, factors impacting the excitation had to be investigated more in detail. To clearly see the unnatural behavior of the development of the excitation force F_3, comparison of figure 26 was done with the excitation force for the concept model. The plot representing F_3 for the concept model is shown in figure 27;

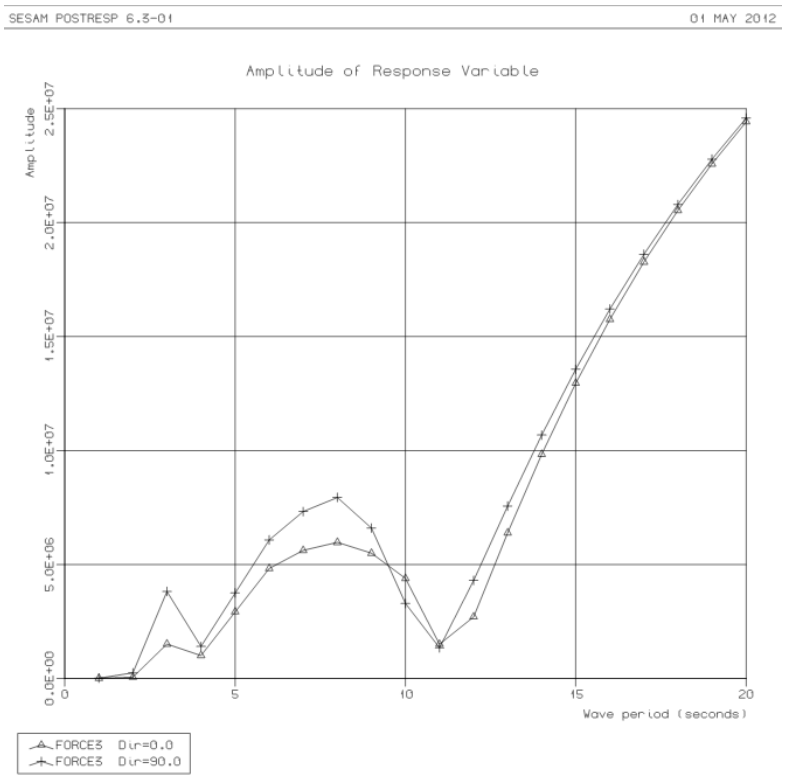

Figure 27 - Excitation force in heave F_3 for the concept model.

The excitation force for the concept model is here observed to be increasing, but not surpassing the value of $2{,}5 * 10^7 N/m$ for wave periods $T \leq 20s$ for the concept model. Expecting an identical shape for the plot of F_3 for models with tunnel cut outs is unrealistic, but a similar shape and magnitude should be expected. When considering figure 26 for the different tunnel lengths, the excitation force has very large values for $L = 20m, L = 30m \; and \; L = 40m$, with amplitudes exceeding $2{,}5 * 10^7 N/m$ significantly. From this comparison the natural conclusion is that either the tunnel`s impact on the heave motion is more significant than what was believed prior to this thesis, or the unexpected large excitation force achieved may be a result of computational or modeling errors.

To look more in detail into what could cause this unexpected behavior, it was natural to evaluate more of the factors impacting the excitation force F_3 in detail. The added mass in heave A_{33} will be evaluated in the following and a plot of A_{33} for tunnel lengths varying between $10m \leq L \leq 78m$ can be seen in figure 28.

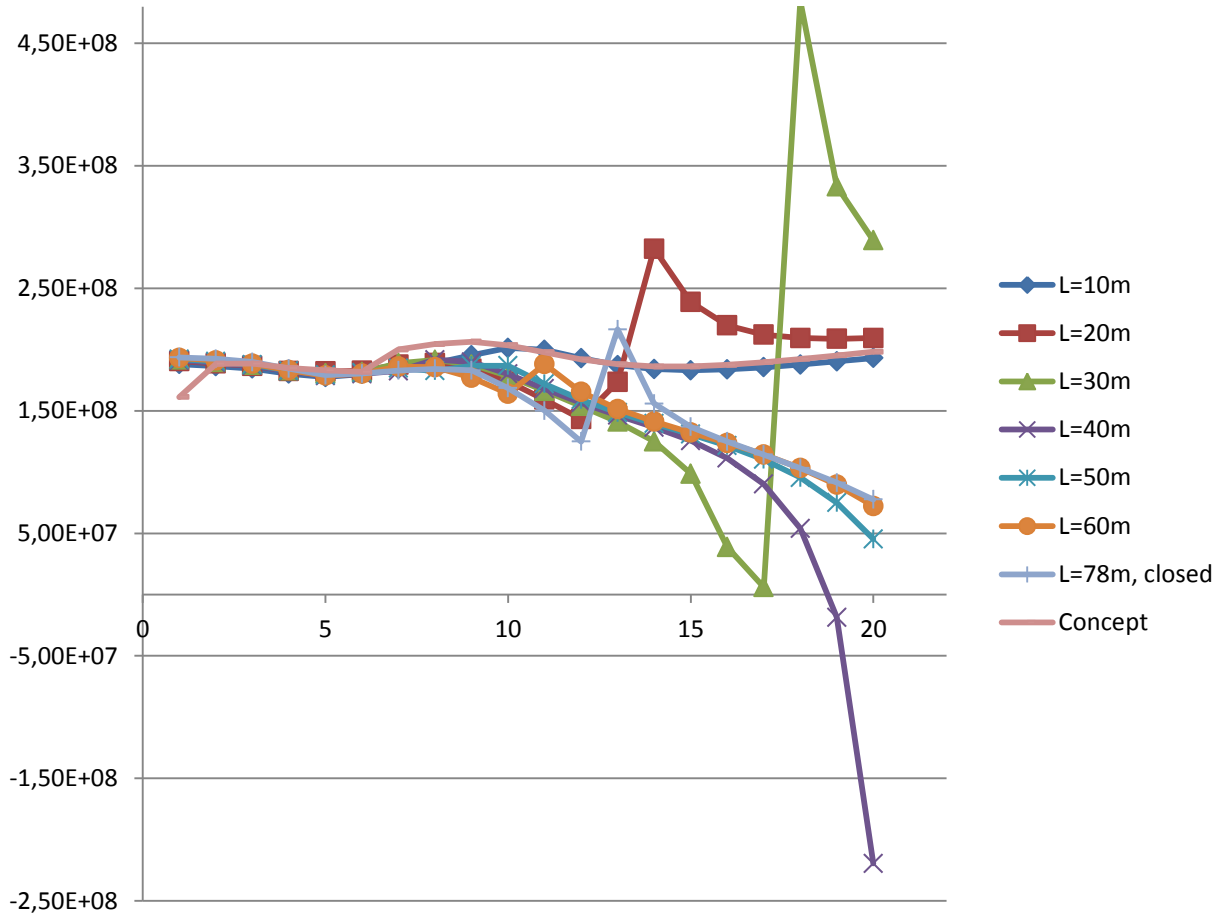

Figure 28 - Added mass A_{33} for models with varying tunnel lengths

This plot shows how the value for the added mass develops for increasing tunnel lengths compared to the added mass for the concept model. As seen in the figure, the added mass gets unrealistic values for tunnel lengths larger that $L \geq 20m$. For these tunnel lengths, the A_{33} is increasing rapidly until tunnel length reaches $L = 40m$, where the added mass starts diverging towards negative infinity. These results are highly unexpected and had to be investigated more in detail to find what factors that could cause these results.

The occurrence of negative added mass is an effect rarely occurring for floating structures of geometries similar to the one considered here, and this effect had to be studied. It was found that for a submerged horizontal cylinder the added mass is negative over a range of frequencies if the depth of submergence is sufficiently small compared to the diameter of a cylinder as mentioned by P.McIver and D.V.Evans (P.McIver and Evans, 1984) according to theory presented by Ogilvie (Ogilvie, 1963). However, it is natural to conclude that this theory not is applicable for describing the negative added mass occurring for the model considered here as the model represents a floating vertical cylinder.

Negative added mass can also be considered as a non-physical effect that occurs for a structure with a geometry which encloses a free surface, similarly to a catamaran (P.McIver and Evans, 1984). The effect

occurs when an incoming wave is directed normally to the longitudinal orientation of the catamaran, and is of such a period and amplitude that it creates a standing wave between the two hulls of the catamaran. When the enclosed standing wave is out of phase with the incoming wave, the effect of negative added mass is observed. The effect occurring is non-physical, but it`s impact on the structure is as if the structure has negative added mass when oscillating. When reviewing this theory in relation to the model presented, one can conclude that the occurrence of a standing wave out of phase inside the tunnel does not explain the strange results acquired for the heave RAO due to two reasons; Firstly, the theory did not explain why the added mass for the models with increasing tunnel length was diverging towards negatively infinity, and secondly; The heave RAO was evaluated for several incoming wave directions and the two-peaked RAO in heave also occurred for wave directions parallel to the tunnel, which excludes the possibility of a standing wave occurring out of phase with the incoming wave.

Considering the facts stated above, and discarding their applicability to the models evaluated in this thesis, it is logical to evaluate if the strange behavior of the added mass might be due to computational errors. To investigate this more in detail, modifications were made on the model to conclude whether it was something wrong with the model geometry that made it incompatible in HydroD. The first modification done was to remove the bottom of the tunnel for a model with tunnel length $L = 35m$. This was done to remove the effect from the tunnel bottom impacting the surface elevation. As the results obtained for the added mass were diverging, it was reasonable to assume that the system had little or no damping. In theory, removing the bottom from the tunnel would allow the energy building up as pressure from increased surface elevations inside the tunnel to leave the system through the bottom. This leads energy away from the system, adds damping, and will in theory limit the forces and motions impacting the structure. The total damping of a system is a combination of viscous damping B_v and potential damping B_{POT} and can be described as $B = B_v + B_{POT}$. Since viscous effects are neglected in these computations, this implies that the viscous damping B_v is equal to zero. For a tunnel with intact bottom, the potential damping B_{POT} is small as the only way for waves to propagate and thus transport energy away from the system is through the relatively small entrance. When both the viscous and potential damping is so small it can be neglected, the system has no damping and the calculations collapses leading to diverging results.

The added mass A_{33} for a model with tunnel length $L = 35m$ without tunnel bottom can be viewed in figure 29;

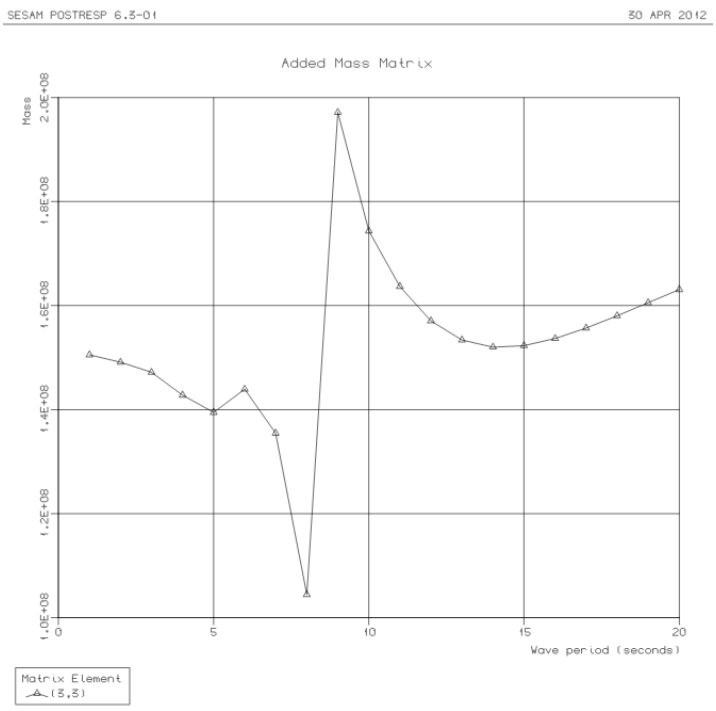

Figure 29 - Added mass A_{33} for tunnel length L=35m, without bottom.

This added mass is of a similar magnitude as that of the concept model, implying that the modifications made to the model by removing the tunnel bottom has successfully added damping to the system. This is an indication that the plot of the excitation force $F_3$for the model with tunnel length $L = 35m$ might be more similar to the excitation force of the concept model. $F_3$for the model with tunnel length $L = 35m$ without tunnel bottom can be seen in figure 30:

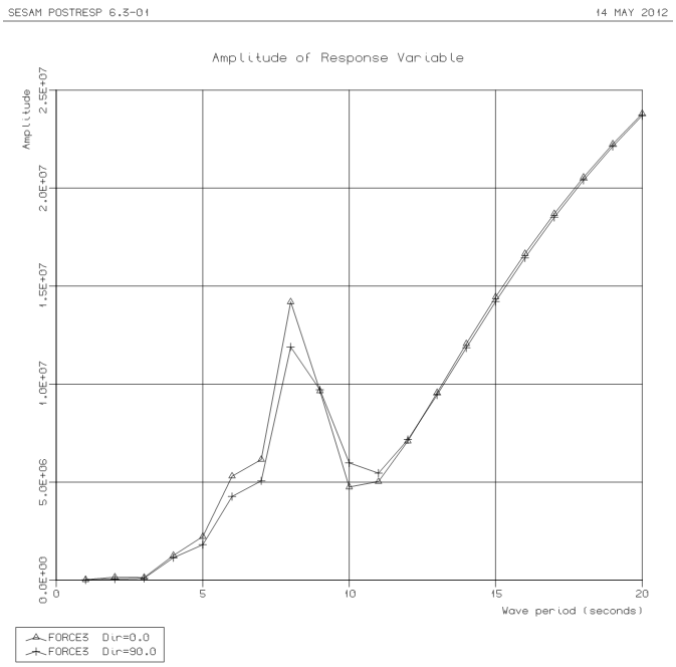

Figure 30 - Excitation force F_3 for tunnel length L=35m, without bottom.

This figure shows that the excitation force $F_3$for a model with tunnel length $L = 35m$ without tunnel bottom has a similar shape and magnitude as the excitation force for the concept model. The excitation force now has a similar peak at periods $T \approx 8s$ and does not surpass the maximum value of $2{,}5 * 10^7 N/m$ which was observed for the concept model in figure 27. From this it is reasonable to expect that the model without tunnel bottom also has a normal, one peaked heave RAO since the irregularities in added mass and excitation force are reduced significantly. The RAO for the heave motion of the model without tunnel bottom can be seen in figure 31:

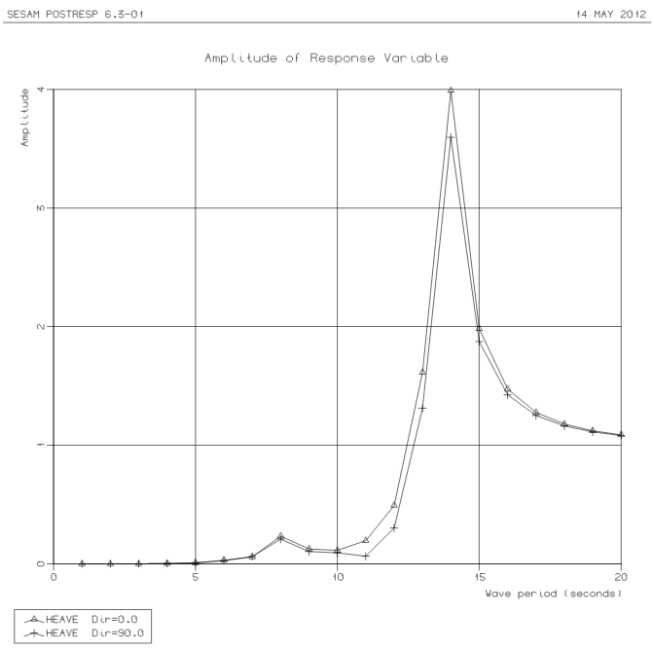

Figure 31 – Heave RAO for tunnel length L=35m, without tunnel bottom.

By evaluation of figure 29-31 and comparing them with the figures for the added mass, excitation force and heave RAO for the concept model and model with intact tunnel bottom, it can be concluded that the calculations in Wadam collapses when applied to models with tunnel cut outs and intact bottoms. Wadam is based on linear methods and neglects viscous effects, and from this it is reasonable to suspect that the viscous effects for the models with intact tunnel bottoms are large, making Wadam unable to perform successful computations. Since the model without tunnel bottom has one peak for the heave RAO, it is logical to conclude that the viscous effects are significantly reduced, making Wadam able to perform the computations successfully. All models evaluated from here on in this master thesis, have been constructed without bottom in the tunnels.

To understand more of why the computations collapse for models with tunnel bottoms, further theory of viscous effects are presented here;

3.2.7 VISCOUS EFFECTS

The theory presented here is mainly applicable for flow around a fully submerged cylinder, but it describes the general aspects of viscous forces, helping to clarify the implications of neglecting viscous effects.

In general there are three basic differential equations describing the motion of a fluid according to Frank M. White (White, 2008);

Continuity: $$\frac{\partial \rho}{\partial t} + \nabla(\rho \boldsymbol{V}) = 0 \qquad \textbf{(3.6)}$$

Momentum: $$\rho \frac{d\boldsymbol{V}}{dt} = \rho \boldsymbol{g} - \nabla p + \nabla \cdot \tau_{ij} \quad \textbf{(3.7)}$$

Energy: $$\rho \frac{d\hat{u}}{dt} + p(\nabla \cdot \boldsymbol{V}) = \nabla \cdot (k \nabla T) + \phi \quad \textbf{(3.8)}$$

Flow with constant ρ, μ and k is a basic simplification often used for small variations in time and space, and this simplifies the equations of fluid motion 3.6-3.8 to:

$$\nabla \cdot \boldsymbol{V} = 0 \quad \textbf{(3.9)}$$

$$\rho \frac{d\boldsymbol{V}}{dt} = \rho \boldsymbol{g} - \nabla p + \mu \nabla^2 \boldsymbol{V} \quad \textbf{(3.10)}$$

$$\rho c_p \frac{dT}{dt} = k \nabla^2 T + \phi \quad \textbf{(3.11)}$$

When assuming an inviscid flow, we indicate that the inertial forces are much more significant than the viscous (friction) forces. This approximation neglects viscosity completely compared to inertial terms, resulting in the equation of momentum being reduced to the Euler`s equation:

Euler`s equation: $$\rho \frac{d\boldsymbol{V}}{dt} = \rho \boldsymbol{g} - \nabla p \quad \textbf{(3.12)}$$

It is known that viscous effects play a small role throughout most of the flowfield when considering flow past thin, streamlined bodies. This is because the Reynolds number $Re = \frac{\rho UL}{\mu}$ is very large for all practical flow problems. The large value of Re is a consequence of the fact that $\mu \ll \rho UL$ for fluids such as air and water. The reciprocal of the Reynolds number multiplies the viscous terms in the equation of motion when we include friction, which explains why viscous effects often can be neglected. However, ignoring viscous effects completely will be a source of error because they give rise to nontrivial drag forces that is absent in theory of inviscid fluids. Additionally, because of frictional effects, flows subjected to increasing pressure behave quite differently from the predictions of inviscid theory. Flow past a cylinder, is for example very complicated due to viscous effects, and over the rear half of the cylinder it bears little relation to the potential flow solution.

Further computer analyzes in this thesis are based on platform models without tunnel bottoms. Different geometrical design solutions for the tunnel orientations have been evaluated with intention of achieving as small wave elevation inside the tunnel as possible.

4 COMPUTATIONAL EVALUATION OF DIFFERENT DESIGN SOLUTIONS

To evaluate the free surface elevation inside a tunnel, the coordinates with the largest vertical motion on the free surface were located. These were located by evaluating a single tunnel design, with tunnel length $L = 35m$ without tunnel bottom according to previously conclusions made in chapter 3. To locate these coordinates, computations were done for incoming wave direction 270 degrees and different points on the free surface were defined from $y = -5m$ (which is located close to the inner tunnel wall) and out to $y = -40m$ which is located on the immediate outside of the tunnel. All the evaluated coordinates were located along the $x = 0$ axis which is the center of the tunnel. From these computations, it was possible to find that the largest surface motion, represented by the response amplitude operator, inside the tunnel was located close to the inner tunnel wall ($-10m < y < -5m$). The plot of these $RAOs$ can be found in appendix B**.** The vertical motion did not differ much between these coordinates, but the elevations measured at $y = -10m$ were slightly higher than the rest. In the following analyses it has been chosen to evaluate the surface elevation at this point to represent the general wave pattern inside the tunnel.

To find an optimal design for the platform it was necessary to determine the incoming wave directions that would result in the smallest surface elevations inside the tunnel. This was an important factor due to the fact that the wave directions causing small surface motions would represent the desired working conditions, impacting the operational uptime for the platform. To find the optimal incoming wave headings, computations were done for a single tunnel entrance for incoming wave headings ranging from $0 - 270$ degrees relative to a general coordinate system and the tunnel being installed in the transverse direction as shown in figure 8. The elevation inside the tunnel was evaluated at $x = 0$, $y = -10m$ as previously concluded, and the explicit results can be found in appendix C. As expected, the results showed that the largest surface elevations inside the tunnel would occur for incoming wave heading equal to 90 degrees as this heading was directly into the tunnel. Incoming wave headings between $0 - 180$ degrees created in general large elevations and are for this reason dismissed as desired working conditions. Further analyses showed that headings in the range of $210 - 240$ degrees resulted in the smallest surface elevation with a maximum $RAO \approx$, and these results were embedded in design #3 and #4 evaluated in the following chapters. These wave headings results in the same surface elevations as waves with heading in the range $300 - 330$ degrees due to symmetry about the y-axis. The computations revealed that a wave heading of 230 degrees gave the smallest surface elevations, and the RAO retrieved here was approximately equal to 1 for all periods up to $T \approx 13s$. From the retrieved results it was defined an incoming wave heading window that would result in the desired working conditions of $RAO \leq 2$.

After having defined the acceptable working conditions, the next logical step was to create designs that had desirable operating conditions as often as possible to achieve an operational uptime as high as possible.

In the following is several design solutions proposed and evaluated. Some of these are solutions that were proposed in the summer project, and needed to be evaluated more in detail, while some are solutions designed to fulfill the criteria of desired incoming wave directions as defined above.

4.1 Outline of Proposed designs

In this master thesis have 4 design solutions been proposed and evaluated as possible designs for a platform with tunnels for ferry entry. Some of the designs were proposed in the summer project during the summer 2011, but were not evaluated in detail and are therefore included here. The designs of interest that will be evaluated are shown in the following;

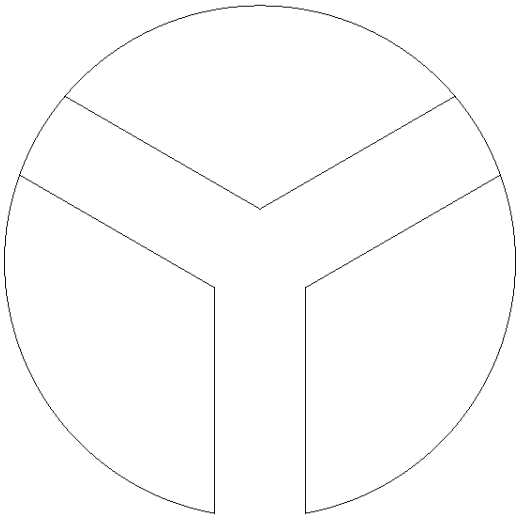

Figure 32 – Proposed design #1

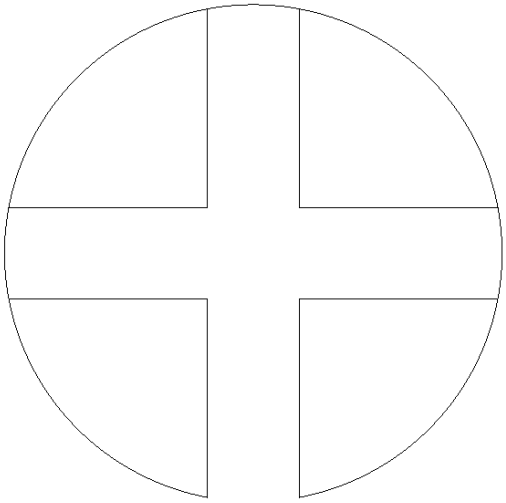

Figure 33 - Proposed design #2

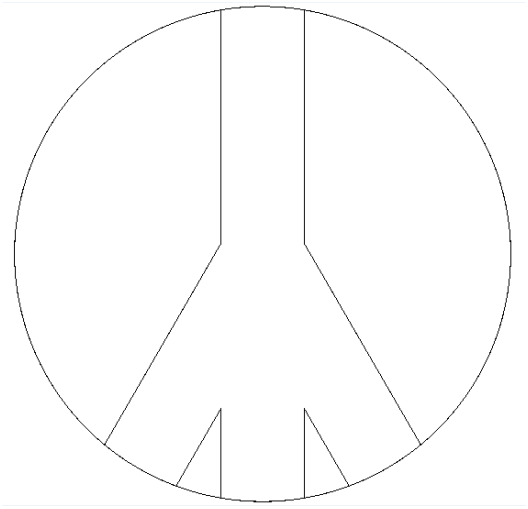

Figure 34 - Proposed design #3

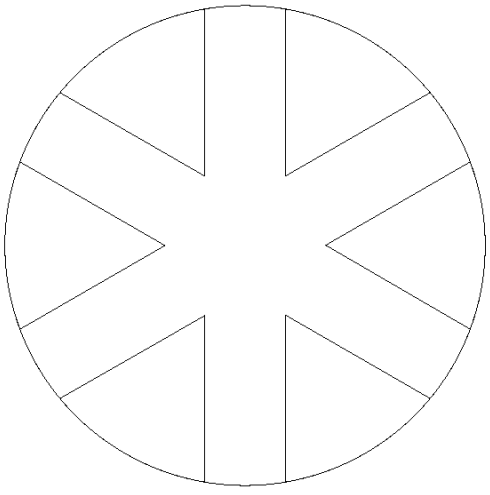

Figure 35 - Proposed design #4

All the 4 designs evaluated here have the following main parameters;

Parameter	Unit	Dimensions
Diameter	m	78
Draft	m	12
Freeboard	m	18
Tunnel breadth	m	13
Distance COB->COG	m	20

Table 2 - Main parameters of proposed design

4.2 Wave condition in the Santos basin

An essential part that needs to be evaluated more in detail before proposing design solutions is the wave statistics in the area where the platform is intended to be located at. These wave statistics are presented graphically in figure 2. The statistics with heading probability of the wave direction is presented in the following histogram;

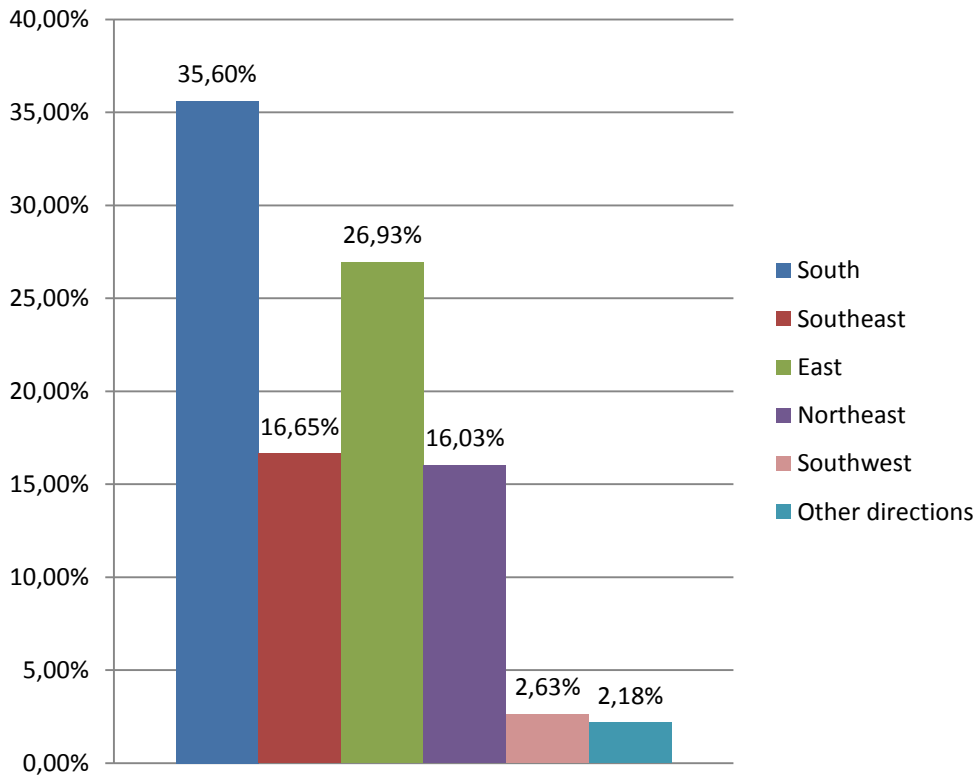

Figure 36 - Percentage average distribution of where the incoming waves are coming from in the Santos basin

When considering the wave statistics in the Santos basin, as presented in figure 2 and 36, it is fair to conclude that most of the waves are coming from directions southwest to northeast. When considering

these statistics into the creation of the platform design, the most important factor to include is to assure that waves incoming from the southwest, south, southeast, east and northeast are reduced the most inside the tunnel used for ferry entry. The waves coming from the north, northwest and west will be of small numbers and magnitudes, and they will result in less dramatic surface elevation inside the tunnel.

It is important to emphasize that the response amplitude operators presented for each design is plotted as a function of the incoming wave heading relevant during ferry entry for the specific design evaluated.

4.3 Proposed design solution #1

In the summer project that this master thesis is a continuation of, a three way entry design was evaluated. The tunnels were evenly distributed over the platform and thus shifted 120 degrees relative to each other. This design was proposed without any detailed wave data accessible, but it was assumed that it would be desirable for a ferry to be able to enter through a tunnel that was located on the leeward side of the platform. The design considered here would result in a modular platform that would be fairly easy to construct, and it was believed that it would result in satisfactory surface elevations inside the tunnels as well. Since the design only has 3 tunnels, it leads to the platform having a large volume displacement and thus being able to carry a large weight compared to designs with a larger number of tunnels.

In the summer project were computations done in HydroD for this design which showed that the design would give satisfactory small surface elevations inside the tunnel. However, the response of the platform retrieved from this computation had the same unphysical behavior regarding the heave motion as those found in chapter 3.1 and discussed further in chapter 3.2. The reason for this behavior was not found in the summer project and the model was manipulated with fictive damping until desirable transfer functions were achieved. This has most likely been a source of error in the results retrieved in the summer project and therefore it was natural to do these computations over again in this master thesis. It is also worth mentioning that the model evaluated in the summer project had tunnels with intact bottoms, which are removed in this master thesis to compensate for the unphysical behavior of the added mass in heave as discussed in chapter 3.2.

The design evaluated is shown in the following:

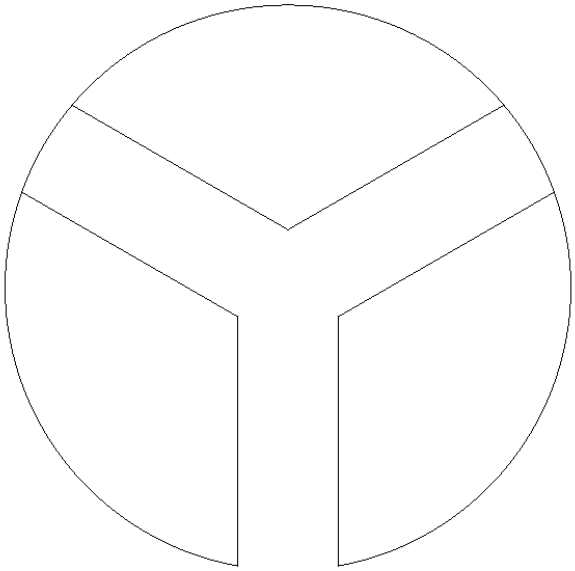

Figure 37 - Proposed design solution #1

Which tunnel an incoming ferry is intended to enter through for this design for different wave headings is shown in figure 38 and described in the following. The wave headings are oriented relative to a general orientation, with origo located in the center of the platform, according to figure 8.

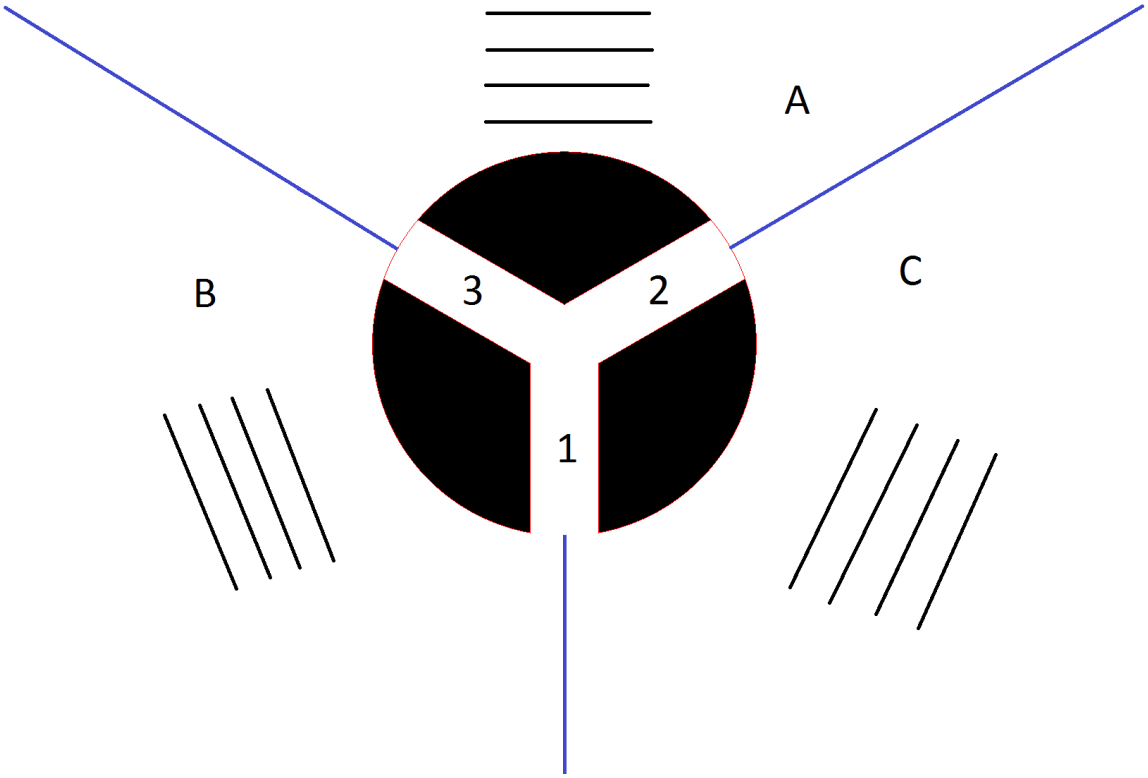

Figure 38 - Relation between incoming wave direction and desired tunnel for ferry entry for design solution #1

1. When waves are incoming from directions within A (with $210 - 330$ degrees wave heading), the smallest surface elevation will occur inside tunnel 1, making this the desired tunnel used for ferry entry.
2. For waves incoming from directions within B (with $330 - 90$ degrees wave heading), the smallest surface elevation will occur inside tunnel 2.
3. For waves incoming from directions within C (with$90 - 210$ and degrees wave heading), the smallest surface elevations will occur inside tunnel 3.

For evaluation of the motions for this design, the computations were done for incoming wave heading $210 - 270$, as these are limited by the number of tunnels and the spreading of these. Note that the computations could have been done for wave directions $210 - 330$ degrees, but that these directions are reduced to half due to symmetry about the y-axis.

The $RAOs$ for the motion in heave, pitch and roll for the platform is presented in the following figures for incoming wave heading $210 - 270$ degrees;

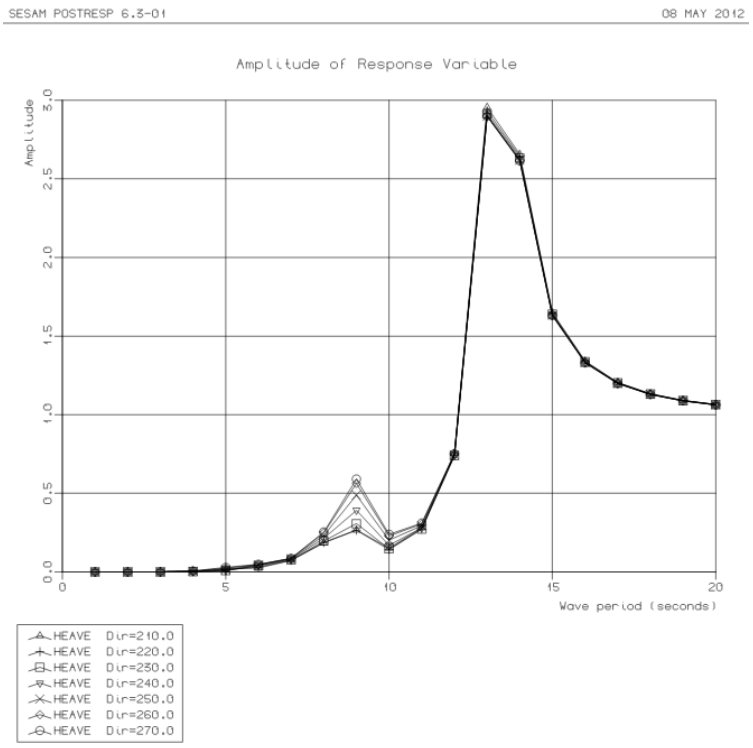

Figure 39 - Heave RAO for design #1

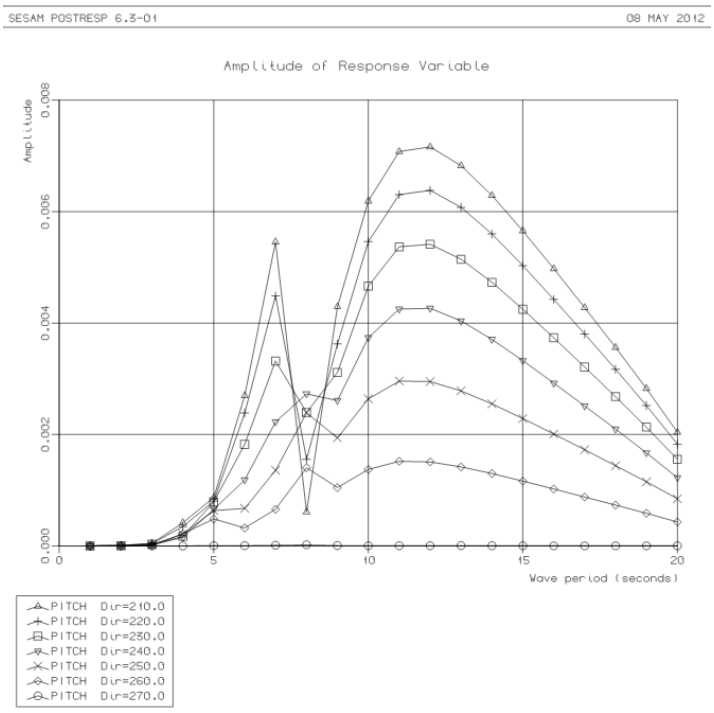

Figure 40 - Pitch RAO for design #1

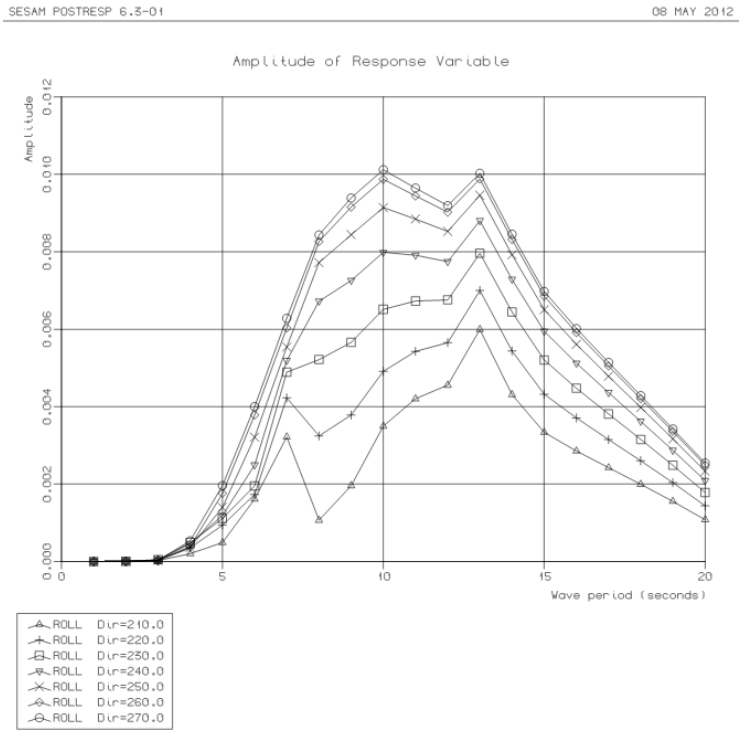

Figure 41 - Roll RAO for design #1

As observed in the plot of the pitch in figure 40, it was a surprising decrease in the RAO for incoming wave periods approximately equal to $T = 8s$. This was an unexpected result and it was natural to examine more in detail what exactly happened in the vicinity of this period. In figure 42 is the pitch motion for the model for incoming wave periods varying between $7s < T < 10s$ with $\Delta T = 0.20s$ presented. This was done to take a closer look at the pitch motion in the vicinity of the period causing the unexpected behavior.

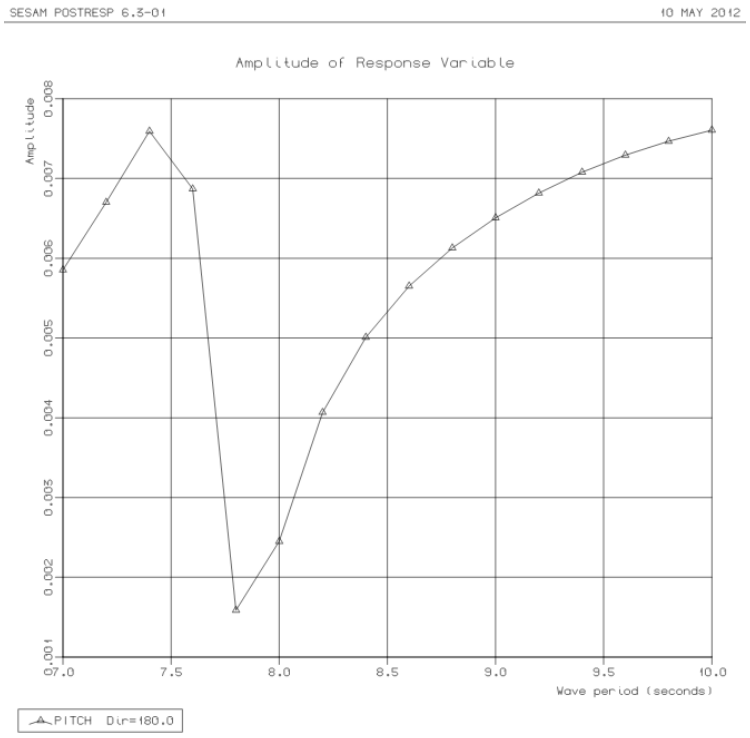

Figure 42 - Pitch RAO for design #1, 7s<T<10s

As figure 42 shows, the decreased value of the pitch is found for several of the periods in the vicinity of $T = 8s$. This shows that the irregularity observed was not caused by a single period computational error. Since it was the pitch motion that behaved unregularly, it was natural to evaluate the added mass A_{33}, A_{53} and A_{55} more in detail for $7s < T < 10s$ to achieve a deeper insight into the found irregularities. The figures for the plots for the added mass are shown in the following;

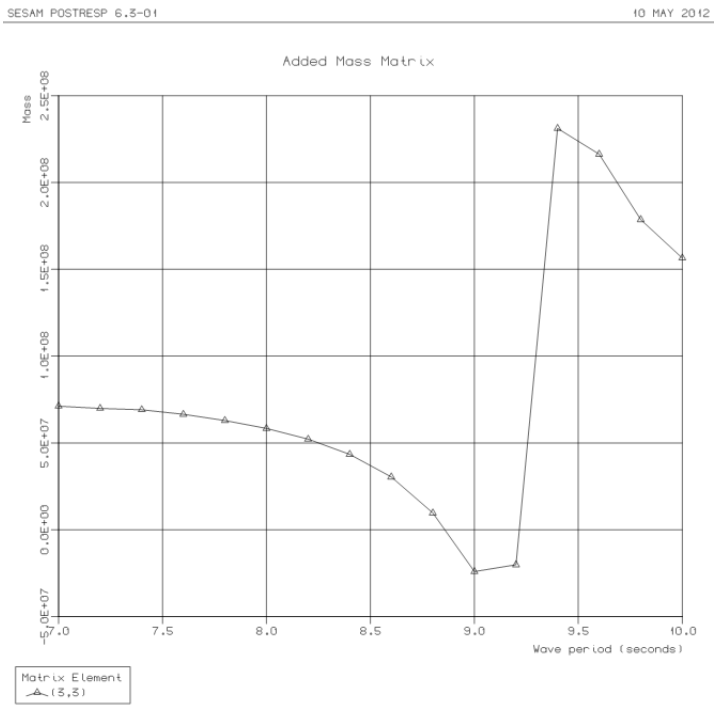

Figure 43 – A_{33} for design #1, 7s<T<10s

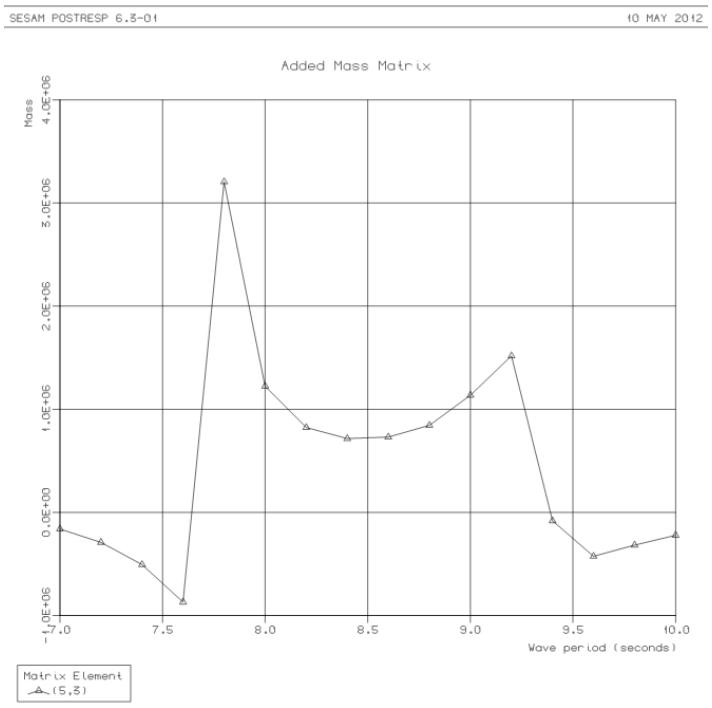

Figure 44 - A_{53} for design #1, 7s<T<10s

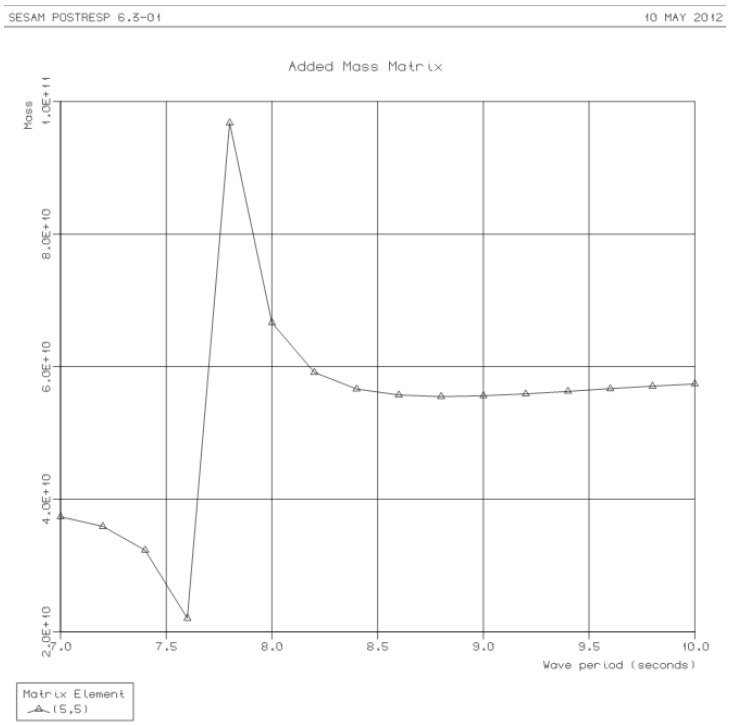

Figure 45 – A_{55} for design #1, 7s<T<10s

When evaluating these figures, it is observed that the irregularities also occur for the added mass for periods surrounding $T = 8s$. From the figures 43-45 it can seem like it is a resonance effect occurring at approximately $T = 7.5s$ which increases significantly in magnitude as a result of small damping in the model. The effect can also be a numerical effect, resulting from irregular frequencies. It is important to note that the effect occurring is a local problem and is limited to periods in the range of $7s - 8s$. These irregularities were discovered at a late stage of the master thesis and due to the time constraint related to the thesis, the effects were not studied any further. It is important to note that the problems are of a magnitude that makes them not ignorable, and the effects should be investigated more in detail before concluding with an optimal design solution. The problems discussed here occurred also for design solution #2 and design solution #4, presented later.

When considering the results retrieved concerning surface elevations inside the tunnel, these have been evaluated at $x = 0, y = -10m$ as determined previously in this thesis, and are done for incoming wave directions varying from $210 - 270$ degrees. Computations for the surface elevation were also done at the tunnel entrance at $x = 0, y = -39m$, as the waves occurring here will be essential for safe entry of a ferry into the tunnels. The result of the surface elevations are shown in figure 46 and 47 below;

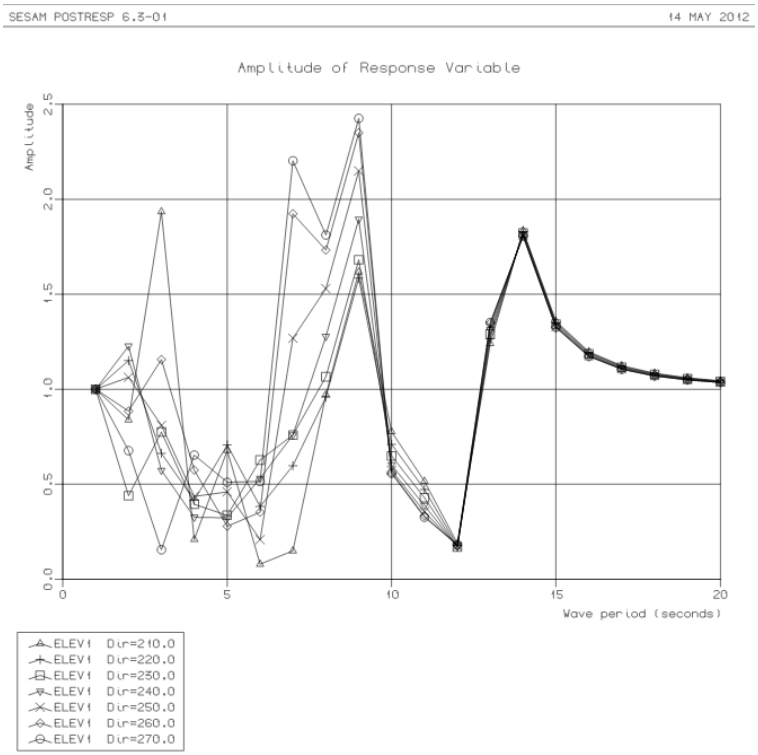

Figure 46 - Surface elevation at y=-10m for design #1.

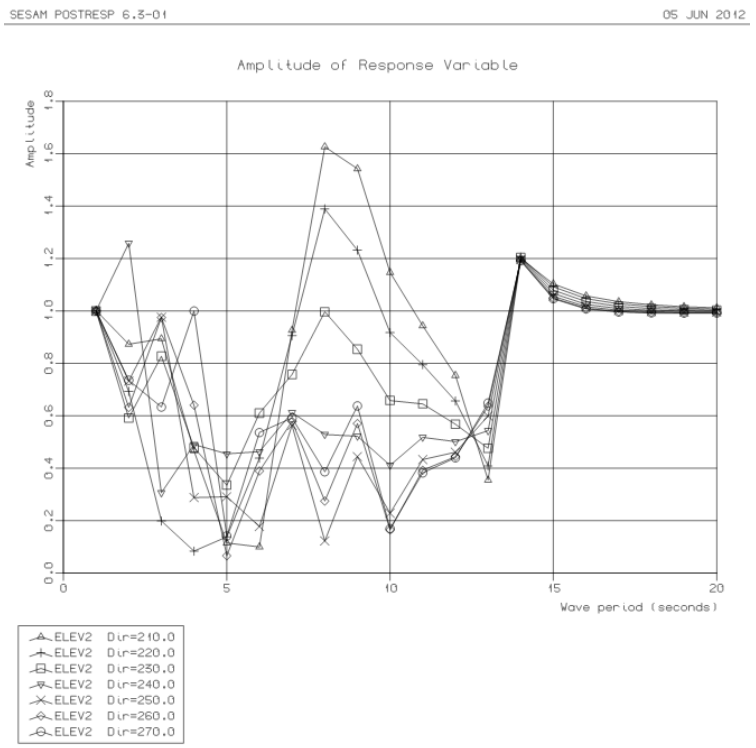

Figure 47 - Surface elevation at tunnel entrance for design #1

As seen in figure 46 the largest wave elevation for design #1 inside the tunnel was found for incoming wave heading 270 degrees where the maximal RAO measured is approximately 2.5. When evaluating the surface elevation at the tunnel entrance, it can be observed that the largest vertical motion is measured for wave heading 210 degrees. The maximal surface amplitude at the tunnel entrance is approximately 1.6.

The results presented here were done for three interconnected tunnels, which mean that the three tunnels are connected to each other at the center of the HUB without the interference of a wharf. This was chosen since this would create a larger inner pool for the waves to propagate in compared to a design with separated tunnels, where a wharf located at the center would create three individual pools. The motions of the design with separated tunnels have also been calculated, and these can be found in appendix D, along with the motion $RAOs$ for all the evaluated designs for separated tunnels solution. It was done computations regarding the surface elevation for a model with separated tunnels as well, but these showed that the surface elevation would increase inside the tunnel compared to an interconnected solution. The plot of these results can be viewed in the appendix E. Based on these results is the design with interconnected tunnels preferred for a three tunnel solution.

4.4 Proposed design solution #2

In the summer project, was a four tunnel design solution also considered, where the tunnels were shifted 90 degrees relative to each other. This was proposed as an alternative solution to design #1 and was proposed as it was believed that the most important factor in reducing the surface elevation in the tunnel was for a ferry to enter on the leeward side of the incoming wave. At this time it was somewhat limited information about the wave orientation in the Santos basin. No computational analyze was done for this design in the summer project to investigate the impact the design had on surface elevations inside the tunnel.

The design is symmetric, making it a modular design and thus easier to construct than more complex geometries. Compared to the proposed design #1, the platform will for design #2 have a larger inner pool as a result of an extra tunnel being cut out. The incoming waves can propagate more in this pool, and it is reasonable to assume that this will result in a reduction in surface elevations inside the tunnel. The design solution proposed has geometry as illustrated in figure 48;

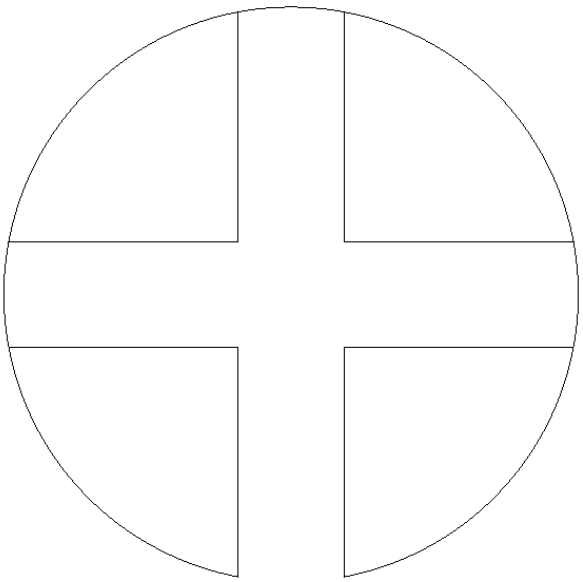

Figure 48 - Proposed design solution #2

Which tunnel an incoming ferry is intended to enter through for different wave headings for this design is shown in figure 49 and described below. The wave headings are oriented relative to a general orientation, with origo located in the center of the platform according to figure 8;

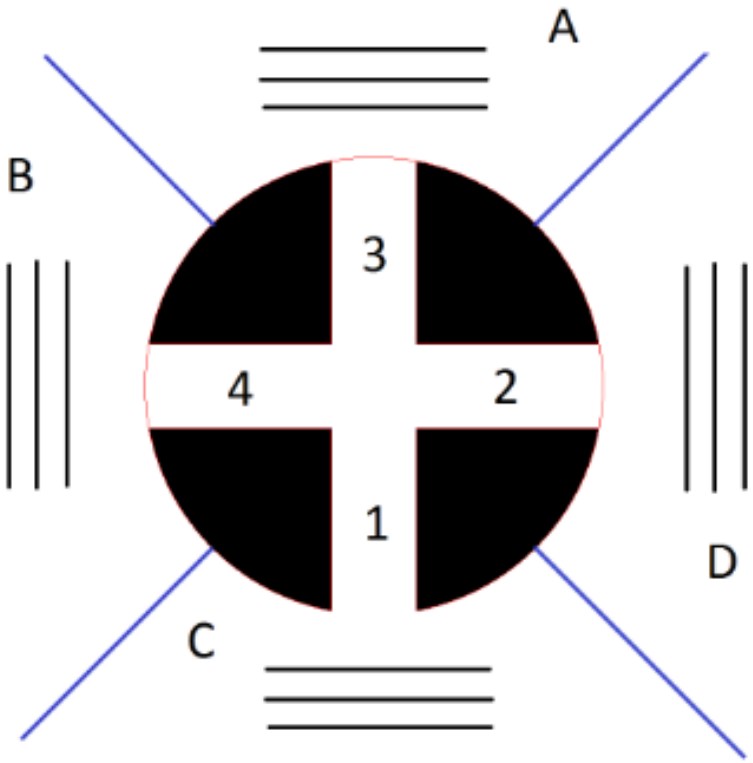

Figure 49 - Relation between incoming wave direction and desired tunnel for ferry entry for design solution #2

1. When waves are incoming from directions within A (with $225 - 315$ degrees wave heading), the smallest surface elevation will occur inside tunnel 1, making this the desired tunnel used for ferry entry.
2. For waves incoming from directions within B (with $315 - 45$ degrees wave propagation direction), the smallest surface elevation will occur inside tunnel 2.
3. For waves incoming from directions within C (with $45 - 135$ degrees wave propagation direction), the smallest surface elevation will occur inside tunnel 3.
4. If the waves are coming from directions within D (with $135 - 225$ degrees wave propagation direction), the ferry is intended to enter through tunnel 4.

For this design solution, the computations were done for incoming wave headings $225 - 270$, as these are limited by the number and spreading of tunnels. Note again that the computations could have been done for wave headings $225 - 315$ degrees, but that this is reduced to half due to symmetry about the y-axis.

The $RAOs$ for the motion in heave, pitch and roll for the platform is presented in the following figures for wave heading $225 - 270$ degrees;

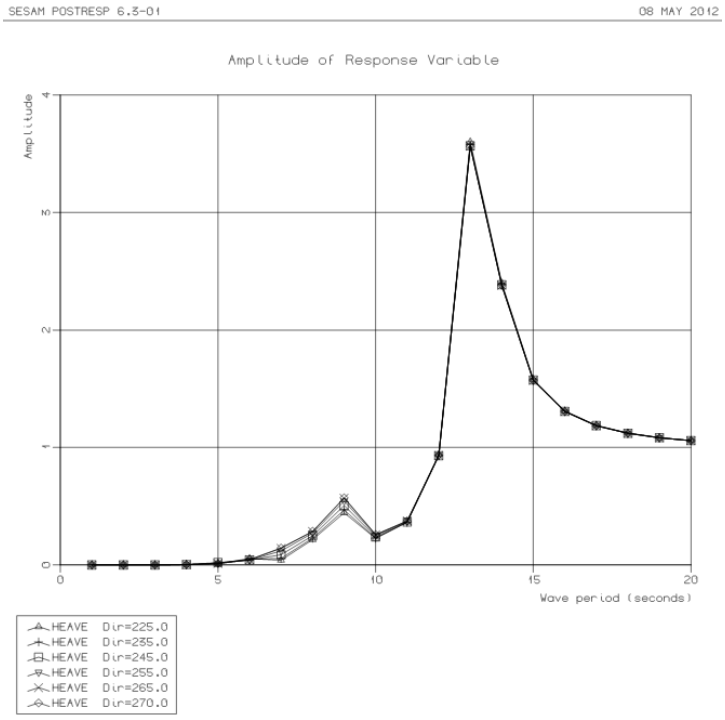

Figure 50 - Heave RAO for design #2

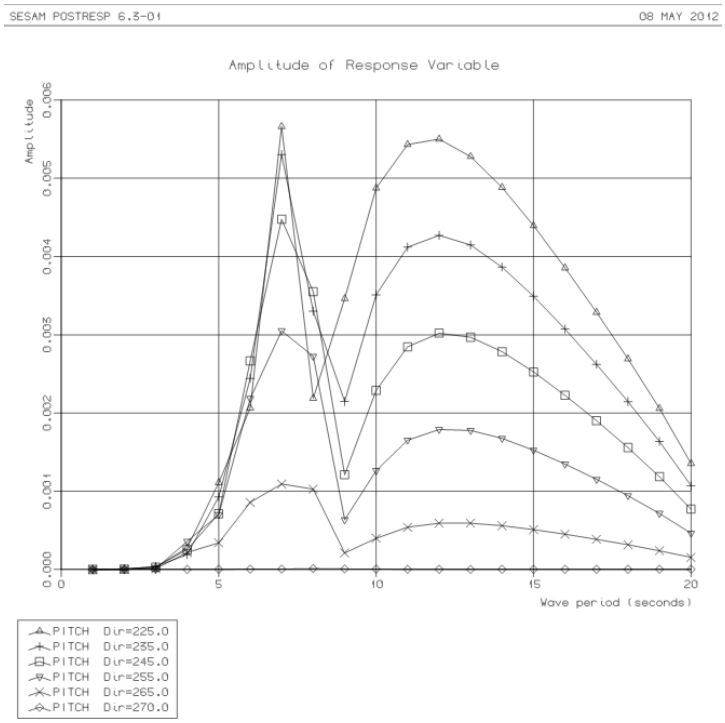

Figure 51 - Pitch RAO for design #2

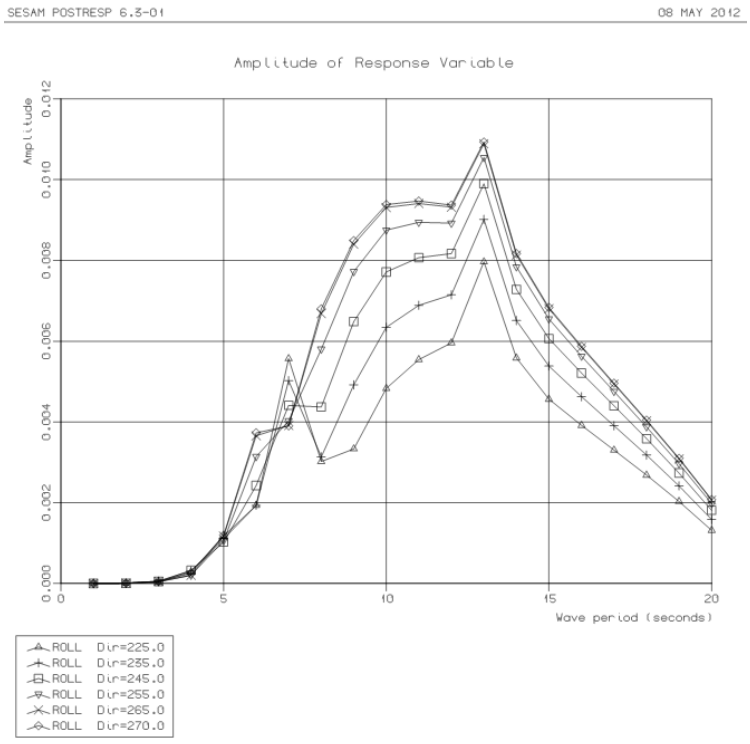

Figure 52 - Roll RAO for design #2

When evaluating the motions of this design solution, figure 50 shows that the heave motion for this design will have a somewhat larger maximum than that of design solution #1.

In general the differences in $RAOs$ between the design #1 and #2 are not of a large magnitude for heave, pitch nor roll. They all have similar shape and approximately the same magnitude, including the illogical behavior in pitch for periods $7s < T < 10s$. The fact that the plots are so similar for two different designs leads me to conclude with a larger certainty that the irregularities in pitch for $7s < T < 10s$ are not caused by modeling errors.

Note the difference in figure 51 and 52 presenting the pitch and roll $RAOs$, which is caused by the fact that the computations are done for wave heading $225 - 270$ degrees, which would have a bigger influence on the roll than the pitch motion of the platform. Wave heading equal to 270 degrees should inn theory lead to pure roll motion.

The surface elevation inside the tunnel for design solution #2 at location $x = 0m, y = -10m$ is shown in figure 53, and the surface elevation at the tunnel entrance is shown in figure 54 in the following;

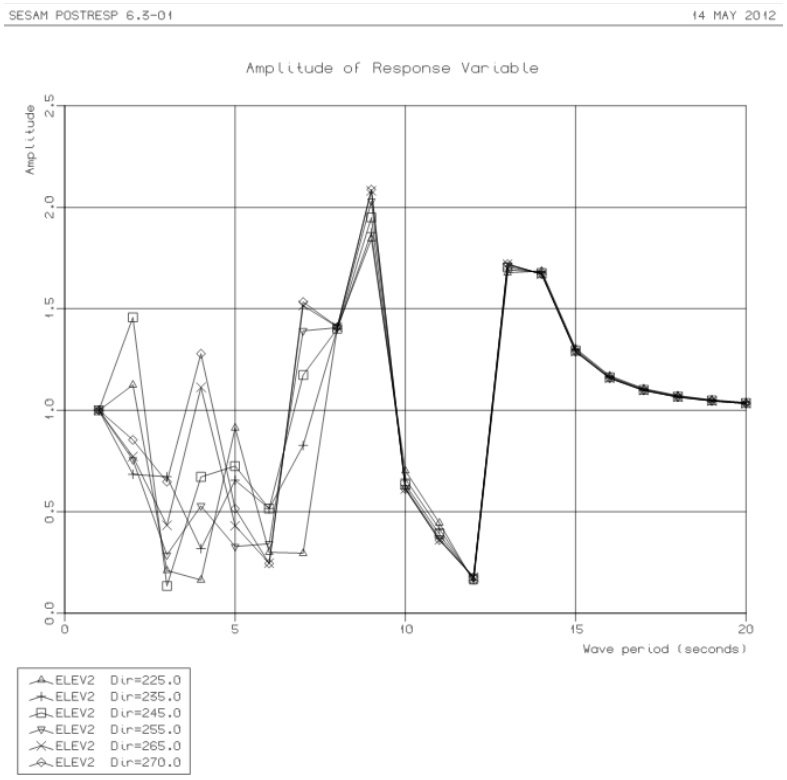

Figure 53 - Surface elevation at y=-10m for design #2

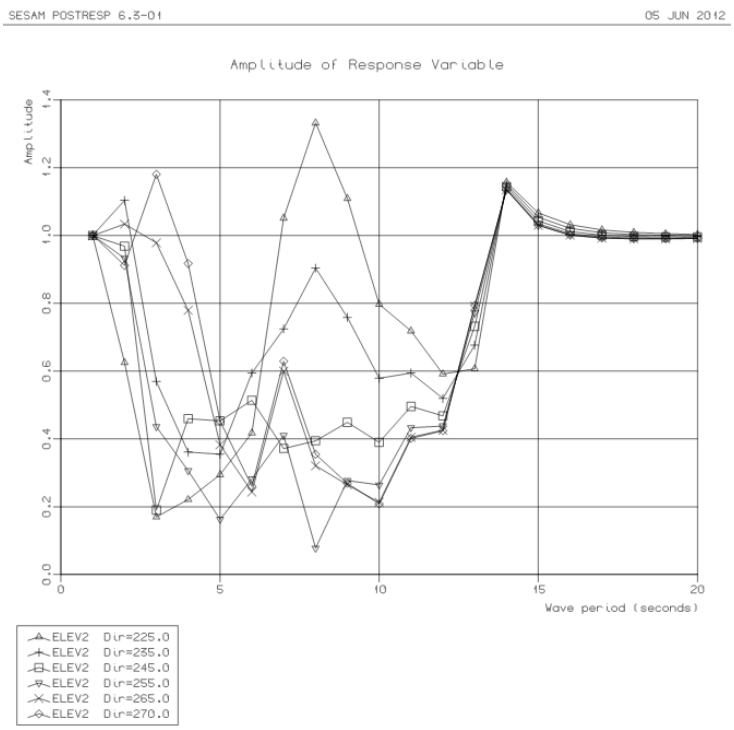

Figure 54 - Surface elevation at tunnel entrance for design #2

Figure 53 shows that the maximal surface elevation achieved inside the tunnel represented by the RAO is a little larger than 2 for period $T = 9$. The magnitude is reduced compared to design #1, which most likely is due to the increased size of the inner "pool" in combination with more favorable wave headings. Regarding the surface elevation found at the tunnel entrance, it is worth noting that the maximal elevation is reduced compared to design #1, causing more preferred entrance condition for a ferry entering the tunnel.

For design #2, as for design #1, computations were done regarding the surface elevation for separated as well as for interconnected tunnels, but no big deviations were found during comparison. These results can be found in appendix E, while the motions of the design with separated tunnels can be found in appendix D presented as $RAOs$

4.5 Proposed design solution #3

Considering the wave statistics presented in chapter 4.2 together with the defined wave window established in chapter 4, it was of interest to evaluate a platform design which utilized these statistics more explicitly. One such design is shown in figure 55;

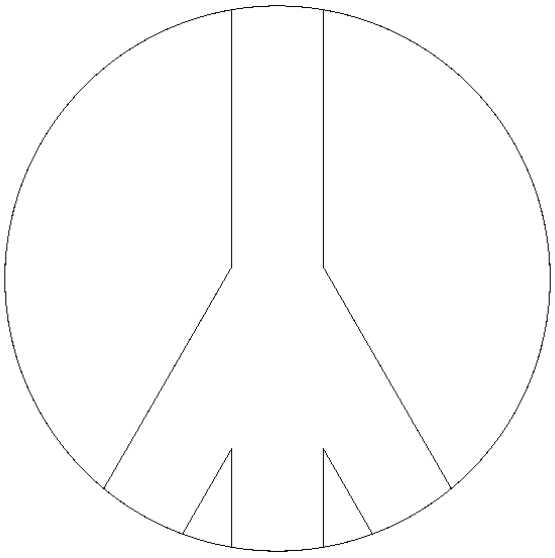

Figure 55 - Proposed design solution #3

The proposed design consists of 4 interconnected tunnels, where three of them are shifted 30 degrees relative each other and one tunnel is located opposite of these. The single tunnel is intended to ensure safe entry for the waves incoming from the north, northwest and southwest. Since these waves are small and relatively rare in occurrence, it was assumed that it would be sufficient with one tunnel to ensure safe entry for the ferries for incoming waves from these directions. The three other tunnels are oriented in a fashion so that when the larger waves are incoming from the southwest, south, southeast, east and northeast, it is always possible for a ferry to enter through a tunnel which has relative incoming wave headings within the established window of acceptance ($210 - 240$ degrees wave heading relative to the tunnel orientation). This should, according to previously presented results, result in maximal reduction of the surface elevation inside the tunnel. Which tunnel a ferry is intended to enter through for different incoming wave headings for this design is illustrated and described in the following;

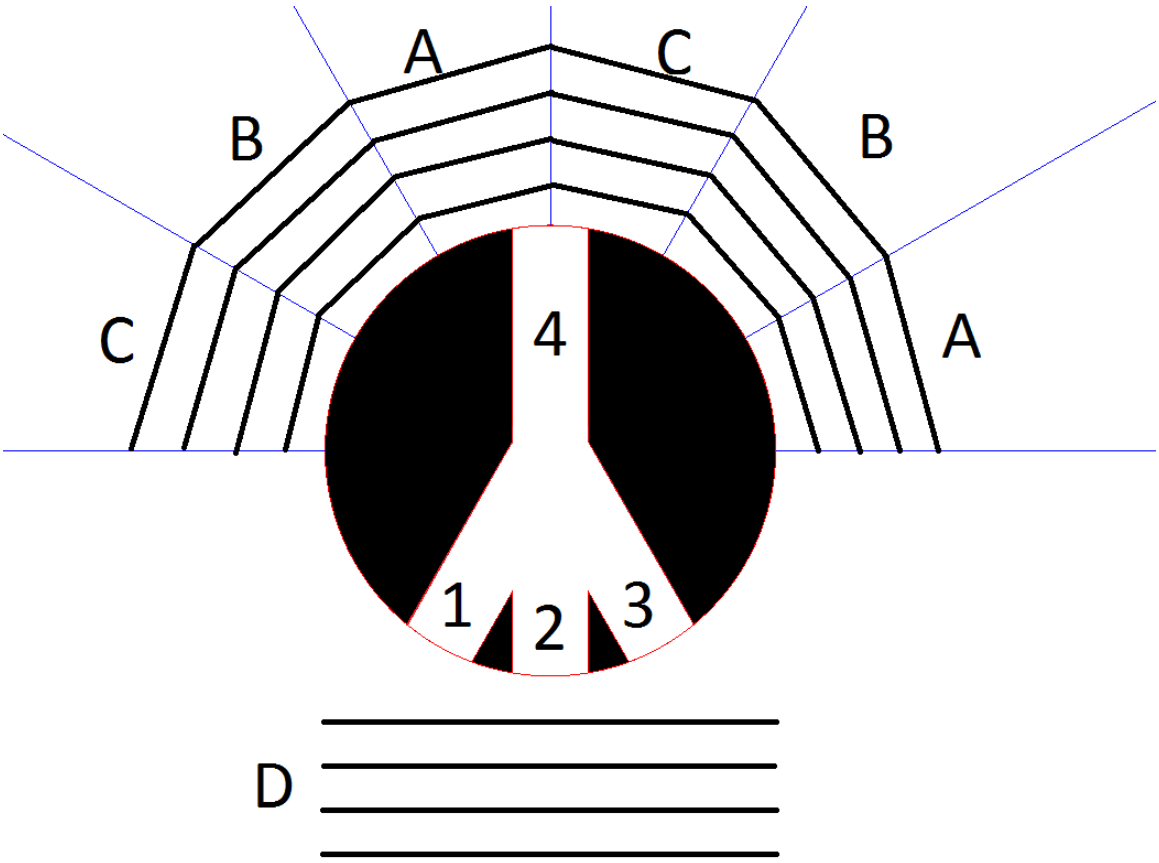

Figure 56 - Relation between incoming wave direction and desired tunnel for ferry entry for design solution #3

1. When waves are incoming from directions within A (with $180 - 210$ and $270 - 300$ degrees wave heading), the smallest surface elevation will occur inside tunnel 1, making this the desired tunnel for ferry entry.
2. For waves incoming from directions within B (with$210 - 240$ and $300 - 330$ degrees wave heading), the smallest surface elevation will occur inside tunnel 2, making this the desired tunnel for ferry entry.
3. For waves incoming from directions within C (with $240 - 270$ and $330 - 360$ degrees wave heading), the smallest surface elevation will occur inside tunnel 3.
4. For waves incoming from directions within D (with 360-180 degrees wave heading), which is a fairly rare case scenario (2.18% of total incoming waves are from this direction (Pianca et al., 2010)), the smallest surface elevation will occur inside tunnel 4.

With this proposed design for the tunnel layout, the ferry is always able to enter through a tunnel that has sufficient shelter and small wave elevations inside the tunnel for a ferry to enter. It seems reasonable to suspect that the operational time with this design solution will be very high; theoretically close to 100%.

In addition to the reduction in wave elevation due to advantageous tunnel locations, the effect of interconnected tunnels is a large inner pool, resulting in a big area that the incoming waves will be able to propagate in.

It was also done computations for the tunnels being separated at the center, and it was found that the wave elevation was of the same magnitude for the two alternatives. Plots representing the elevation for separated tunnels can be found in appendix D.

When considering this design, it is apparent that the platform will be more unstable in the transverse direction than in the longitudinal direction due to its unsymmetrical geometry. This is a result of the second moment of area related to the x-axis; $I_{xx} = \int y^2 dA$, being smaller than the second moment of area related to the y-axis, $I_{yy} = \int x^2 dA$. The implications of this is a smaller initial metacenter radius $BM = \frac{I}{\nabla}$ and thus a smaller metacentric height, as $GM = KB + BM - KG$, assuming KB and KG are held constant. This was confirmed when the design solution was evaluated in HydroD, where the big difference in transverse (GM_4) and longitudinal (GM_5) metacentric height from the result file underlined this. For this design, it was retrieved metacentric height for $GM_4 = 2.02\text{m}$ and for $GM_5 = 17.29\text{m}$, for a distance from the center of buoyancy (COB) to the center of gravity (COG) defined to be $20m$. A $GM_4 \approx 2m$ is a too low metacentric height to fulfill the necessary stability criteria of a floating structure, but this can be modified by installing a vertical wall at the center of the HUB. The large difference in metacentric height implies that a platform with this design will be more vulnerable for large roll motions than it will be for pitch motions.

The $RAOs$ for the motions of a platform with this design is shown in figure 57-59 for heave, roll and pitch motions respectively. Plots are done for wave heading $210 - 240$ degrees;

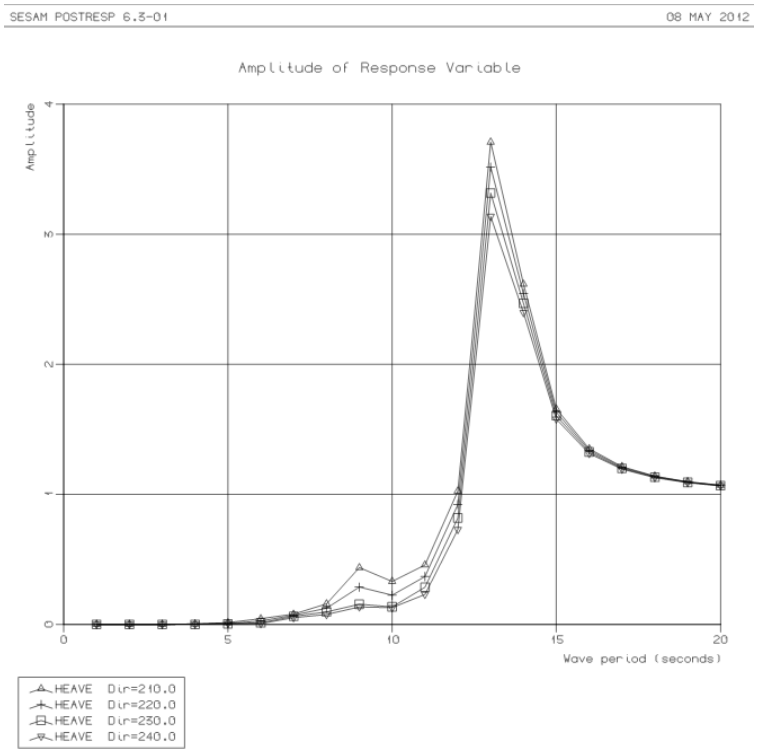

Figure 57 - Heave RAO for design #3

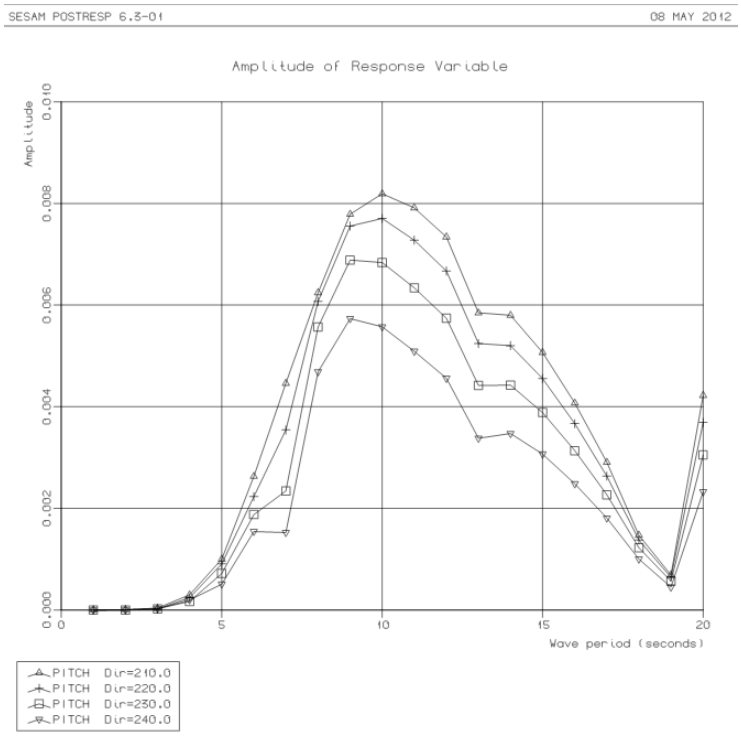

Figure 58 - Pitch RAO for design #3

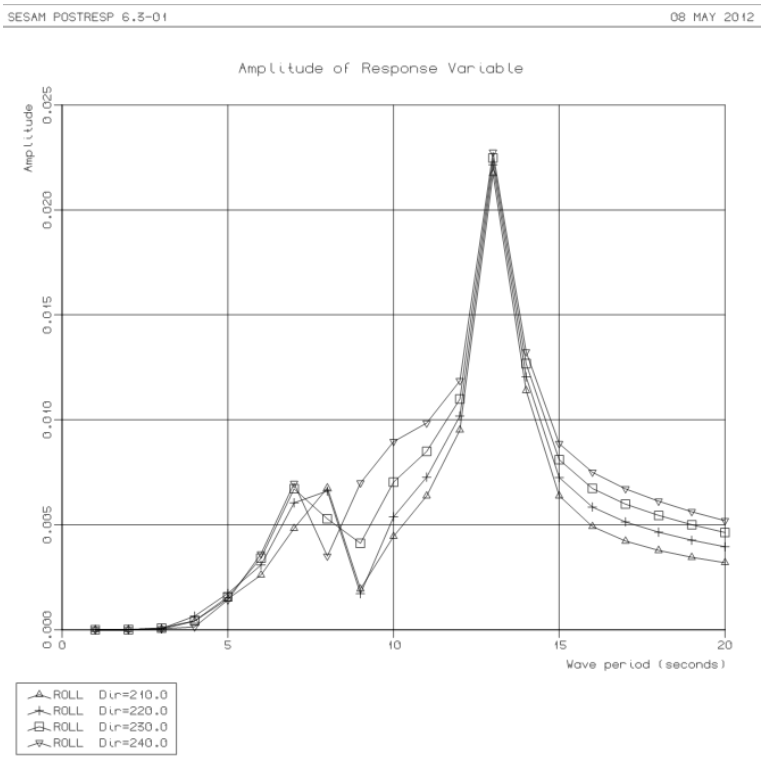

Figure 59 - Roll RAO for design #3

The heave motion of this design has a similar magnitude for the maximum RAO as design solution #2 and is approximately equal 3.5. This is logical as they have the same number of tunnels, thus displacing the same volume and having a similar resistance to vertical motion.

The pitch motion illustrated in figure 58 for design #3 has a similar shape and magnitude as the compared platform with the standard Sevan design (Sevan, 2010), as illustrated with the concept model in figure 10.

As shown by the plot in figure 59, the roll RAO for this design has maximal amplitude more than twice the size of that for design #1 shown in figure 41. This is a result of the decreased second moment of area related to the x-axis as discussed previously. This indicates that the reduction in transverse metacentric height GM_4 for design #3 will cause roll motions larger than what is acceptable.

Concerning the surface elevations that will occur inside the tunnel for this design, this is shown in figure 60, and the elevation at the tunnel entrance is shown in figure 61 in the following;

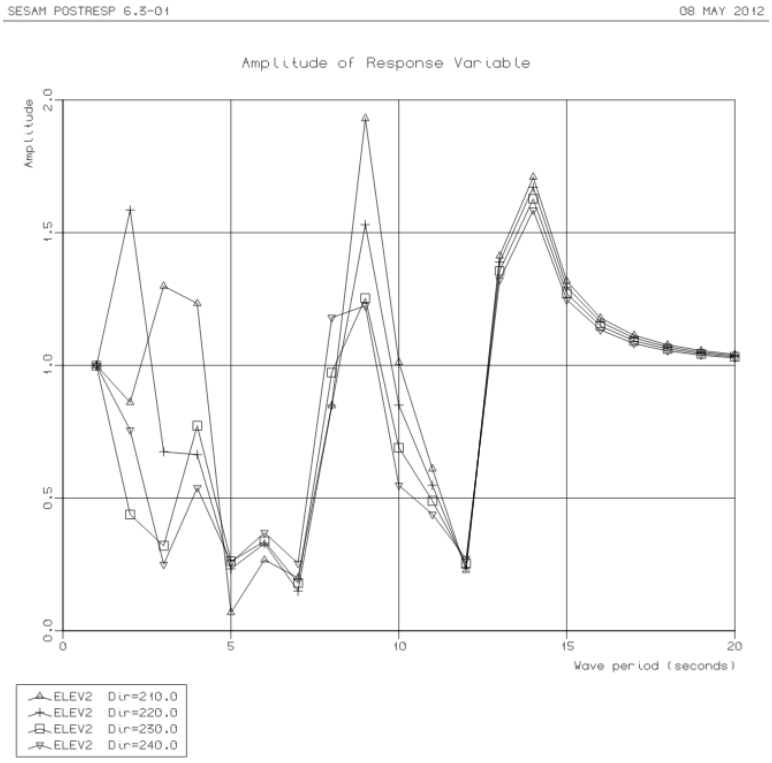

Figure 60 - Surface elevation at y=-10m for design #3

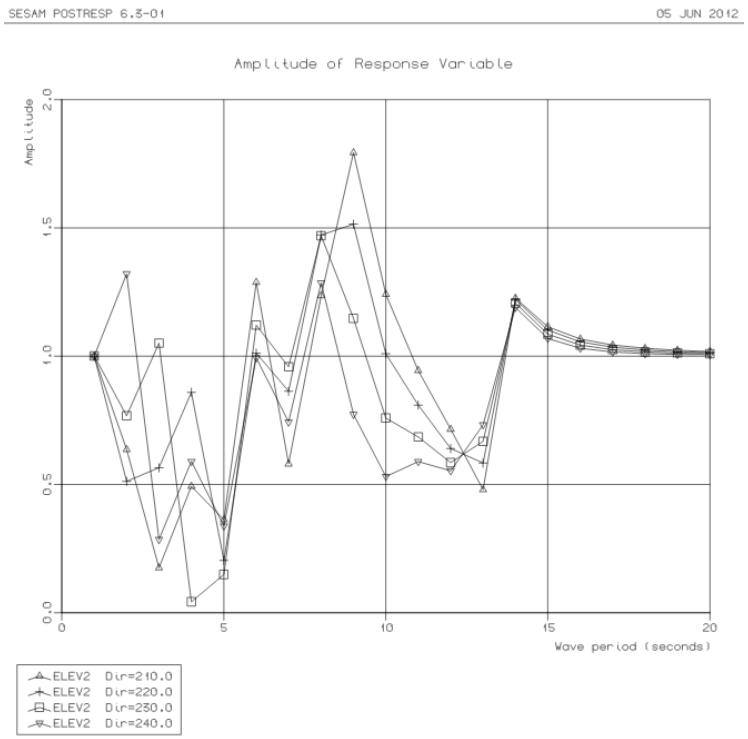

Figure 61 - Surface elevation at the tunnel entrance for design #3

Compared to the wave elevation at $y = -10m$ for design #1 as shown in figure 46, the elevation is significantly reduced for design #3. The difference in elevation at $y = -10m$ between design #2 and design #3 is not of a magnitude to be of any significance. Considering the elevation at the tunnel entrance, it is larger for design #3 than design #2, resulting in less optimal entrance conditions.

For this design, as for design #1 and #2 were computations done regarding the surface elevation for separated tunnels and these results can be found in appendix E. The motions of the design with separated tunnels can be found in appendix D, presented as $RAOs$.

In addition to the unsatisfactory stability in transverse direction for design #3 as illustrated by the plot for the roll RAO, the proposed solution consists of a complex geometry and will lead to challenges during construction.

4.6 Proposed design solution #4

When considering the problems occurring for design solution #3 regarding the transverse instability, it was natural to evaluate a structure that had a more symmetrical geometry in addition to the advantageous wave headings. This was of interest because as it was considered to be of essential importance that the platform had satisfactory resistance to motion in all directions. To achieve this, it was a necessity that GM_4 and GM_5 were within the same order of magnitude. Considering this, in addition to the window of acceptance established in chapter 4, it was natural to analyze a design solution with a symmetric geometry and with tunnel locations providing desired relative wave headings. The evaluated design can be seen in figure 62 in the following;

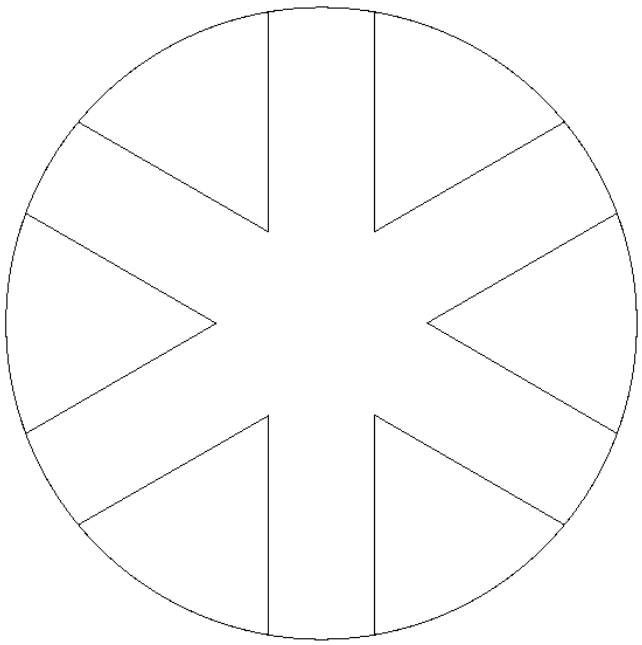

Figure 62 - Proposed design solution #4

The design proposed gives optimal entry conditions for ferries for all incoming wave headings, and in addition the waves entering through an open tunnel port have a very large inner pool to propagate in. In theory, design #4 should result in the smallest surface elevation inside the tunnels of the designs evaluated in this master thesis.

A factor worth noting that might cause problems with this design is that due to many tunnels in the design, this results in a reduced water displacement, and might lead to limitations considering the total weight of the platform. A platform with this design, a diameter of $78m$, draft $9m$ and a lip diameter of $47.5m$ with height $3m$ would lead to a total volume of displacement equal to approximately $41000\ m^3$. This corresponds to a total platform weight of approximately $42000\ ton$ which is half the weight of the platform provided for comparison (Sevan, 2010). The platform used for comparison is a FPSO, and it is reasonable to assume that it has to be able to carry a larger weight load represented by all the equipment and oil stored. Whether this load is twice as large as the weight of the platform presented in design #4 is uncertain and this has to be evaluated more closely if the design is to be considered to be constructed. For this thesis, no information regarding the needed carrying weight was provided which made it impossible to conclude whether design #4 provided the satisfactory buoyancy or not.

Which tunnel an incoming ferry is intended to enter through for different wave headings for this design is shown in figure 63 and is described in the following. The wave headings are oriented relative to a general orientation, with origo located in the center of the platform, according to figure 8;

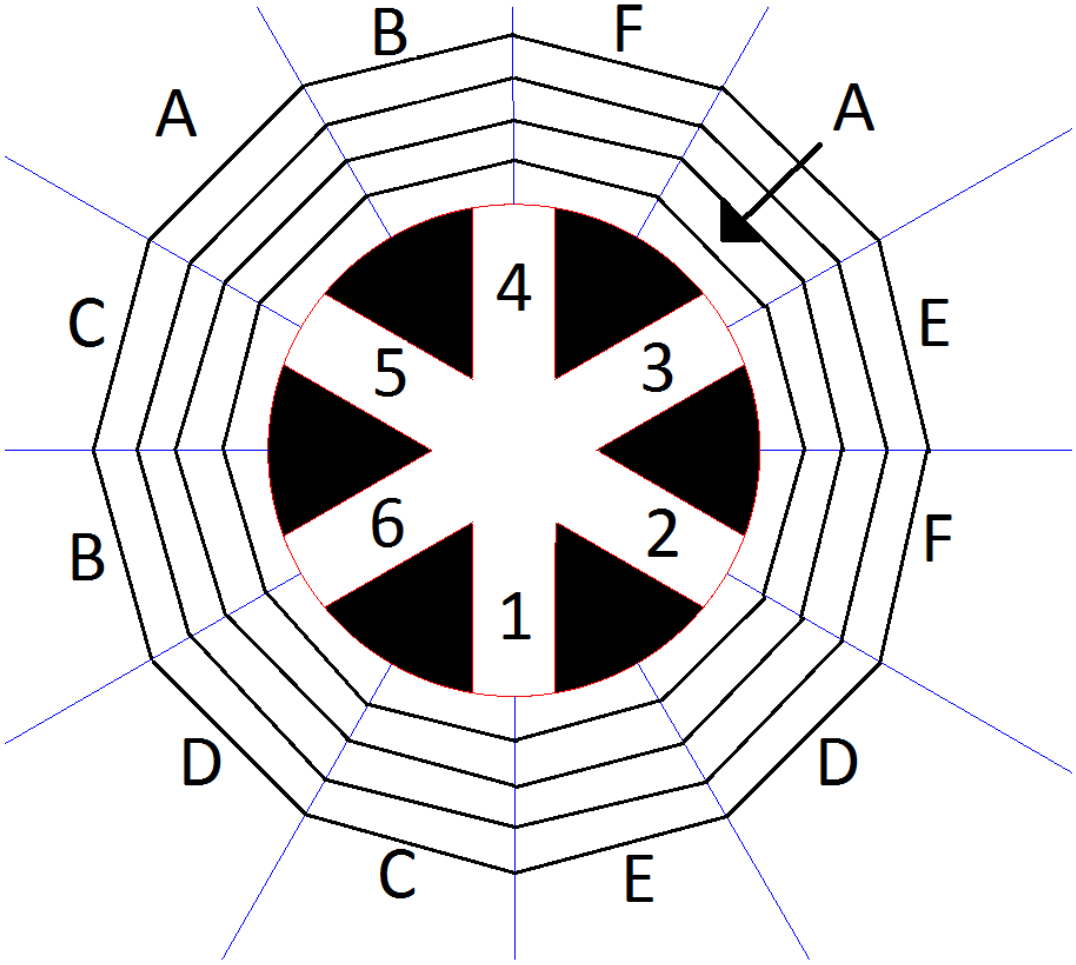

Figure 63 - Relation between incoming wave direction an tunnel of entry for design solution #4

1. For waves incoming from directions within A (with $210 - 240$ and $300 - 330$ degrees wave heading), the smallest surface elevation will occur in tunnel 1, and this will then be the desired for ferry entry.
2. Waves incoming from directions within B (with $270 - 300$ and $0 - 30$ degrees wave heading) will result in the smallest surface elevation in tunnel 2, making this the desired tunnel for ferry entry.
3. Waves incoming from directions C ($330 - 0$ and $60 - 90$ degrees wave heading) will result in the smallest surface elevation in tunnel 3.
4. Waves incoming from directions D ($30 - 60$ and $120 - 150$ degrees wave heading) will result in the smallest surface elevation in tunnel 4.
5. Waves incoming from directions E ($90 - 120$ and $180 - 210$ degrees wave heading) will result in the smallest elevation in tunnel 5.
6. Waves incoming from directions F ($150 - 180$ and $60 - 90$ degrees wave heading) will result in the smallest elevation in tunnel 6.

Considering the stability of the platform, the second moment of area about the x-axis for this design $I_{xx} = \int y^2 dA$, is the same as the moment of area about the y-axis, $I_{yy} = \int x^2 dA$. This results in equal initial metacenter radius $BM = \frac{I}{\nabla}$ in transverse and longitudinal direction, and consequently equal metacentric height $GM_4 = GM_5$. For this design $GM_4 = GM_5 \approx 12.1m$, which is a large metacentric height. This was calculated using the same distance from the COB to COG as for all the other designs evaluated in this thesis ($COG - COB \ = 20m$).

The motion of this design is illustrated by the RAO plots in the following figures for wave heading $210 - 240$ degrees;

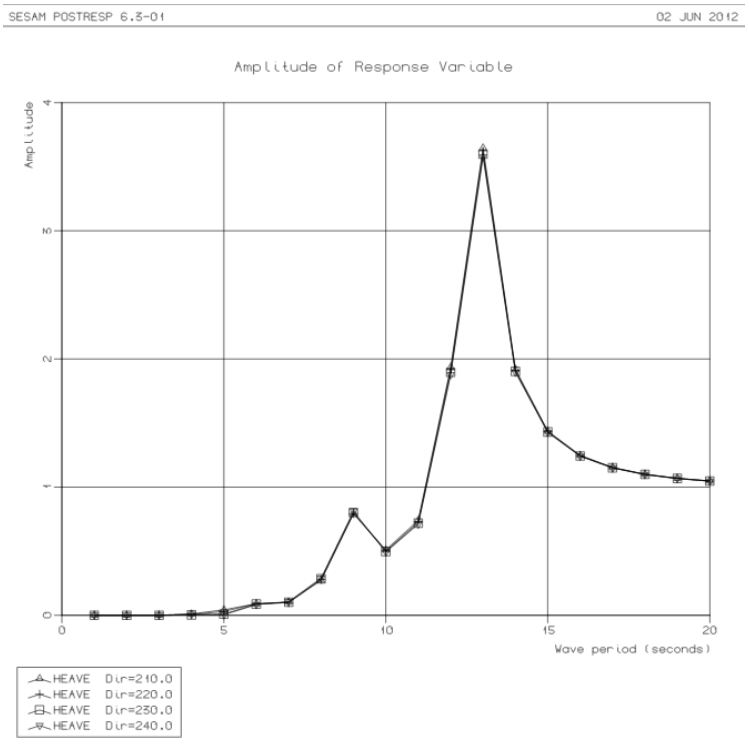

Figure 64 - Heave RAO for design #4

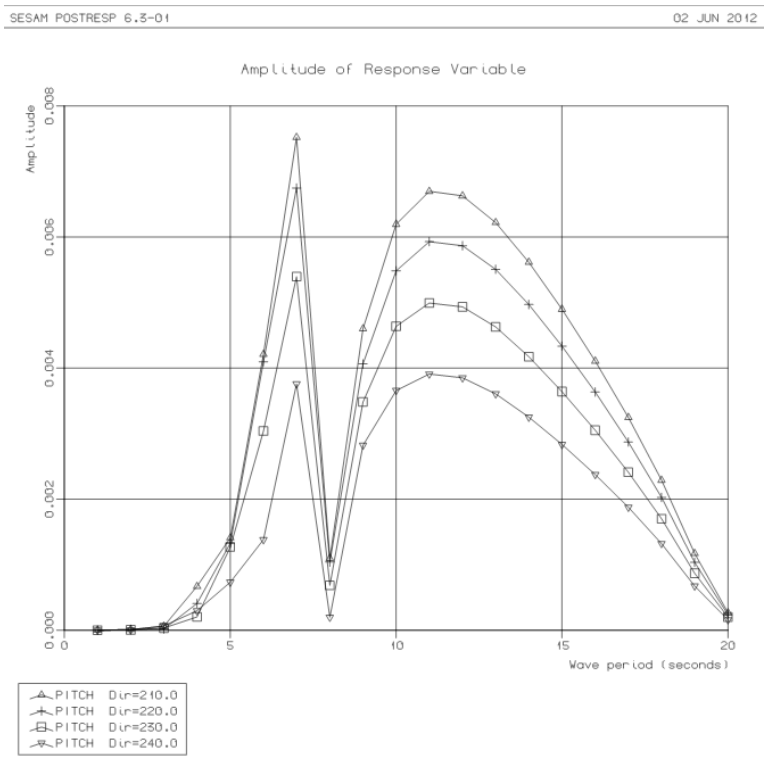

Figure 65 - Pitch RAO for design #4

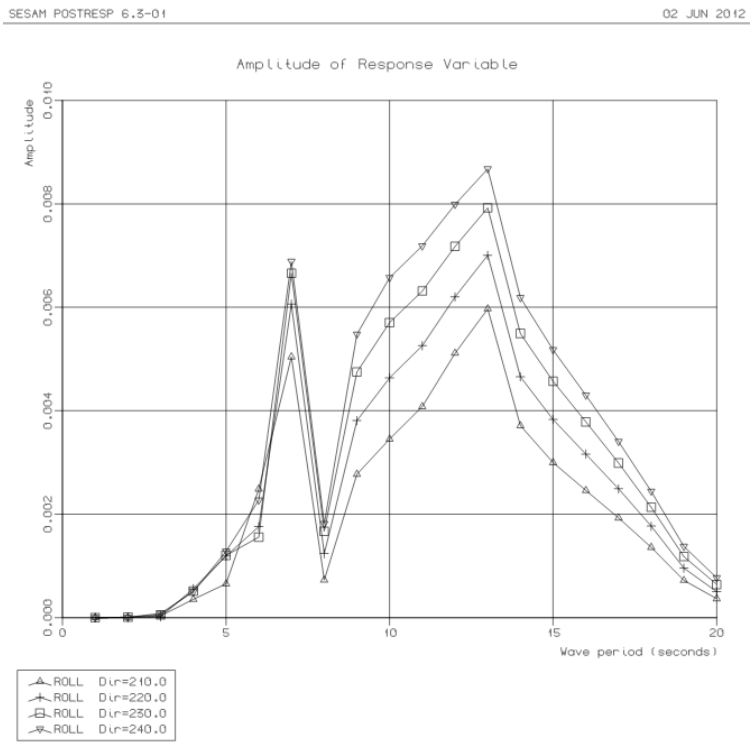

Figure 66 - Roll RAO for design #4

The heave motion of the platform for this design follows the heave RAO for the other designs fairly close and has a maximum of approximately 3.5 which is similar to design #2 and #3.

The roll and pitch motion $RAOs$ have a resembling shape for this design, which is a natural consequence of a symmetric design and wave headings contributing approximately the same to motion in pitch and roll.

The surface elevation inside the tunnel is illustrated in figure 67 and the elevations at the tunnel entrance can be seen in figure 68;

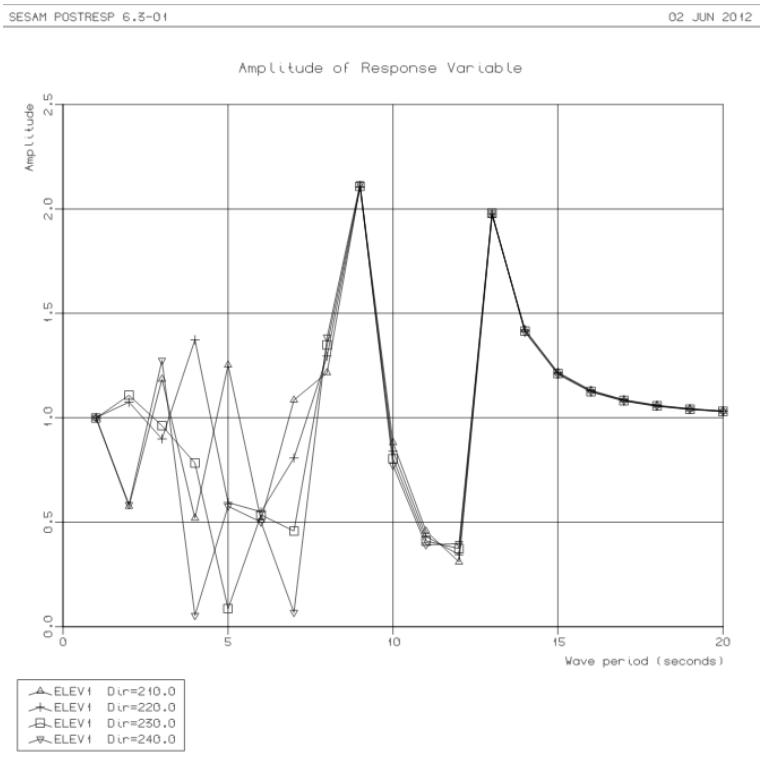

Figure 67 - Surface elevations at y=-10m for design #4

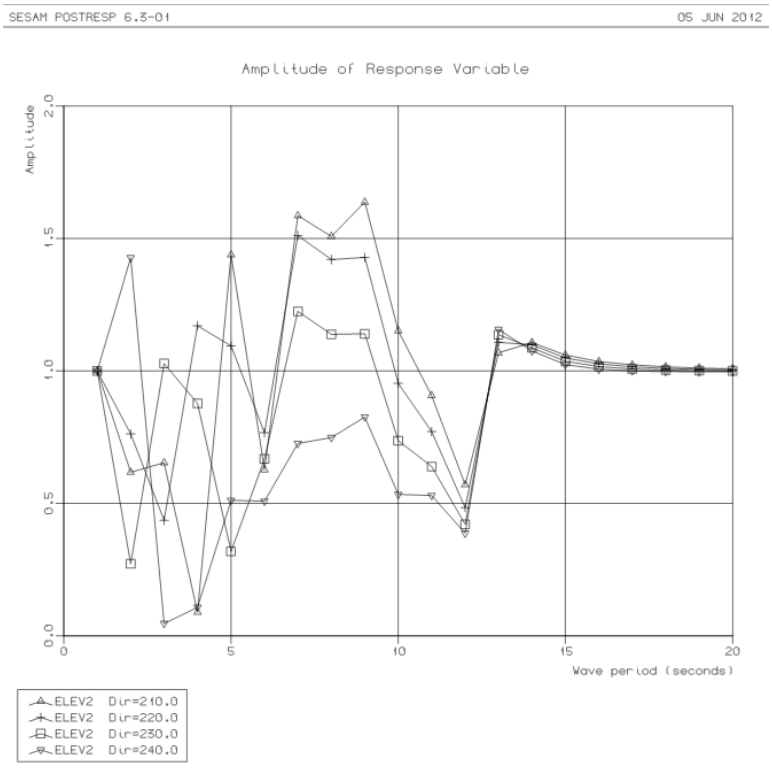

Figure 68 - Surface elevation at the tunnel entrance for design #4

The elevations inside the tunnel shown in figure 67 follow the same shape as the other evaluated designs, with two main peaks. The maximal elevations measured for this design are somewhat larger than those for design #3, but are similar in magnitude as those retrieved for design #2. The elevation measured at $T \approx 13s$ for this design is the largest measured of the 4 evaluated designs.

Considering figure 68, it shows that the surface elevation for design #4 evaluated at the tunnel entrance is approximately equal to that for design #1, with a maximal magnitude of approximately 1.6.

Computations were also done for tunnels with an installed placed wharf at the center of the HUB. This computation showed that the elevations at $y = -10m$ was somewhat smaller than that for the design without the wharf. This was somewhat surprising, as it was not in correspondence to the results retrieved for the other designs. The results retrieved showed that it for this design might be advantageous to place a wharf in the center of the HUB regarding the surface elevation in the tunnel. The plot of the surface elevation for design #4 with an installed wharf at the center of the HUB is found in appendix E, and the motions of the design with a central wharf is presented in appendix D as response amplitude operators.

It is also worth mentioning here that the design evaluated here is a modular structure, making it relatively simple to construct as it consist of 6 equal modules.

4.7 Comparison of computational results for the different design solutions

The different design solutions will have different abilities affecting the motions of the platform. These motions are presented in the following as short term response curves. The STRs here are defined in the same way as in chapter 3.2.5, where the STR is plotted for the peak period $T_P = 1.41 * T_z$ and the significant amplitude = $\frac{1}{2} *$ significant double amplitude, where the significant double amplitude = 2* the standard deviation of the response. The STR in heave, pitch and surge are plotted for wave heading 0 degrees while the STR in sway and roll is plotted for wave heading 270 degrees. This was done as it was the wave headings resulting in the largest model motions that were of interest here;

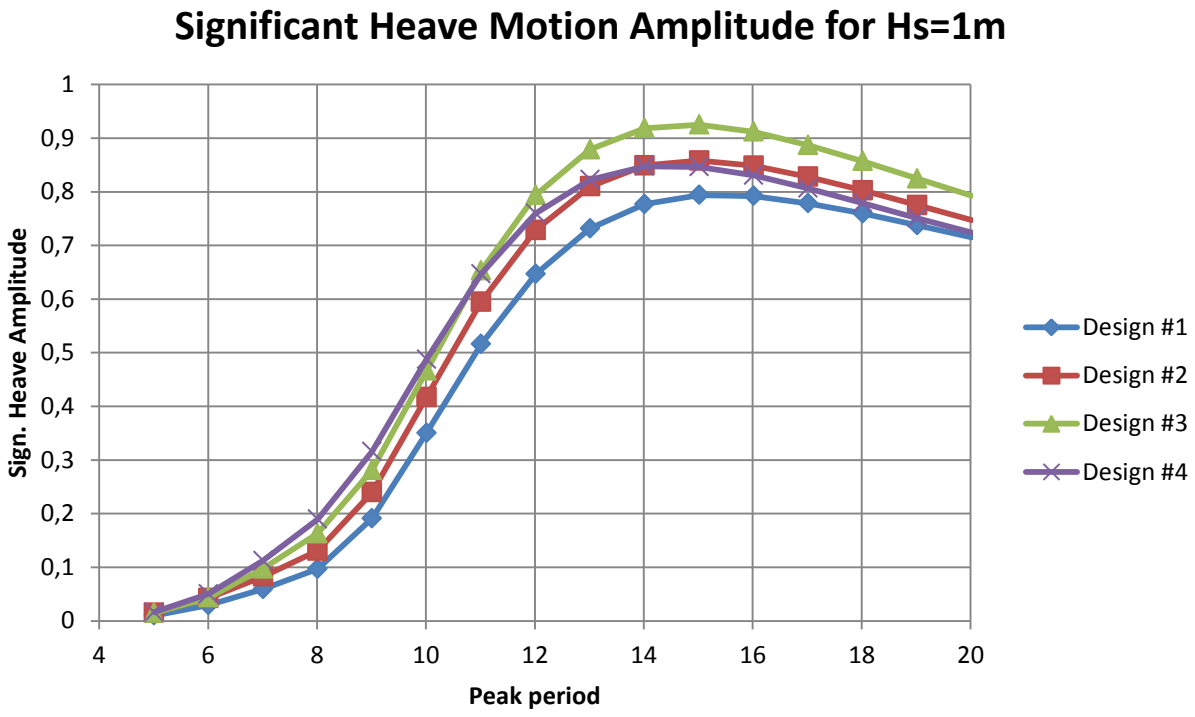

Figure 69 - STR in heave for design #1-4

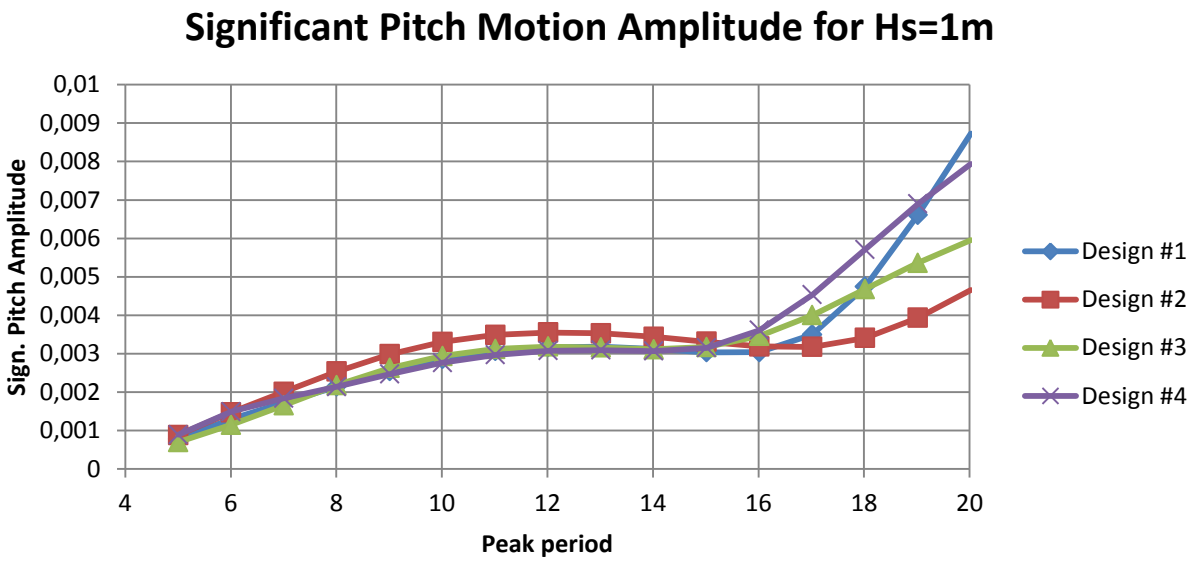

Figure 70 - STR in pitch for design #1-4

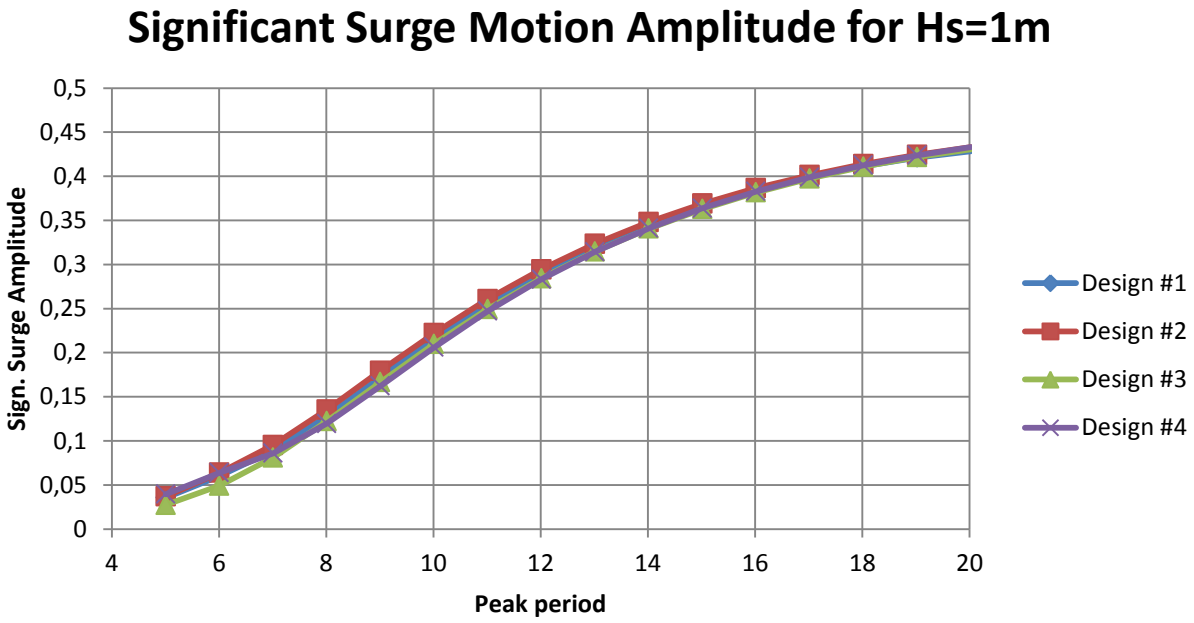

Figure 71 - STR in surge for design #1-4

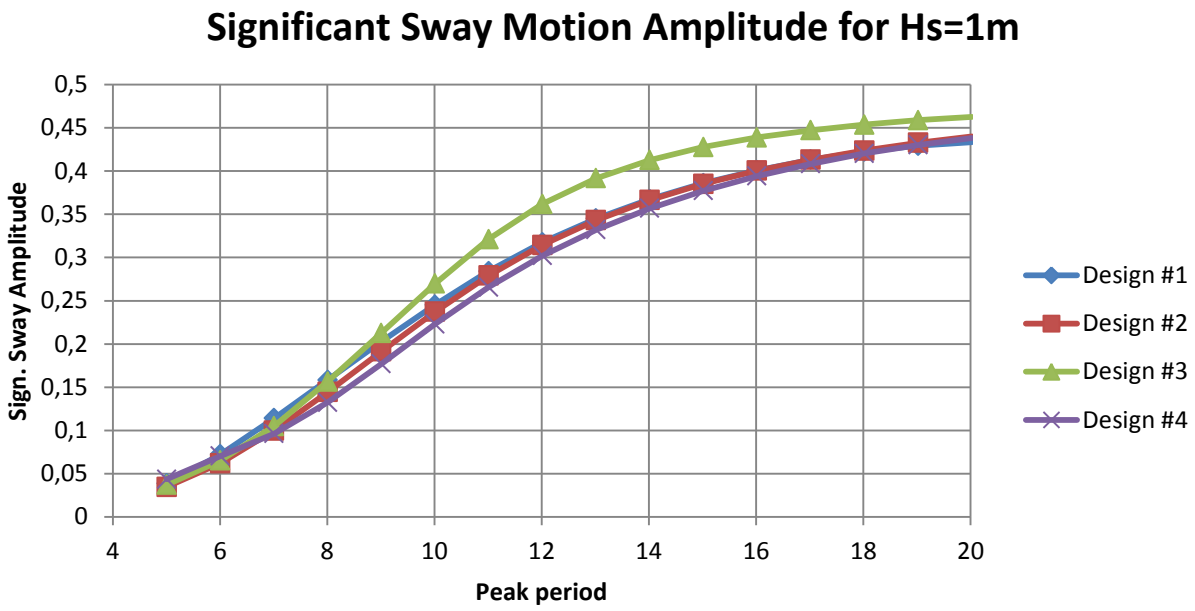

Figure 72 - STR in sway for design #1-4

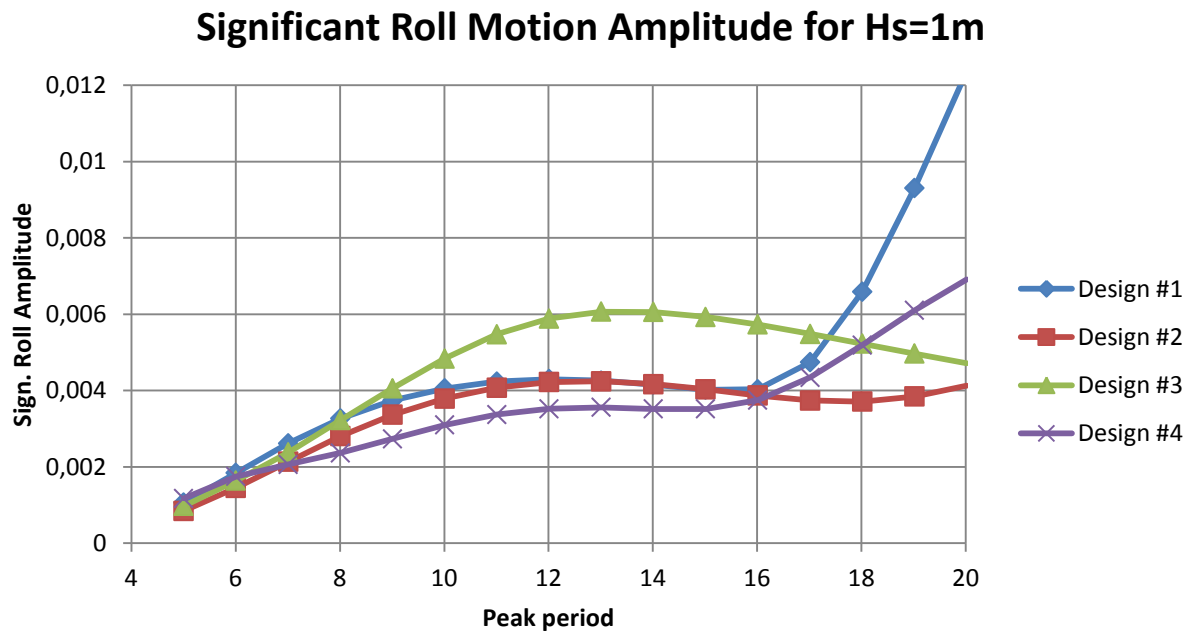

Figure 73 - STR in roll for design #1-4

When the figures representing the motions of the 4 designs were evaluated, it became apparent that the 4 platforms would behave somewhat differently. Design #1 will have the smallest motion in heave while design #3 has the largest, as shown in figure 69. The biggest differences in motions are appearing

for the pitch and roll motion for wave periods $T_p \geq 18s$. In pitch will design #1 and #4 have the biggest motions, but they don`t stand out before the largest periods are evaluated. In the plot for the roll motion does design #1 stand out for $T_p \geq 18s$ as it increases rapidly for high periods. This is a surprising result, as the geometry should not imply that this design should experience any particular instability for large periods in roll. From the unexpected exponential growth observed, it can seem like the growth might be due to computational errors as it is diverging, but this has not been confirmed. It is important to note that design #3 stands out resulting in larger roll motions for $10s \leq T_p \leq 17s$. This is not unexpected, for reasons discussed in chapter 4.5, but as these periods will occur more regularly, the large motion achieved here represents a significant threat to the stability of the platform.

When comparing the surface elevation at $y = -10m$ and $y = -39m$ for the designs #1-4, this was done by doing computations for all relevant wave headings during ferry entry, before extracting the wave heading resulting in the largest amplitude. The consequence of this was that the surface elevations for the designs #1-4 have been evaluated for different wave headings. For instance; results in surface elevations for design #1 was evaluated using wave headings $210 - 270$ degrees. Here the elevation at $y = -10m$ was the largest for wave heading 270 degrees while at $y = -39m$ the largest elevation was found for wave heading 210 degrees. On the other hand, computations done for design #3 showed that the largest values for the STR at $y = -10m$ and $y = -39m$ both occurred for wave heading 210, and the STR for the elevations in the two points for design #3 is presented for this wave heading.

Note again that the elevations found at $y = -10m$ are chosen to represent the surface elevation inside the tunnel, as concluded in chapter 4. The elevations found at $y = -39m$ are chosen to represent the wave pattern at the tunnel entrance which will be critical during ferry entry. This might be a source of error, as the maximal elevation might occur at some other locations. However, the motions measured at these points should give an indication as to what could be expected of vertical motion of the surface.

The short term response for the surface elevation in $y = -10m$ for design #1-4 is presented in figure 74 and at the tunnel entrance $y = -39m$ is presented in figure 75 below;

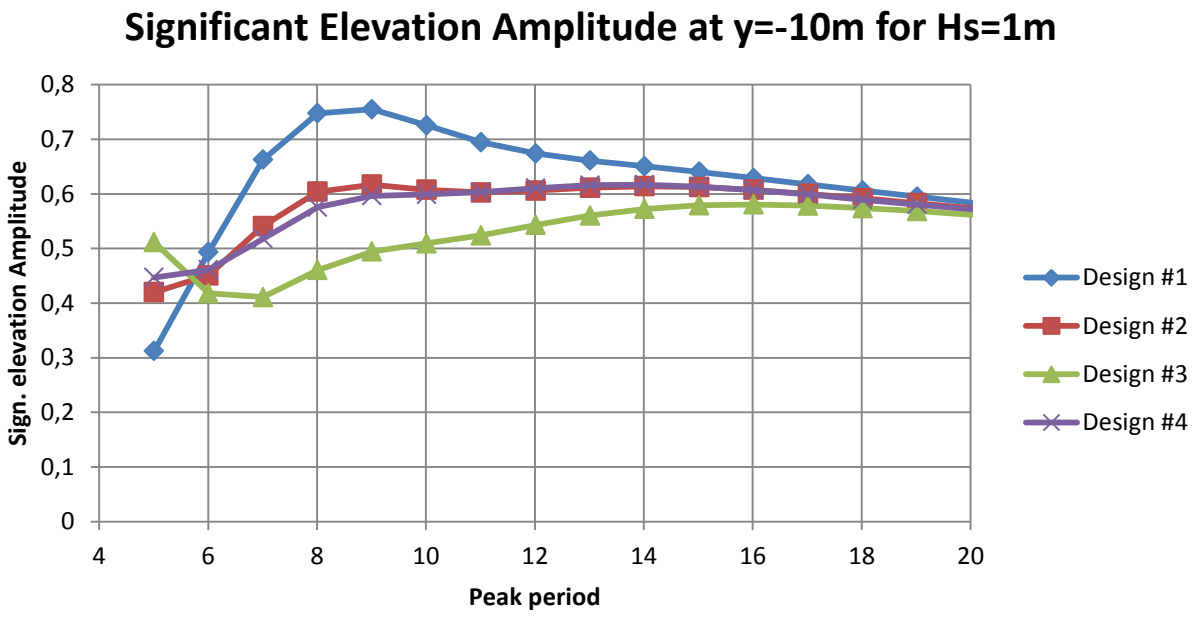

Figure 74 - Short term response for surface elevation at y=-10m for design #1-4

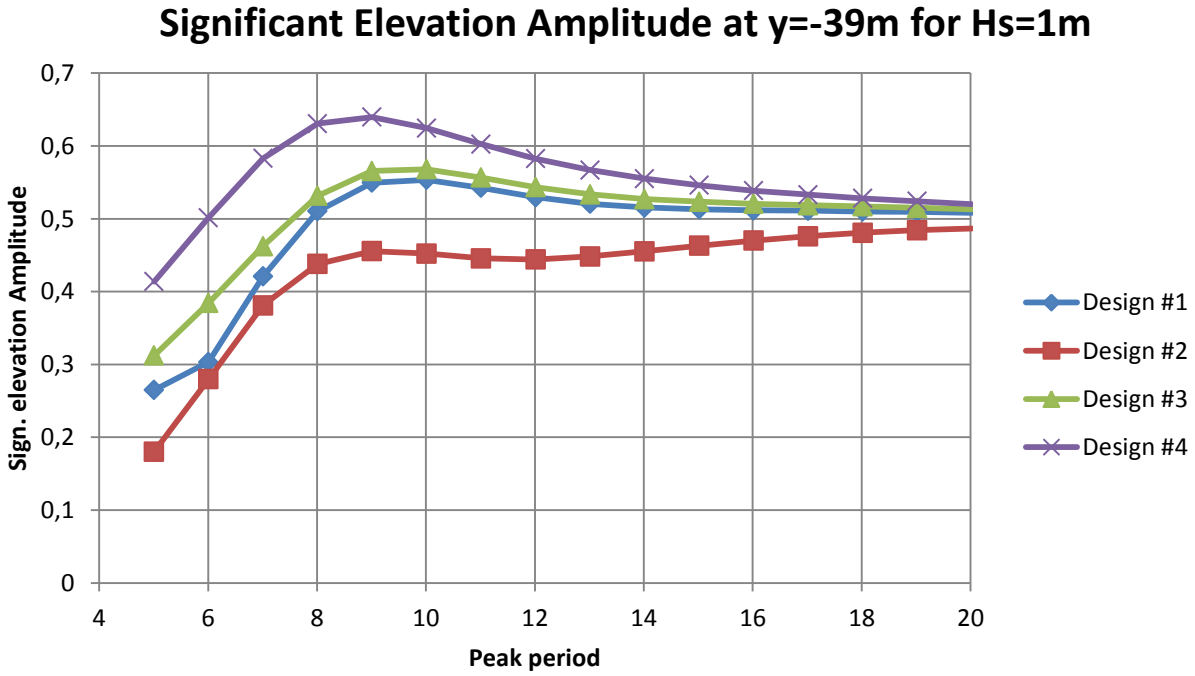

Figure 75 - Short term response for surface elevation at y=-39m for design #1-4

As observed in figure 74 and 75, the elevations experienced will be very similar for the 4 designs for high wave periods. This is a natural effect, as it for larger wave periods will be the motion of the platform that will dictate the wave pattern, and for high periods the platform will follow the wave. For shorter wave periods will it be the diffraction of waves around the platform and the pressure buildup between the inside and outside of the tunnel that will affect the elevations the most.

Assuming that impact between the ferry- top and the tunnel roof during entry/exiting is the limiting factor for operability, a study of regularity has been done. The limiting factor was first determined by evaluation of the summer project prior to this thesis (Syvertsen et al., 2011). The factor was here determined to be equal to $5m$ resulting in a wave height equal to $10m$ as this would lead to collision between the ferry and the tunnel roof. The operational study has here been done by utilizing linearity, the STR presentation of the surface elevation and the determined limiting factor. Through the presentation of the surface elevation as STRs, it was now possible to retrieve the significant wave height corresponding to this determined limiting factor as $H_s \leq \frac{10m}{2*Sign.STR\ amp}$, where $Sign.Str\ amp$ were found in figure74 and 75 for the 4 designs. After retrieving the H_s for the different wave periods, the wave data in the Santos basin (Petrobras, 2008) was studied to retrieve the measured H_s- values for different peak periods T_p, i.e using the wave scatter diagram. If it had been measured a wave height in the Santos basin higher than that calculated by the limiting factor, this wave was noted. This was done for all measured peak periods, and then all the noted waves were summed together. The total number of waves summarized represented the total number of waves that resulted in unsatisfactory surface elevations, regarding the limiting factor. This number was related to the total number of measured waves, as to find a percentage of how often the unsatisfactory conditions would occur. This was done for both points evaluated, and for all 4 designs proposed. The Excel sheet which contains this data and the data for the plots shown in figure 74 and 75 can be found in appendix F**.** The results of the operability study can be seen in table 3;

Operability at:	Design #1	Design #2	Design #3	Design #4
y=-10m (in %)	99,9256	99,9375	99,96726	99,9375
y=-39m (in %)	99,96726	100	99,97619	99,95238

Table 3 - Regularity for design #1-4 with limiting factor =5m

As seen in table 3 above, all 4 designs result in a very high operational time if only considering the surface elevations on the inside and the immediate outside of the tunnel. Based on these results, which gives the 4 designs approximately 100% operational time, none of the 4 designs stand out as the preferred one over the others. To achieve more conclusive results, the limiting factor was reduced to be $2.5m$. The Excel sheet containing the data for these regularity calculations can be found in appendix G. The resulting regularity with 2.5m as the limiting factor is shown in table 4;

Operability at:	Design #1	Design #2	Design #3	Design #4
y=-10m (in %)	95,78597	97,14303	98,73222	97,14303
y=-39m (in %)	98,68163	99,47027	98,48819	97,72335

Table 4 - Regularity for design #1-4 with limiting factor =2.5m

For each design will the lowest of the regularity percentages determine the maximal uptime for the design. This results in design #1 being able to have ferries entering the hull 95.79% of the time, design #2 having ferries entering 97.14% of the time, design #3 having ferries entering 98.48% of the time and design #4 can have ferries entering the hull 97.14% of the time. Based on this study, which considers only the surface elevation as the determining factor for the regularity of the platform, design #3 would be the preferred design.

5 TUNNEL MODIFICATIONS

In the project prior to this master thesis it has been proposed some modifications that can be done to the tunnel design. Some of the most important of these modifications are mentioned here.

5.1 Central wharf separating the tunnels

When the different design solutions have been evaluated, the designs considered have been for interconnected tunnels and for separated tunnels, considering only the surface elevation inside the tunnel as the factor of interest. In a practical aspect, it is important to note that there are other factors that also need to be considered when evaluating what design solution to choose. For instance it will be of interest for a ferry to have a central wharf at the end of a tunnel which it can perform a controlled collision with when entering. This will make the loading and unloading of personnel safer as the ferry can be tied at the front, and thus restrict its motion in surge. This kind of wharf at the center will make the tunnels separated and is an argument for deciding on a design solution that favors separated tunnels, even though computations show that this might lead to somewhat higher surface elevations.

Different designs of this wharf can give a reduction in wave elevation that may compensate for the expected increased elevation caused by separation of the tunnels;

- A wharf can be installed with two separate floors, where the lower of these are installed in a height $1m$ above the mean water level, and the second floor is installed approximately $4m$ above the mean water level. This causes a gap between the first and the second floor where all waves with $\zeta_A > 1m$ would wash over the first floor, losing a significant amount of its energy and thus reducing the reflected wave.
- A parabolic shaped beach installed at the center of the platform may also help reducing the surface motion.

5.2 Perforated bottom

If the platform is constructed with bottom in the tunnels, it will be of interest to optimize this bottom in order to reduce the wave height. This may be done by perforating the bottom to provide pressure compensation as the wave is entering the tunnel. The optimization of the floor will result in a reduction of the surface elevation inside the tunnel in the Sevan hull. To find the total impact that a perforated bottom will have on the surface elevation, the problems occurring from the creation of vortices outside the tunnel for a Sevan 650 hull will need to be mapped. It is reasonable to assume that a Sevan platform will create smaller vortices than a ship used for docking due to the decreased heave and pitch motions a Sevan platform experience compared to a ship (Løken, 2011).

6 CONCLUSION

The main scope of work in this thesis was to evaluate the wave pattern at the entrance of and inside tunnels installed on a logistical HUB based on the characteristic Sevan design. Different design solutions were proposed to minimize these surface elevations as well as the motions of the platform.

It was found that computations done in Wadam produced unnatural heave motions when a platform with a single tunnel with intact bottom was evaluated. It was concluded that this was caused by the impact of viscous effects which Wadam is unable to include in its computations. It was found that the added mass in heave for these models diverged towards negative infinity for increasing tunnel length as a result of little or no damping. This was compensated for by removing the tunnel bottom for the models to add damping to the system.

In this master thesis were 4 design solutions for the layout of the tunnels proposed and the motions for the models with these designs were evaluated. It was found that a 3 tunnel solution would result in the smallest platform motions, with the exception of in roll for wave periods larger than $T_p \geq 18s$. The large roll motion recorded for these periods was concluded to most likely be the result of computational errors.

For the 4 designs evaluated, it was concluded that a proposed design consisting of 4 interconnected tunnels, three of them being shifted 30 degrees relative each other and one tunnel located opposite of these three, would be the optimal design regarding the surface elevation inside the tunnel. The design was made specifically for minimizing this surface elevation based on the given wave situation known to occur in the Santos basin. The design resulted in the largest operability with a regularity of 98.49%, based on the wave pattern at the inside of the tunnel and at the entrance. Computations done for this design showed that it would be subject to large roll motions as a result of a small transverse metacentric height. Modifications could be done to the design to increase this small metacentric height for example by installing a vertical plate at the center of the HUB.

The Wadam computations for some of the proposed designs collapsed when calculating the pitch and roll motion for local periods $7s < T_p < 10s$. This was concluded to be either a resonance effect as a result of small damping in the model or a numerical effect resulting from irregular frequencies.

To establish a more complete overview of the wave pattern and platform motions that will occur, further computations should be done utilizing a computer program based on e.g. Navier Stokes equation, as to include kinematic effects.

7 LIST OF REFERENCES

BAUER, H. F. 1965. Nonlinear propellant sloshing in a rectangular container on infinite length.

DEAN, D. 1992. Water Wave Mechanics for Engineering and Scientists.

DNV. *GeniE- Engineering for the future* [Online]. Available: http://www.dnv.com/services/software/products/sesam/sesamfixedstructures/genie.asp.

DNV. *HydroD- Stability and hydrodynamic assessment of floating structures* [Online]. Available: http://www.dnv.com/services/software/products/sesam/sesamfloatingstructures/hydrod.asp.

DNV. *Postresp- statistical response calculation* [Online]. Available: http://www.dnv.com/services/software/products/sesam/sesamfloatingstructures/postresp.asp.

DNV. *Wadam- frequency domain hydrodynamic analysis* [Online]. Available: http://www.dnv.com/services/software/products/nauticus/hull/wadam.asp.

FALTINSEN, O. M. 1974. A nonlinear theory of sloshing in rectangular tanks.

FALTINSEN, O. M. 1998. *Sea Loads on Ships and Offshore Structures*.

FALTINSEN, O. M. & TIMOKHA, A. 2001. An adaptive multidimensional approach to nonlinear sloshing in a rectangular tank.

FALTINSEN, O. M. & TIMOKHA, A. N. 2002a. Analytically-oriented approaches to two-dimensional fluid sloshing in a rectangular tank.

FALTINSEN, O. M. & TIMOKHA, A. N. 2002b. Asymptotic modal approximation of nonlinear resonant sloshing in a rectangular tank with small fluid depth.

IBRAHIM, R. A. 2005. *Liquid Sloshing Dynamics - Theory and Applications*.

LUKOVSKII & TIMOKHA 1999. Nonlinear theory of sloshing in mobile tanks: classical and non-classical problems.

LØKEN, E. 2011. Hydrodynamic analysis of logistic HUB for personnel transfer.

OGILVIE, T. F. 1963. Firts- and second-order forces on a cylinder submerged under a free surface.

P.MCIVER & EVANS, D. V. 1984. The occurrence of negative added mass in free-surface problems involving submerged oscillating bodies.

PETROBRAS 2008. Metocean data in the Santos basin.

PIANCA, C., MAZZINI, P. & SIEGLE, E. 2010. Brazilian offshore wave climate based on NWW3 reanalysis. Available: http://www.scielo.br/scielo.php?pid=S1679-87592010000100006&script=sci_arttext#nt.

R.KHOSROPOUR, COLE, S. & STRAYER, T. 1995. Resonant free surface waves in a rectangular basin.

SEVAN 2010. Jordbær FPSO Development Project.

SYVERTSEN, K. & LOPES, C. The SSP: A New Class of Hull for the Oil Industry.

SYVERTSEN, K. & SMEDAL, A. 2005. *Offshore platform for drilling after or production of hydrocarbons*. United States of America patent application.

SYVERTSEN, T. E., SYVERTSEN, H., HANSSEN, E. B. & LØKEN, E. 2011. Logistical HUB.

VERHAGEN & WIJNGAARDEN 1965. Nonlinear oscillations of fluid in a container.

WHITE, F. M. 2008. Fluid Mechanics.

YOUNG-SUN & CHUNG-BANG 1996. Sloshing characteristics in rectangular tanks with a submerged block.

APPENDIX A

Response Amplitude Operators in heave for models with a single tunnel with intact bottom of varying length L

L=10m:

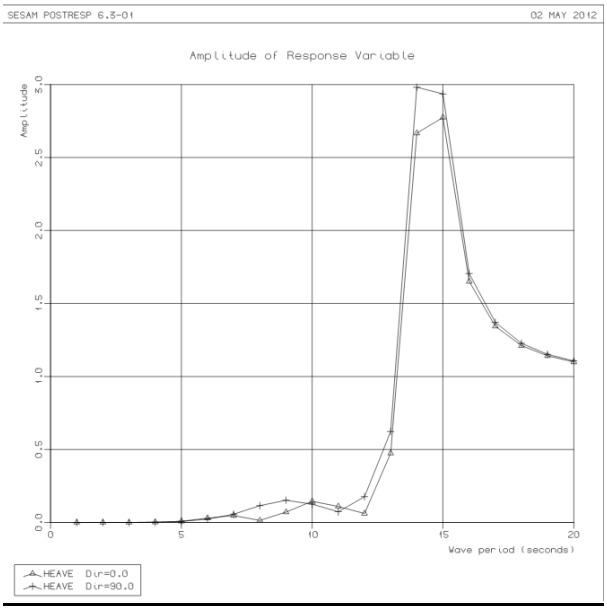

L=20m:

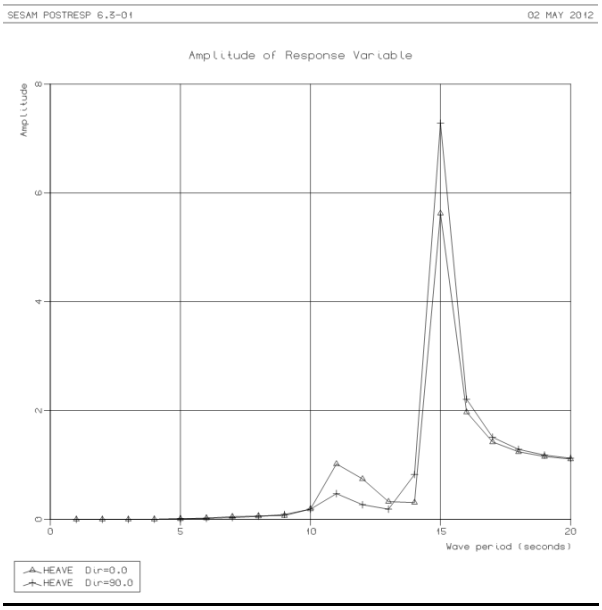

L=30m:

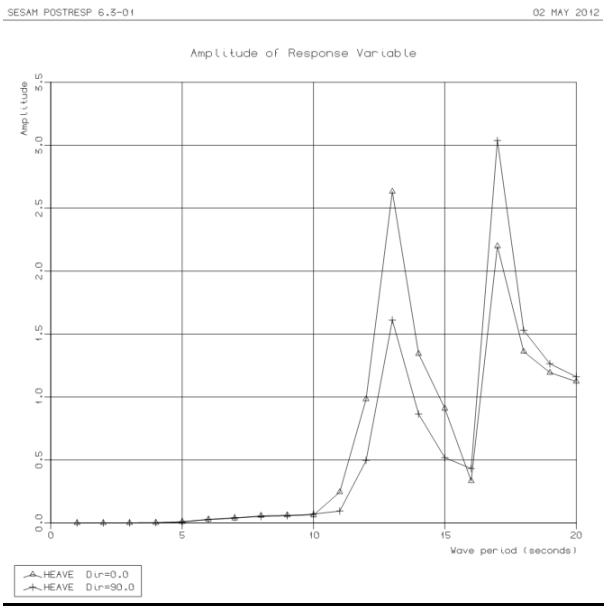

L=40m:

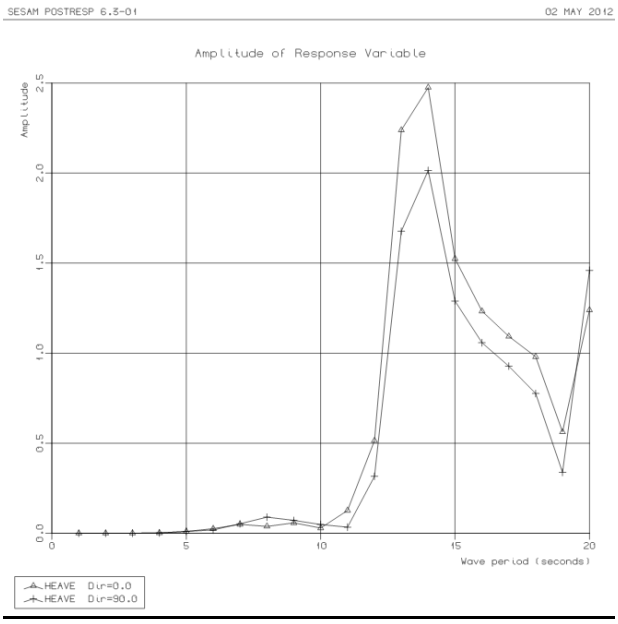

L=50m:

SESAM POSTRESP 6.3-01 02 MAY 2012

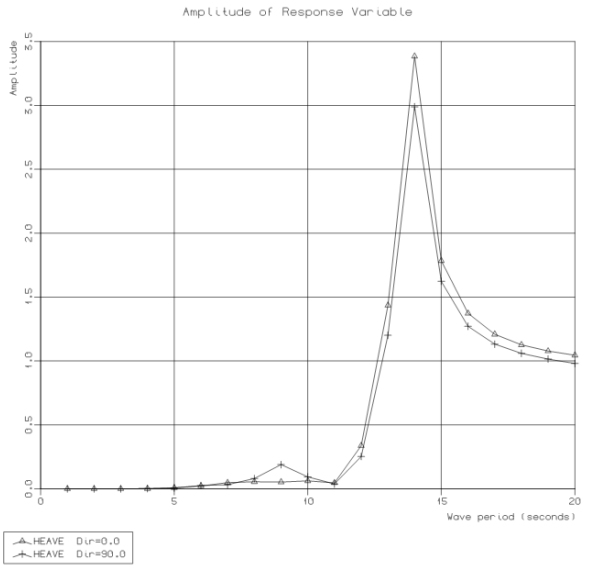

L=60m:

SESAM POSTRESP 6.3-01 02 MAY 2012

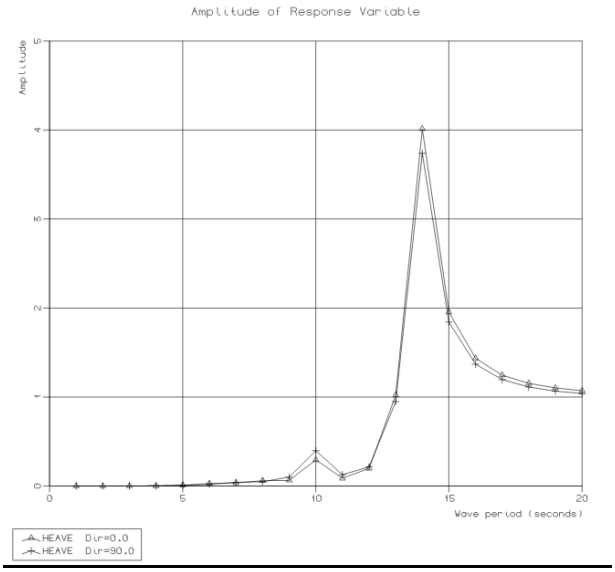

L=70m:

SESAM POSTRESP 6.3-01 03 MAY 2012

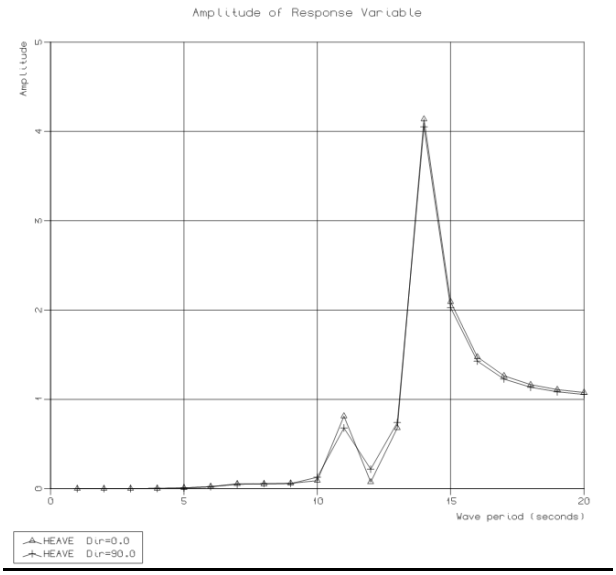

L=78m:

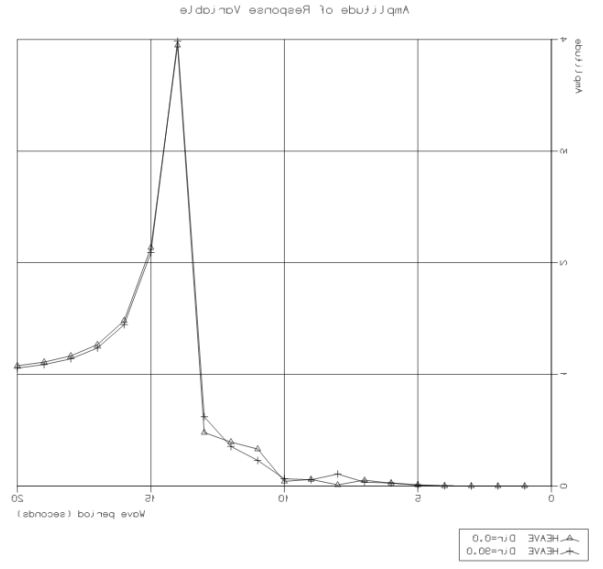

APPENDIX B

Surface elevations for a model with a single tunnel of length L=35m, without bottom, for varying y- coordinates and incoming wave heading = 270 degrees

y=-5m

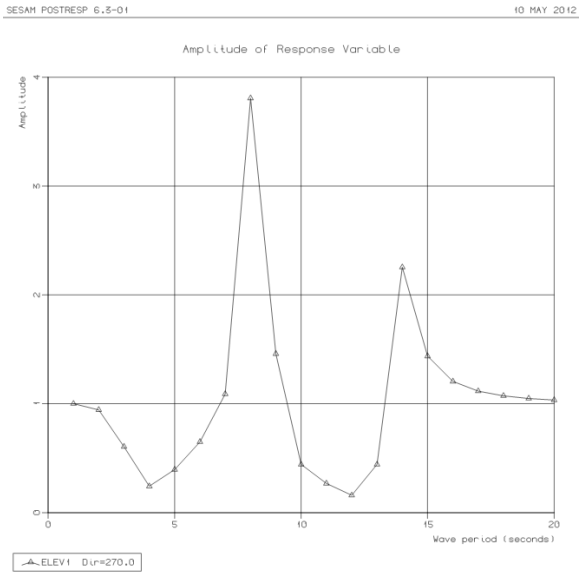

y=-10m

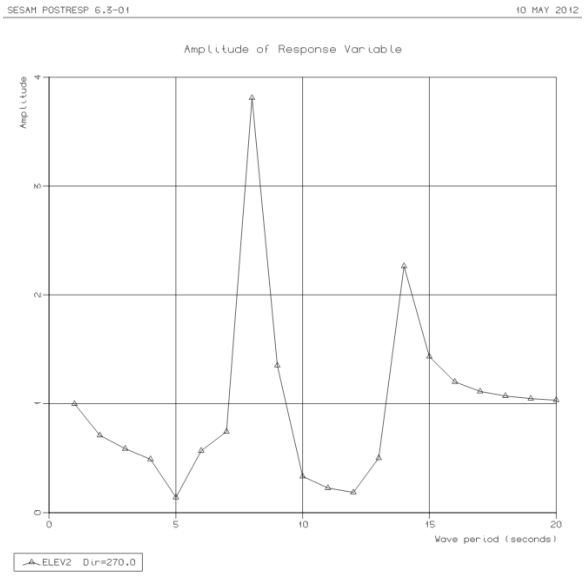

y=-15m

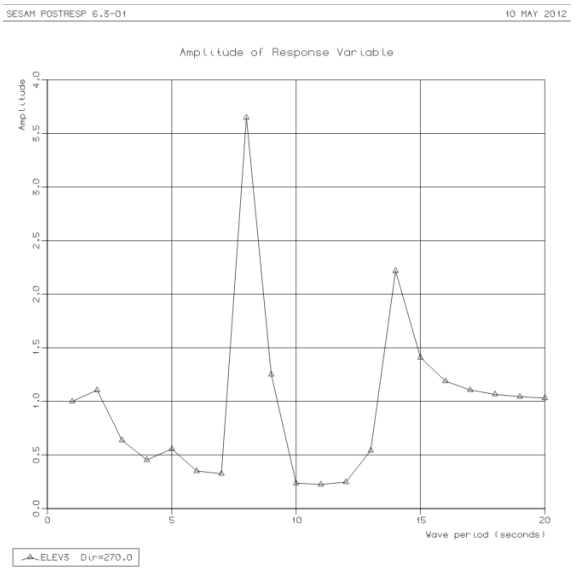

y=-20m

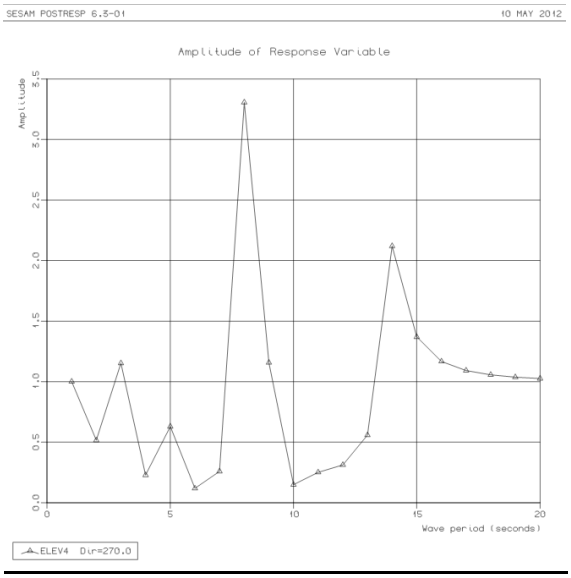

y=-25m

SESAM POSTRESP 6.3-01 10 MAY 2012

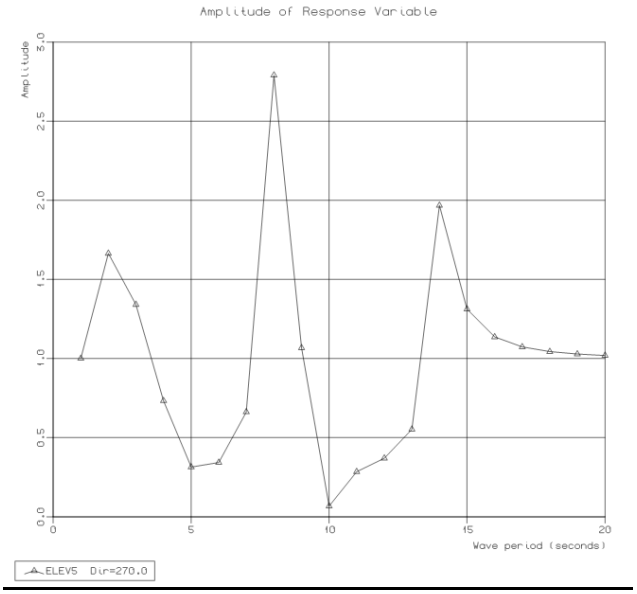

y=-30m

SESAM POSTRESP 6.3-01 10 MAY 2012

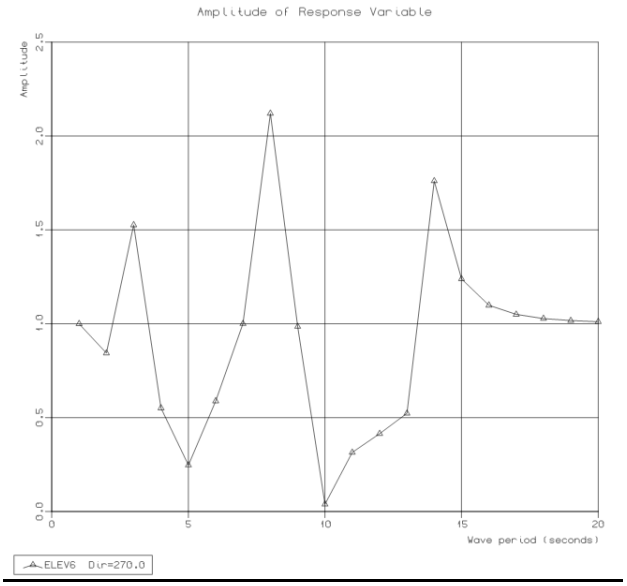

y=-35m

SESAM POSTRESP 6.3-01 10 MAY 2012

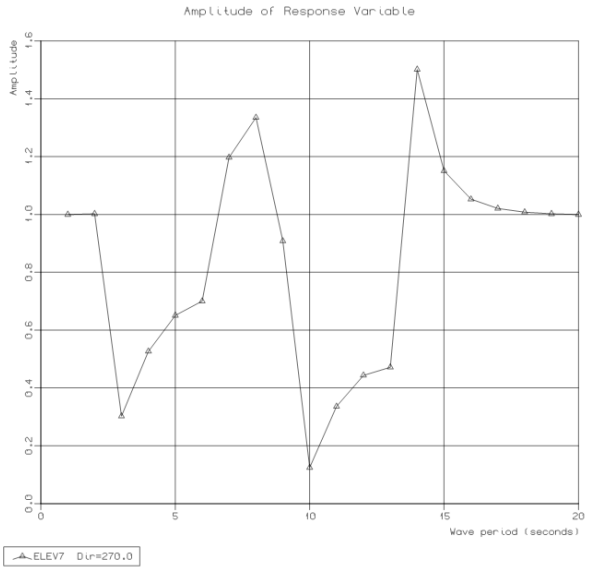

y=-40m

SESAM POSTRESP 6.3-01 10 MAY 2012

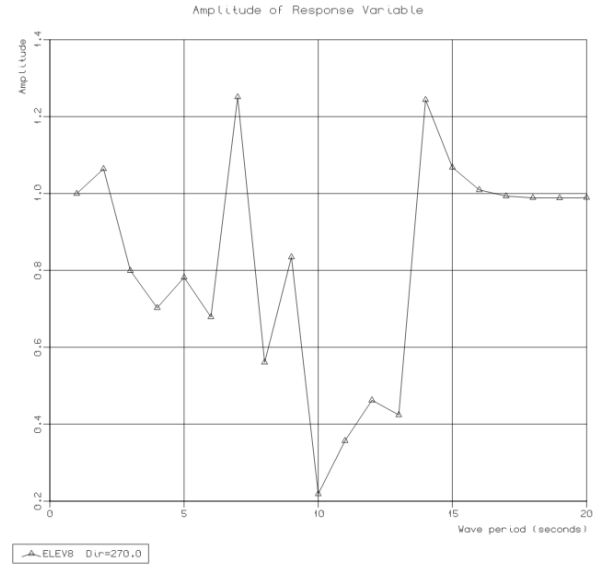

APPENDIX C

Surface elevation for a model with a single tunnel of length L=35m, without bottom, at y=-10m and for varying incoming wave headings

Incoming wave direction = 0-20 degrees

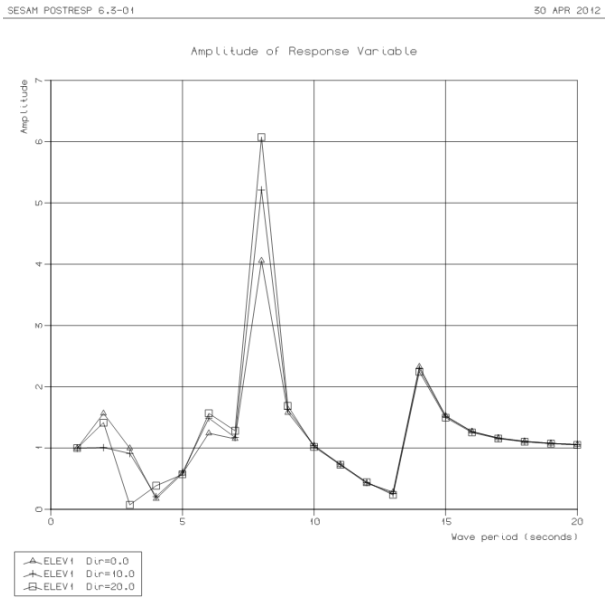

Incoming wave direction = 30-50 degrees

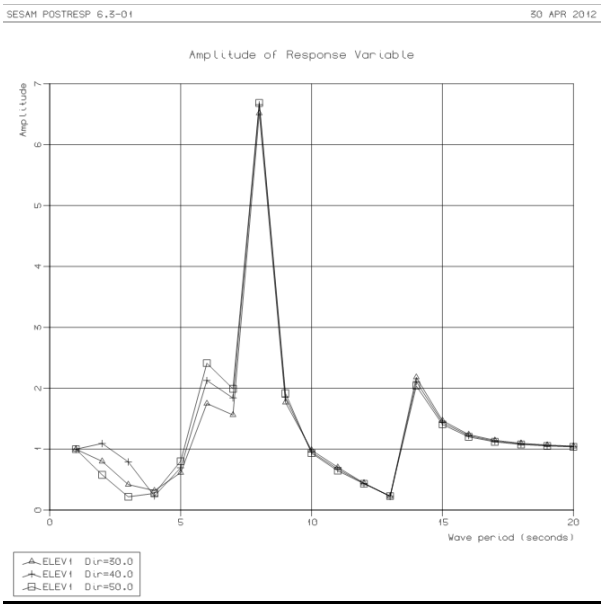

Incoming wave direction = 60-80 degrees

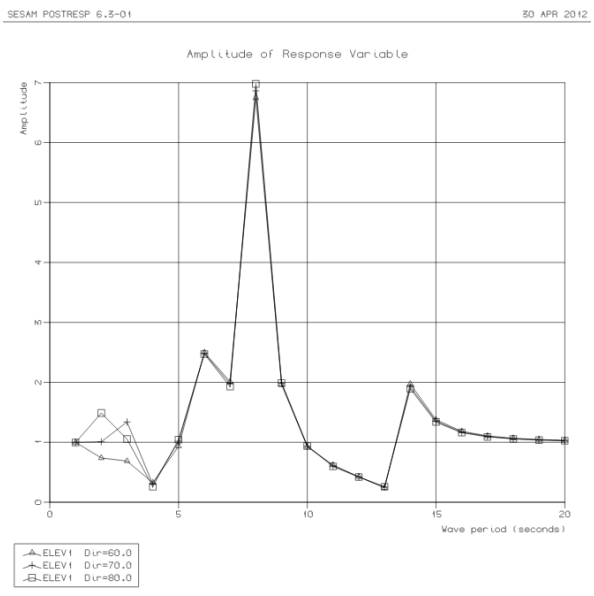

Incoming wave direction = 90 degrees

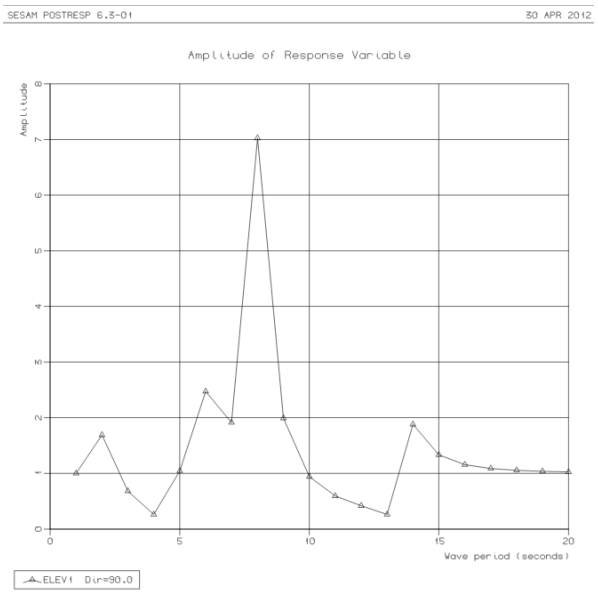

Incoming wave direction = 180-200 degrees

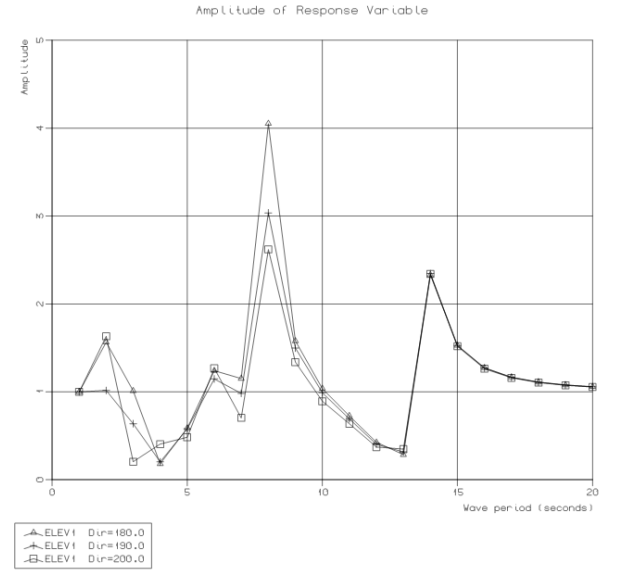

Incoming wave direction = 210-230 degrees

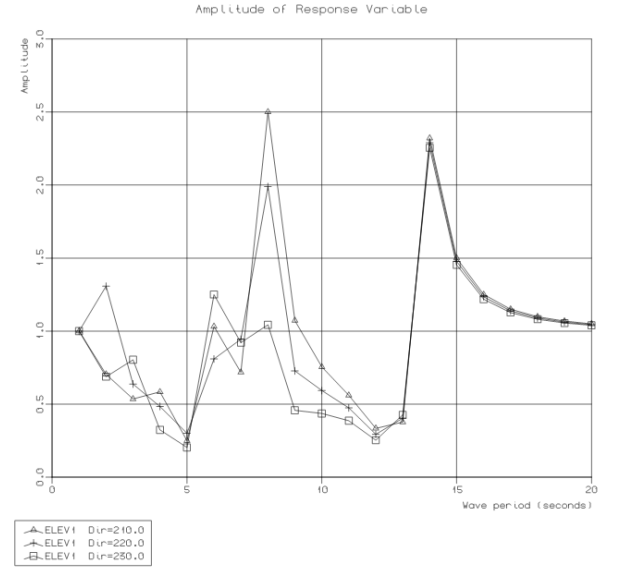

Incoming wave direction =240-260 degrees

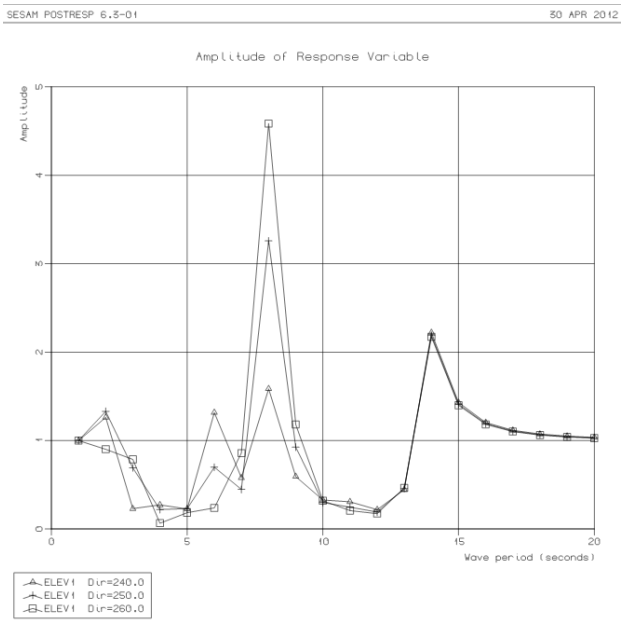

Incoming wave direction =270 degrees

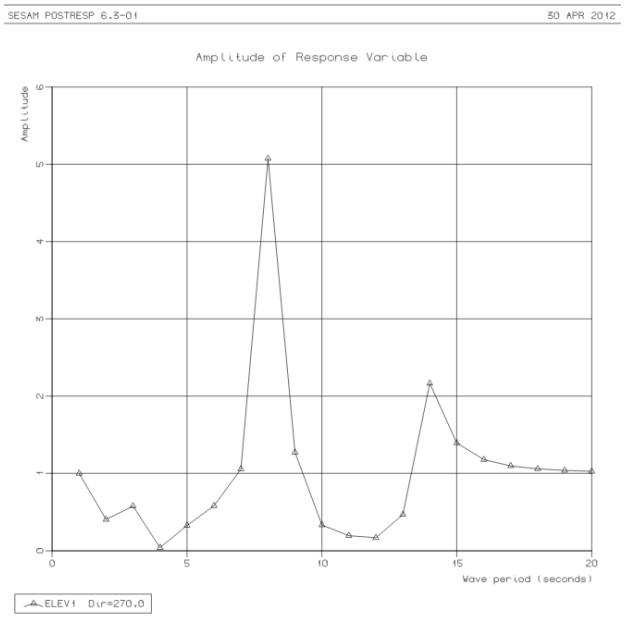

APPENDIX D

Motions for the 4 evaluated designs with central wharf separating the tunnels

Heave RAO for design #1, separated tunnels:

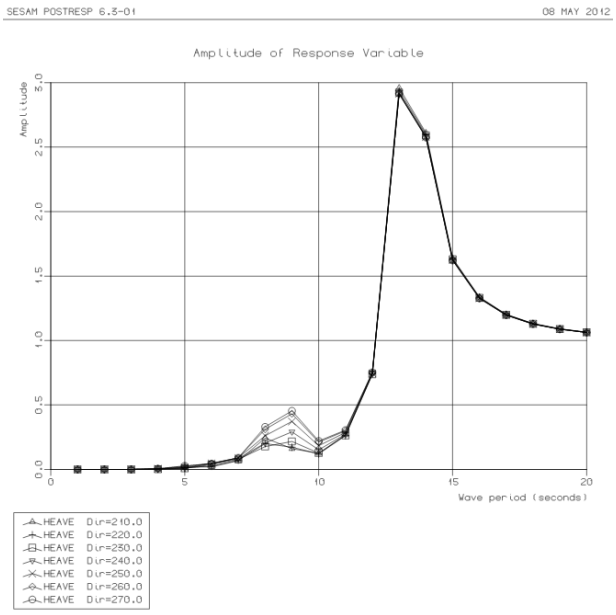

Heave RAO for design #2, separated tunnels:

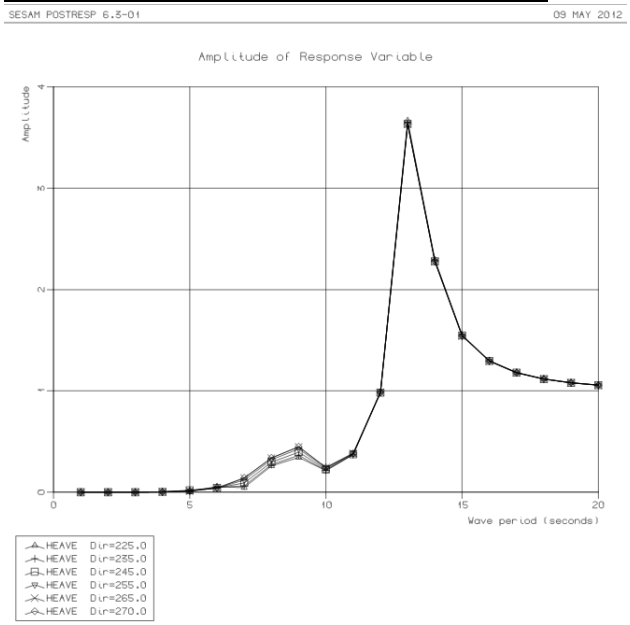

Heave RAO for design #3, separated tunnels:

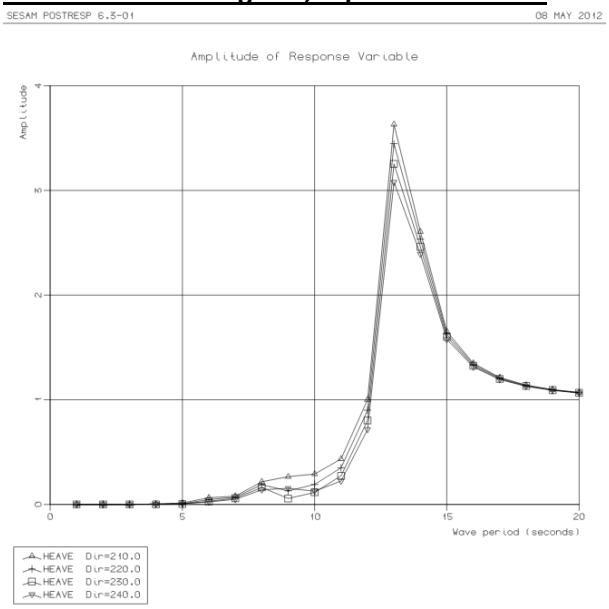

Heave RAO for design #4, separated tunnels:

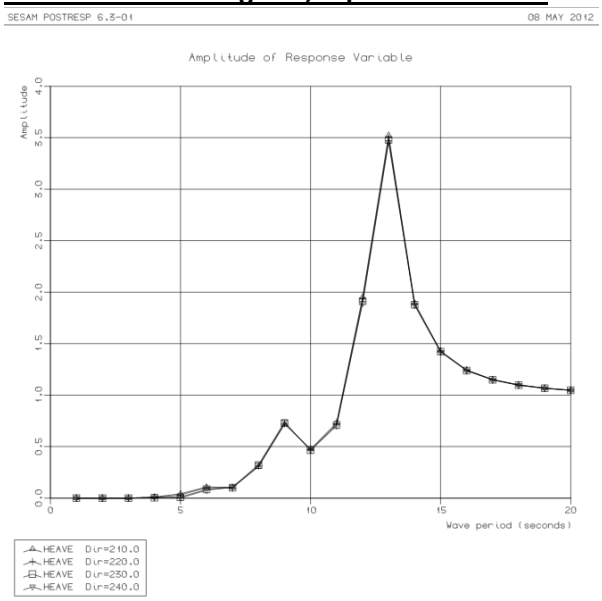

Pitch RAO for design #1, separated tunnels:

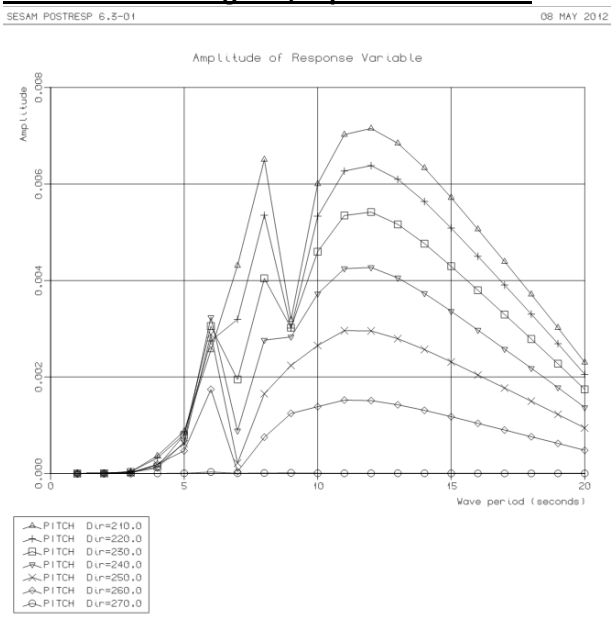

Pitch RAO for design #2, separated tunnels:

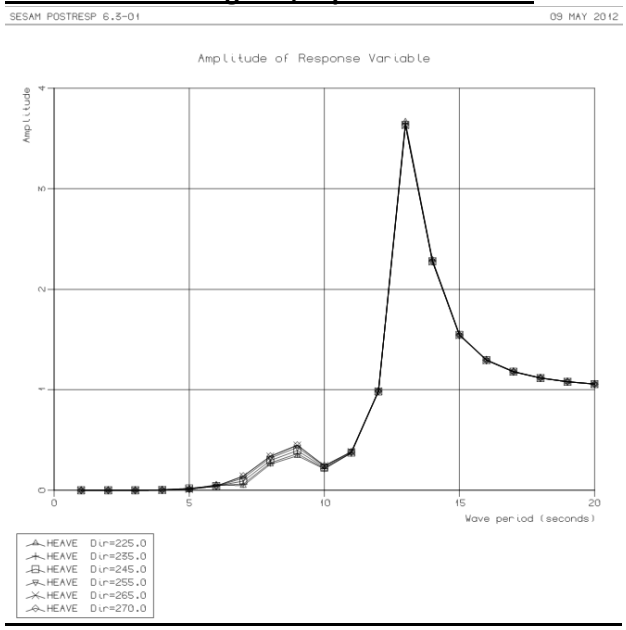

Pitch RAO for design #3, separated tunnels:

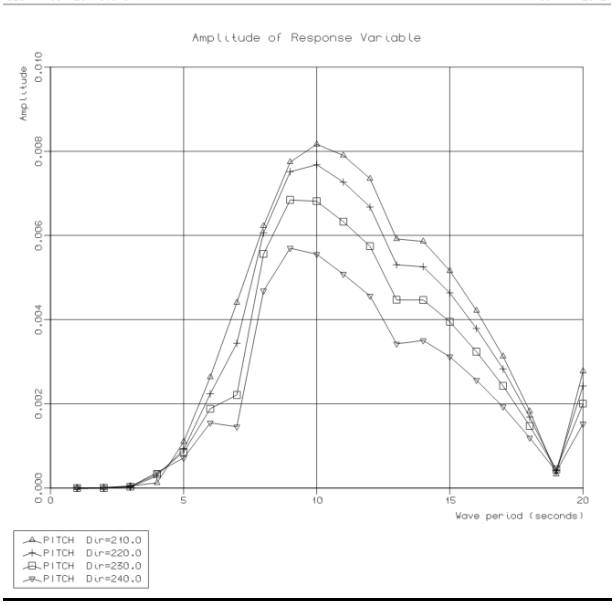

Pitch RAO for design #4, separated tunnels:

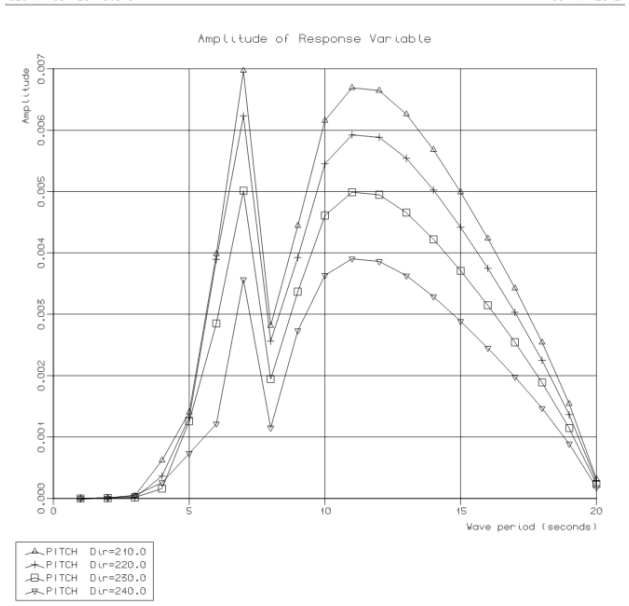

Roll RAO for design #1, separated tunnels:

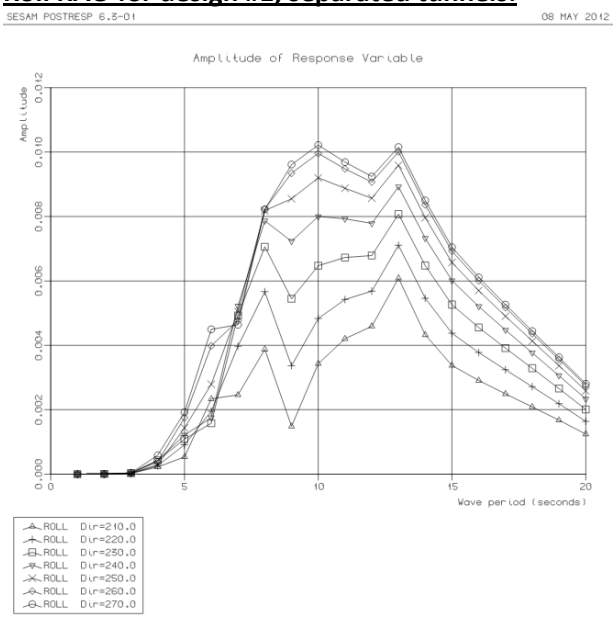

Roll RAO for design #2, separated tunnels:

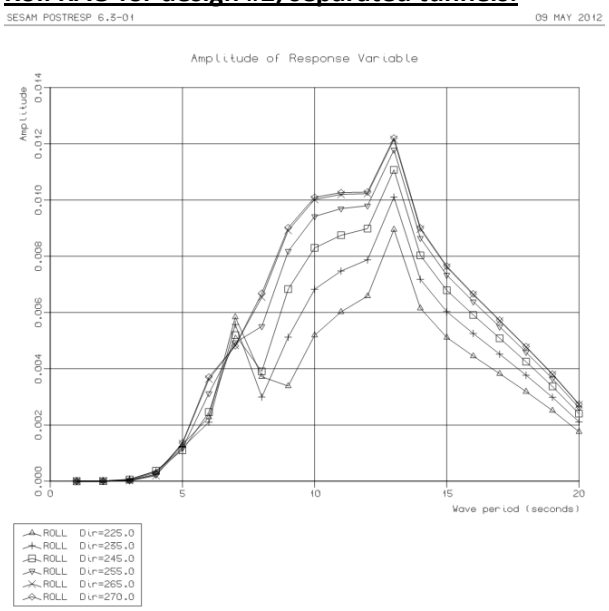

Roll RAO for design #3, separated tunnels:

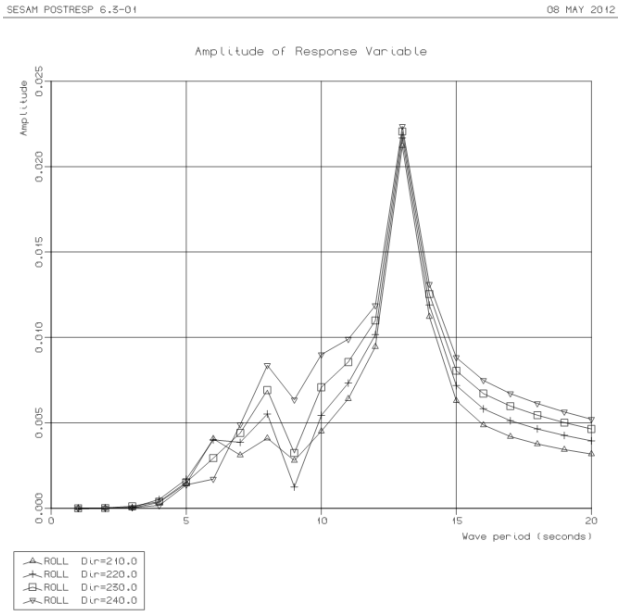

Roll RAO for design #4, separated tunnels:

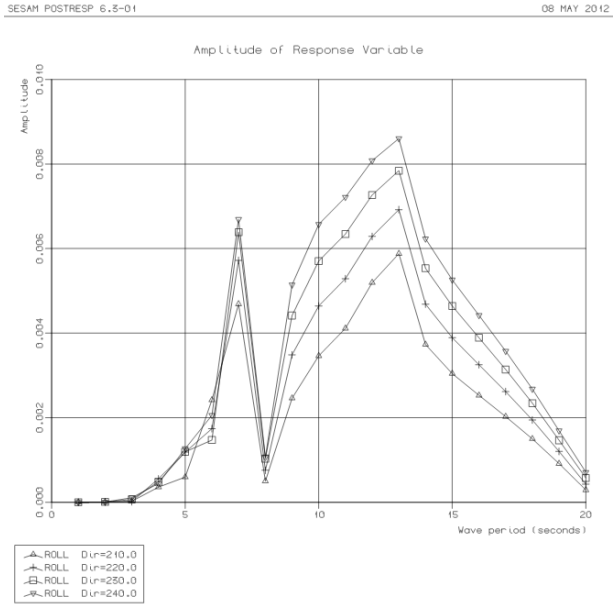

APPENDIX E

Surface elevation at y=-10m for design #1-4 with central wharf separating the tunnels

Design #1:

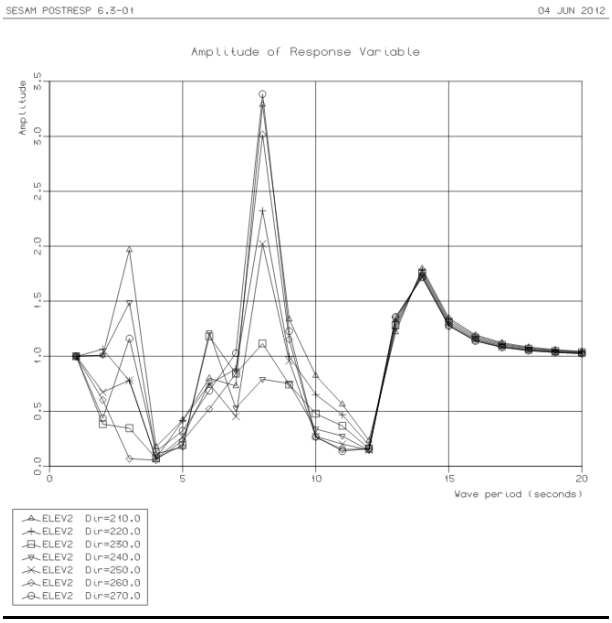

Design #2:

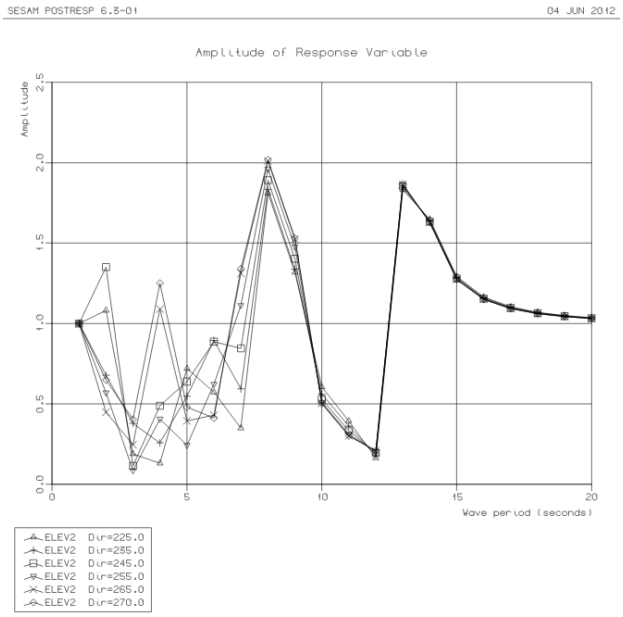

Design #3:

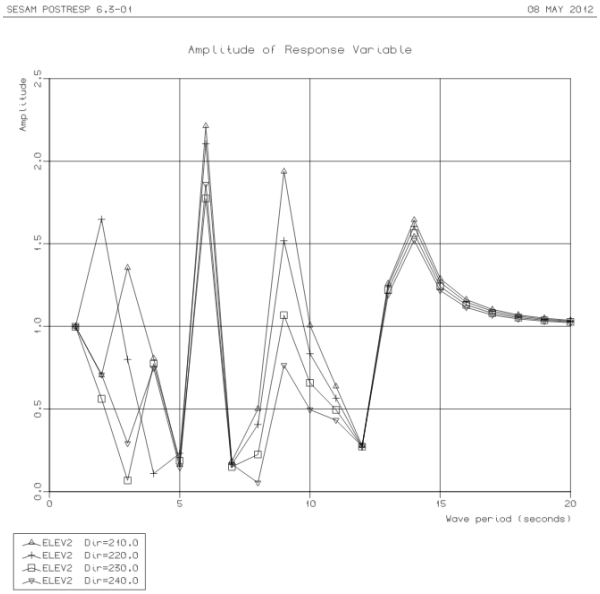

Design #4:

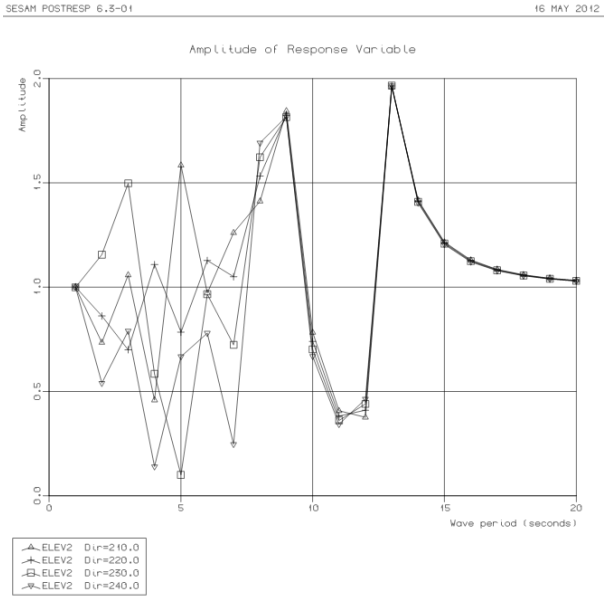

APPENDIX F

Surface elevation at y=-10m for design #1-4 as Short Term Responses. The limiting factor for the regularity study is sat to be 5m.

STR FOR ELEVATION AT Y=-10

Total number of waves recorded: 33602

Design #1:

Short Term Response number 7: ELEV1 Dir=270.0 P1-P16

Tz	Response	Tp	Sign.amp	Resulting limiting Hs [m]	Is it recorded larger than limiting Hs for given Tp?	If yes, how many waves is reecorded?
---	---					
3,55	6,25E-01	5,0055	0,3123	16,01024656	No	0
4,26	9,86E-01	6,0066	0,4932	10,1378751	No	0
4,97	1,33E+00	7,0077	0,6625	7,547169811	No	0
5,68	1,50E+00	8,0088	0,7475	6,688963211	No	0
6,39	1,51E+00	9,0099	0,755	6,622516556	No	0
7,1	1,45E+00	10,011	0,7255	6,891798759	Yes	4
7,81	1,39E+00	11,0121	0,6945	7,199424046	Yes	6
8,52	1,35E+00	12,0132	0,674	7,418397626	Yes	4
9,23	1,32E+00	13,0143	0,661	7,56429652	Yes	4
9,94	1,30E+00	14,0154	0,6505	7,686395081	No	0
10,65	1,28E+00	15,0165	0,6405	7,806401249	Yes	1
11,36	1,26E+00	16,0176	0,629	7,949125596	Yes	6
12,07	1,24E+00	17,0187	0,6175	8,097165992	No	0
12,78	1,21E+00	18,0198	0,606	8,250825083	No	0
13,49	1,19E+00	19,0209	0,595	8,403361345	No	0
14,2	1,17E+00	20,022	0,584	8,561643836	No	0
						25

Percentage uptime
99,9256

Design #2:

Short Term Response number 6: ELEV1 Dir=270.0 P1-P16

Tz	Response	Tp	Sign.amp	Resulting limiting Hs [m]	Is it recorded larger than limiting Hs for given Tp?	If yes, how many waves is reecorded?
---	---					
3,55	8,40E-01	5,0055	0,42005	11,90334484	No	0
4,26	9,02E-01	6,0066	0,45095	11,08770374	No	0
4,97	1,08E+00	7,0077	0,541	9,242144177	No	0
5,68	1,21E+00	8,0088	0,604	8,278145695	No	0
6,39	1,23E+00	9,0099	0,617	8,103727715	No	0
7,1	1,22E+00	10,011	0,6075	8,230452675	Yes	2
7,81	1,21E+00	11,0121	0,6025	8,298755187	Yes	5
8,52	1,21E+00	12,0132	0,606	8,250825083	Yes	5
9,23	1,22E+00	13,0143	0,6115	8,176614881	Yes	3
9,94	1,23E+00	14,0154	0,614	8,143322476	No	0
10,65	1,23E+00	15,0165	0,6125	8,163265306	No	0
11,36	1,22E+00	16,0176	0,6075	8,230452675	Yes	6
12,07	1,20E+00	17,0187	0,6	8,333333333	No	0
12,78	1,18E+00	18,0198	0,592	8,445945946	No	0
13,49	1,17E+00	19,0209	0,583	8,576329331	No	0
14,2	1,15E+00	20,022	0,574	8,710801394	No	0
						21

Percentage uptime
99,9375

Design #3:

Short Term Response number 1: ELEV1 Dir=210.0 P1-P16

Tz	Response	Tp	Sign.amp	Resulting limiting Hs [m]	Is it recorded larger than limiting Hs for given Tp?	If yes, how many waves is reecorded?	
3,55	1,02E+00	5,0055	0,5115	9,775171065	No	0	
4,26	8,36E-01	6,0066	0,4179	11,96458483	No	0	
4,97	8,22E-01	7,0077	0,41105	12,16397032	No	0	
5,68	9,21E-01	8,0088	0,4606	10,85540599	No	0	
6,39	9,89E-01	9,0099	0,4945	10,11122346	No	0	
7,1	1,02E+00	10,011	0,5095	9,813542689	No	0	
7,81	1,05E+00	11,0121	0,524	9,541984733	Yes	2	
8,52	1,09E+00	12,0132	0,543	9,208103131	Yes	3	
9,23	1,12E+00	13,0143	0,5605	8,920606601	Yes	2	
9,94	1,15E+00	14,0154	0,5725	8,733624454	No	0	
10,65	1,16E+00	15,0165	0,579	8,635578584	No	0	
11,36	1,16E+00	16,0176	0,5805	8,613264427	Yes	4	
12,07	1,16E+00	17,0187	0,5785	8,643042351	No	0	
12,78	1,15E+00	18,0198	0,574	8,710801394	No	0	
13,49	1,14E+00	19,0209	0,5685	8,795074758	No	0	
14,2	1,12E+00	20,022	0,562	8,896797153	No	0	
						11	**Percentage uptime**
							99,96726

Design #4:

Short Term Response number 6: ELEV1 Dir=210.0 P1-P16

Tz	Response	Tp	Sign.amp	Resulting limiting Hs [m]	Is it recorded larger than limiting Hs for given Tp?	If yes, how many waves is reecorded?	
3,55	8,94E-01	5,0055	0,4469	11,18818528	No	0	
4,26	9,22E-01	6,0066	0,461	10,84598698	No	0	
4,97	1,04E+00	7,0077	0,518	9,652509653	No	0	
5,68	1,15E+00	8,0088	0,5755	8,688097307	No	0	
6,39	1,19E+00	9,0099	0,5965	8,382229673	No	0	
7,1	1,20E+00	10,011	0,599	8,347245409	Yes	2	
7,81	1,21E+00	11,0121	0,6035	8,285004143	Yes	5	
8,52	1,22E+00	12,0132	0,6105	8,19000819	Yes	5	
9,23	1,23E+00	13,0143	0,616	8,116883117	Yes	3	
9,94	1,23E+00	14,0154	0,617	8,103727715	No	0	
10,65	1,23E+00	15,0165	0,6135	8,14995925	No	0	
11,36	1,21E+00	16,0176	0,607	8,23723229	Yes	6	
12,07	1,20E+00	17,0187	0,599	8,347245409	No	0	
12,78	1,18E+00	18,0198	0,5895	8,481764207	No	0	
13,49	1,16E+00	19,0209	0,5805	8,613264427	No	0	
14,2	1,14E+00	20,022	0,5715	8,748906387	No	0	
						21	**Percentage uptime**
							99,9375

Surface elevation at tunnel entrance y=-39m for design #1-4 as Short Term Responses. The limiting factor for the regularity study is sat to be 5m.

STR FOR ELEVATION AT Y=-39

Total number of waves recorded: 33602

Design #1:

Short Term Response number 8: ELEV2 Dir=210.0 P1-P16

Tz	Response	Tp	Sign. amp	**Resulting limiting Hs [m]**	**Is recorded larger than limiting Hs for given Tp?**	**If yes, how many waves is reecorded?**	
--------	----------						
3,55	5,30E-01	5,0055	0,2649	18,87504719	No	0	
4,26	6,07E-01	6,0066	0,30325	16,48804617	No	0	
4,97	8,42E-01	7,0077	0,4209	11,87930625	No	0	
5,68	1,02E+00	8,0088	0,5105	9,794319295	No	0	
6,39	1,10E+00	9,0099	0,5495	9,099181074	No	0	
7,1	1,11E+00	10,011	0,5535	9,033423668	Yes	1	
7,81	1,09E+00	11,0121	0,5425	9,216589862	Yes	2	
8,52	1,06E+00	12,0132	0,5295	9,442870633	Yes	3	
9,23	1,04E+00	13,0143	0,5205	9,606147935	Yes	2	
9,94	1,03E+00	14,0154	0,5155	9,699321048	No	0	
10,65	1,03E+00	15,0165	0,513	9,746588694	No	0	
11,36	1,02E+00	16,0176	0,5115	9,775171065	Yes	3	
12,07	1,02E+00	17,0187	0,511	9,784735812	No	0	
12,78	1,02E+00	18,0198	0,51	9,803921569	No	0	
13,49	1,02E+00	19,0209	0,5095	9,813542689	No	0	
14,2	1,02E+00	20,022	0,508	9,842519685	No	0	
						11	**Percantage uptime**
							99,96726

Design #2:

Short Term Response number 7: ELEV2 Dir=225.0 P1-P16

Tz	Response	Tp	Sign.amp	**Resulting limiting Hs [m]**	**Is recorded larger than limiting Hs for given Tp?**	**If yes, how many waves is reecorded?**	
--------	----------						
3,55	3,61E-01	5,0055	0,18035	27,72387025	No	0	
4,26	5,60E-01	6,0066	0,2798	17,86990708	No	0	
4,97	7,62E-01	7,0077	0,38105	13,12163758	No	0	
5,68	8,76E-01	8,0088	0,43805	11,41422212	No	0	
6,39	9,11E-01	9,0099	0,45545	10,97815347	No	0	
7,1	9,05E-01	10,011	0,4523	11,05460977	No	0	
7,81	8,91E-01	11,0121	0,4457	11,21830828	No	0	
8,52	8,88E-01	12,0132	0,4442	11,2561909	No	0	
9,23	8,97E-01	13,0143	0,44825	11,15448968	No	0	
9,94	9,11E-01	14,0154	0,4553	10,98177026	No	0	
10,65	9,26E-01	15,0165	0,46295	10,80030241	No	0	
11,36	9,40E-01	16,0176	0,47	10,63829787	No	0	
12,07	9,52E-01	17,0187	0,47595	10,50530518	No	0	
12,78	9,62E-01	18,0198	0,48075	10,40041602	No	0	
13,49	9,69E-01	19,0209	0,48435	10,32311345	No	0	
14,2	9,74E-01	20,022	0,48675	10,27221366	No	0	
						0	**Percantage uptime**
							100

Design #3:

Short Term Response number 5: ELEV2 Dir=210.0 P1-P16

Tz	Response	Tp	Sign.amp	Resulting limiting Hs [m]	Is recorded larger than limiting Hs for given Tp?	If yes, how many waves is reecorded?	
3,55	6,25E-01	5,0055	0,31225	16,01281025	No	0	
4,26	7,69E-01	6,0066	0,3844	13,00728408	No	0	
4,97	9,25E-01	7,0077	0,4624	10,81314879	No	0	
5,68	1,06E+00	8,0088	0,5315	9,407337723	No	0	
6,39	1,13E+00	9,0099	0,5655	8,84173298	No	0	
7,1	1,14E+00	10,011	0,568	8,802816901	Yes	1	
7,81	1,11E+00	11,0121	0,5565	8,984725966	Yes	2	
8,52	1,09E+00	12,0132	0,5435	9,199632015	Yes	3	
9,23	1,07E+00	13,0143	0,5335	9,372071228	Yes	2	
9,94	1,05E+00	14,0154	0,527	9,487666034	No	0	
10,65	1,05E+00	15,0165	0,5235	9,551098376	No	0	
11,36	1,04E+00	16,0176	0,5205	9,606147935	No	0	
12,07	1,04E+00	17,0187	0,5185	9,643201543	No	0	
12,78	1,03E+00	18,0198	0,517	9,671179884	No	0	
13,49	1,03E+00	19,0209	0,515	9,708737864	No	0	
14,2	1,03E+00	20,022	0,513	9,746588694	No	0	
						8	**Percantage uptime**
							99,97619

Design #4:

Short Term Response number 7: ELEV2 Dir=210.0 P1-P16

Tz	Response	Tp	Sign.amp	Resulting limiting Hs [m]	Is recorded larger than limiting Hs for given Tp?	If yes, how many waves is reecorded?	
3,55	8,28E-01	5,0055	0,41375	12,08459215	No	0	
4,26	1,00E+00	6,0066	0,5015	9,970089731	No	0	
4,97	1,17E+00	7,0077	0,583	8,576329331	No	0	
5,68	1,26E+00	8,0088	0,6305	7,930214116	No	0	
6,39	1,28E+00	9,0099	0,6395	7,818608288	No	0	
7,1	1,25E+00	10,011	0,6245	8,006405124	Yes	2	
7,81	1,21E+00	11,0121	0,6025	8,298755187	Yes	5	
8,52	1,17E+00	12,0132	0,5825	8,583690987	Yes	4	
9,23	1,13E+00	13,0143	0,567	8,818342152	Yes	2	
9,94	1,11E+00	14,0154	0,555	9,009009009	No	0	
10,65	1,09E+00	15,0165	0,546	9,157509158	No	0	
11,36	1,08E+00	16,0176	0,5385	9,285051068	Yes	3	
12,07	1,07E+00	17,0187	0,533	9,380863039	No	0	
12,78	1,06E+00	18,0198	0,528	9,46969697	No	0	
13,49	1,05E+00	19,0209	0,524	9,541984733	No	0	
14,2	1,04E+00	20,022	0,52	9,615384615	No	0	
						16	**Percantage uptime**
							99,95238

APPENDIX G

Surface elevation at y=-10m for design #1-4 as Short Term Responses. The limiting factor for the regularity study is sat to be 2.5m

STR FOR ELEVATION AT Y=-10

Total number of waves recorded: 33602

Design #1:

Short Term Response number 7: ELEV1 Dir=270.0 P1-P16

Tz	Response	Tp	Sign.amp	Resulting limiting Hs [m]	Is it recorded larger than limiting Hs for given Tp?	If yes, how many waves is reecorded?	
--------	----------					0	
3,55	6,25E-01	5,0055	0,3123	8,005123279	No	0	
4,26	9,86E-01	6,0066	0,4932	5,068937551	No	0	
4,97	1,33E+00	7,0077	0,6625	3,773584906	Yes	1	
5,68	1,50E+00	8,0088	0,7475	3,344481605	Yes	88	
6,39	1,51E+00	9,0099	0,755	3,311258278	Yes	314	
7,1	1,45E+00	10,011	0,7255	3,44589938	Yes	310	
7,81	1,39E+00	11,0121	0,6945	3,599712023	Yes	230	
8,52	1,35E+00	12,0132	0,674	3,709198813	Yes	107	
9,23	1,32E+00	13,0143	0,661	3,78214826	Yes	122	
9,94	1,30E+00	14,0154	0,6505	3,84319754	Yes	93	
10,65	1,28E+00	15,0165	0,6405	3,903200625	Yes	71	
11,36	1,26E+00	16,0176	0,629	3,974562798	Yes	57	
12,07	1,24E+00	17,0187	0,6175	4,048582996	Yes	23	
12,78	1,21E+00	18,0198	0,606	4,125412541	No	0	
13,49	1,19E+00	19,0209	0,595	4,201680672	No	0	
14,2	1,17E+00	20,022	0,584	4,280821918	No	0	
						1416	**Percentage uptime**
							95,78597

Design #2:

Short Term Response number 6: ELEV1 Dir=270.0 P1-P16

Tz	Response	Tp	Sign.amp	Resulting limiting Hs [m]	Is it recorded larger than limiting Hs for given Tp?	If yes, how many waves is reecorded?	
--------	----------						
3,55	8,40E-01	5,0055	0,42005	5,95167242	No		
4,26	9,02E-01	6,0066	0,45095	5,543851868	No		
4,97	1,08E+00	7,0077	0,541	4,621072089	No		
5,68	1,21E+00	8,0088	0,604	4,139072848	Yes	14	
6,39	1,23E+00	9,0099	0,617	4,051863857	Yes	128	
7,1	1,22E+00	10,011	0,6075	4,115226337	Yes	211	
7,81	1,21E+00	11,0121	0,6025	4,149377593	Yes	134	
8,52	1,21E+00	12,0132	0,606	4,125412541	Yes	107	
9,23	1,22E+00	13,0143	0,6115	4,088307441	Yes	122	
9,94	1,23E+00	14,0154	0,614	4,071661238	Yes	93	
10,65	1,23E+00	15,0165	0,6125	4,081632653	Yes	71	
11,36	1,22E+00	16,0176	0,6075	4,115226337	Yes	57	
12,07	1,20E+00	17,0187	0,6	4,166666667	Yes	23	
12,78	1,18E+00	18,0198	0,592	4,222972973	No	0	
13,49	1,17E+00	19,0209	0,583	4,288164666	No	0	
14,2	1,15E+00	20,022	0,574	4,355400697	No	0	
						960	**Percentage uptime**
							97,14303

Design #3:

Short Term Response number 1: ELEV1 Dir=210.0 P1-P16

Tz	Response	Tp	Sign.amp	Resulting limiting Hs [m]	Is it recorded larger than limiting Hs for given Tp?	If yes, how many waves is reecorded?	
3,55	1,02E+00	5,0055	0,5115	4,887585533	No	0	
4,26	8,36E-01	6,0066	0,4179	5,982292414	No	0	
4,97	8,22E-01	7,0077	0,41105	6,08198516	No	0	
5,68	9,21E-01	8,0088	0,4606	5,427702996	No	0	
6,39	9,89E-01	9,0099	0,4945	5,055611729	Yes	16	
7,1	1,02E+00	10,011	0,5095	4,906771344	Yes	55	
7,81	1,05E+00	11,0121	0,524	4,770992366	Yes	77	
8,52	1,09E+00	12,0132	0,543	4,604051565	Yes	54	
9,23	1,12E+00	13,0143	0,5605	4,460303301	Yes	68	
9,94	1,15E+00	14,0154	0,5725	4,366812227	Yes	40	
10,65	1,16E+00	15,0165	0,579	4,317789292	Yes	45	
11,36	1,16E+00	16,0176	0,5805	4,306632214	Yes	50	
12,07	1,16E+00	17,0187	0,5785	4,321521175	Yes	21	
12,78	1,15E+00	18,0198	0,574	4,355400697	No	0	
13,49	1,14E+00	19,0209	0,5685	4,397537379	No	0	
14,2	1,12E+00	20,022	0,562	4,448398577	No	0	
						426	**Percentage uptime**
							98,73222

Design #4:

Short Term Response number 6: ELEV1 Dir=210.0 P1-P16

Tz	Response	Tp	Sign.amp	Resulting limiting Hs [m]	Is it recorded larger than limiting Hs for given Tp?	If yes, how many waves is reecorded?	
3,55	8,94E-01	5,0055	0,4469	5,594092638	No	0	
4,26	9,22E-01	6,0066	0,461	5,422993492	No	0	
4,97	1,04E+00	7,0077	0,518	4,826254826	No	0	
5,68	1,15E+00	8,0088	0,5755	4,344048653	Yes	14	
6,39	1,19E+00	9,0099	0,5965	4,191114837	Yes	128	
7,1	1,20E+00	10,011	0,599	4,173622705	Yes	211	
7,81	1,21E+00	11,0121	0,6035	4,142502071	Yes	134	
8,52	1,22E+00	12,0132	0,6105	4,095004095	Yes	107	
9,23	1,23E+00	13,0143	0,616	4,058441558	Yes	122	
9,94	1,23E+00	14,0154	0,617	4,051863857	Yes	93	
10,65	1,23E+00	15,0165	0,6135	4,074979625	Yes	71	
11,36	1,21E+00	16,0176	0,607	4,118616145	Yes	57	
12,07	1,20E+00	17,0187	0,599	4,173622705	Yes	23	
12,78	1,18E+00	18,0198	0,5895	4,240882103	No	0	
13,49	1,16E+00	19,0209	0,5805	4,306632214	No	0	
14,2	1,14E+00	20,022	0,5715	4,374453193	No	0	
						960	**Percentage uptime**
							97,14303

Surface elevation at tunnel entrance y=-39m for design #1-4 as Short Term Responses. The limiting factor for the regularity study is sat to be; 2.5m

STR FOR ELEVATION AT Y=-39

Total number of waves recorded: 33602

Design #1:

Short Term Response number 8: ELEV2 Dir=210.0 P1-P16

Tz	Response	Tp	Sign. amp	**Resulting limiting Hs [m]**	**Is recorded larger than limiting Hs for given Tp?**	**If yes, how many waves is reecorded?**	
--------	----------						
3,55	5,30E-01	5,0055	0,2649	9,437523594	No	0	
4,26	6,07E-01	6,0066	0,30325	8,244023083	No	0	
4,97	8,42E-01	7,0077	0,4209	5,939653124	No	0	
5,68	1,02E+00	8,0088	0,5105	4,897159647	No	0	
6,39	1,10E+00	9,0099	0,5495	4,549590537	Yes	48	
7,1	1,11E+00	10,011	0,5535	4,516711834	Yes	125	
7,81	1,09E+00	11,0121	0,5425	4,608294931	Yes	103	
8,52	1,06E+00	12,0132	0,5295	4,721435316	Yes	54	
9,23	1,04E+00	13,0143	0,5205	4,803073967	Yes	33	
9,94	1,03E+00	14,0154	0,5155	4,849660524	Yes	13	
10,65	1,03E+00	15,0165	0,513	4,873294347	Yes	19	
11,36	1,02E+00	16,0176	0,5115	4,887585533	Yes	36	
12,07	1,02E+00	17,0187	0,511	4,892367906	Yes	12	
12,78	1,02E+00	18,0198	0,51	4,901960784	No	0	
13,49	1,02E+00	19,0209	0,5095	4,906771344	No	0	
14,2	1,02E+00	20,022	0,508	4,921259843	No	0	
						443	**Percantage uptime**
							98,68163

Design #2:

Short Term Response number 7: ELEV2 Dir=225.0 P1-P16

Tz	Response	Tp	Sign.amp	**Resulting limiting Hs [m]**	**Is recorded larger than limiting Hs for given Tp?**	**If yes, how many waves is reecorded?**	
--------	----------						
3,55	3,61E-01	5,0055	0,18035	13,86193513	No	0	
4,26	5,60E-01	6,0066	0,2798	8,934953538	No	0	
4,97	7,62E-01	7,0077	0,38105	6,56081879	No	0	
5,68	8,76E-01	8,0088	0,43805	5,70711106	No	0	
6,39	9,11E-01	9,0099	0,45545	5,489076737	Yes	1	
7,1	9,05E-01	10,011	0,4523	5,527304886	Yes	36	
7,81	8,91E-01	11,0121	0,4457	5,60915414	Yes	55	
8,52	8,88E-01	12,0132	0,4442	5,628095452	Yes	27	
9,23	8,97E-01	13,0143	0,44825	5,577244841	Yes	10	
9,94	9,11E-01	14,0154	0,4553	5,490885131	Yes	3	
10,65	9,26E-01	15,0165	0,46295	5,400151204	Yes	9	
11,36	9,40E-01	16,0176	0,47	5,319148936	Yes	25	
12,07	9,52E-01	17,0187	0,47595	5,25265259	Yes	12	
12,78	9,62E-01	18,0198	0,48075	5,200208008	No	0	
13,49	9,69E-01	19,0209	0,48435	5,161556726	No	0	
14,2	9,74E-01	20,022	0,48675	5,136106831	No	0	
						178	**Percantage uptime**
							99,47027

Design #3:

Short Term Response number 5: ELEV2 Dir=210.0 P1-P16

Tz	Response	Tp	Sign.amp	Resulting limiting Hs [m]	Is recorded larger than limiting Hs for given Tp?	If yes, how many waves is reecorded?	
3,55	6,25E-01	5,0055	0,31225	8,006405124	No	0	
4,26	7,69E-01	6,0066	0,3844	6,50364204	No	0	
4,97	9,25E-01	7,0077	0,4624	5,406574394	No	0	
5,68	1,06E+00	8,0088	0,5315	4,703668862	Yes	3	
6,39	1,13E+00	9,0099	0,5655	4,42086649	Yes	48	
7,1	1,14E+00	10,011	0,568	4,401408451	Yes	125	
7,81	1,11E+00	11,0121	0,5565	4,492362983	Yes	103	
8,52	1,09E+00	12,0132	0,5435	4,599816007	Yes	54	
9,23	1,07E+00	13,0143	0,5335	4,686035614	Yes	68	
9,94	1,05E+00	14,0154	0,527	4,743833017	Yes	40	
10,65	1,05E+00	15,0165	0,5235	4,775549188	Yes	19	
11,36	1,04E+00	16,0176	0,5205	4,803073967	Yes	36	
12,07	1,04E+00	17,0187	0,5185	4,821600771	Yes	12	
12,78	1,03E+00	18,0198	0,517	4,835589942	No	0	
13,49	1,03E+00	19,0209	0,515	4,854368932	No	0	
14,2	1,03E+00	20,022	0,513	4,873294347	No	0	
						508	**Percantage uptime**
							98,48819

Design #4:

Short Term Response number 7: ELEV2 Dir=210.0 P1-P16

Tz	Response	Tp	Sign.amp	Resulting limiting Hs [m]	Is recorded larger than limiting Hs for given Tp?	If yes, how many waves is reecorded?	
3,55	8,28E-01	5,0055	0,41375	6,042296073	No		
4,26	1,00E+00	6,0066	0,5015	4,985044865	No		
4,97	1,17E+00	7,0077	0,583	4,288164666	No		
5,68	1,26E+00	8,0088	0,6305	3,965107058	Yes	14	
6,39	1,28E+00	9,0099	0,6395	3,909304144	Yes	128	
7,1	1,25E+00	10,011	0,6245	4,003202562	Yes	211	
7,81	1,21E+00	11,0121	0,6025	4,149377593	Yes	134	
8,52	1,17E+00	12,0132	0,5825	4,291845494	Yes	54	
9,23	1,13E+00	13,0143	0,567	4,409171076	Yes	68	
9,94	1,11E+00	14,0154	0,555	4,504504505	Yes	40	
10,65	1,09E+00	15,0165	0,546	4,578754579	Yes	45	
11,36	1,08E+00	16,0176	0,5385	4,642525534	Yes	50	
12,07	1,07E+00	17,0187	0,533	4,69043152	Yes	21	
12,78	1,06E+00	18,0198	0,528	4,734848485	No	0	
13,49	1,05E+00	19,0209	0,524	4,770992366	No	0	
14,2	1,04E+00	20,022	0,52	4,807692308	No	0	
						765	**Percantage uptime**
							97,72335